bioRxiv preprint doi: https://doi.org/10.64898/2026.07.30.741915; this version posted November 9, 2026. The copyright holder for this preprint (which was not certified by peer review) is the author/funder, who has granted bioRxiv a license to display the preprint in perpetuity. It is made available under a CC-BY 4.0 International license.



A nuclear targeting approach enables efficient transgenesis in the milkweed bug *Oncopeltus fasciatus*

Yu Shirai[1 *], Yousuf Hashmi[1,2], Ashley Watts[1,3], Jonchee A. Kao[4,5], Cassandra G. Extavour[1,4,6 *]

1. Department of Organismic and Evolutionary Biology, Harvard University, Cambridge, MA, USA

2. Present address: Committee on Regeneration, Development, and Stem Cell Biology, University of Chicago, Chicago, IL, USA

3. Present address: Office of Education, Rutgers New Jersey Medical School, 185 South Orange Ave, Newark, NJ, USA

4. Department of Molecular and Cellular Biology, Harvard University, Cambridge, MA, USA

5. Present address: Department of Applied Biosciences, Graduate School of Agriculture, Kyoto University, Kyoto, Japan

6. Howard Hughes Medical Institute, Chevy Chase, MD, USA

* Correspondence: Yu Shirai, Cassandra G. Extavour

Email: shiraiyu@fas.harvard.edu, extavour@oeb.harvard.edu

bioRxiv preprint doi: https://doi.org/10.64898/2026.07.30.741915; this version posted November 9, 2026. The copyright holder for this preprint (which was not certified by peer review) is the author/funder, who has granted bioRxiv a license to display the preprint in perpetuity. It is made available under a CC-BY 4.0 International license.

Abstract

Insects show extreme diversity and have long intrigued biologists. Although gene editing and transgenesis should enable the use of almost any insect species for biological research, species-specific challenges remain and conditions must be optimized carefully. Here, using the milkweed bug *Oncopeltus fasciatus*, we first generate a useful eye- and body-color mutant strain by CRISPR/Cas9-mediated genome editing. Using this strain, we develop an efficient *piggyBac*-mediated transgenesis system with a nuclear targeting approach. Incorporating 1× and 3× nuclear localization signals into *piggyBac* mRNA substantially enhances overall transformation efficiency in *O. fasciatus*. Taking advantage of the mutant strain and the efficient transgenesis system, we integrated multiple expression cassettes ranging from 1.8 to 7.2 kb, including attP strains for phiC31-mediated integration and histone-labelled strains for live imaging. We further show that the Q system, a binary expression system, is functional in this species, paving the way for sophisticated genetic manipulations. Together, our results expand the genetic toolkit of *O. fasciatus* as a comparative model insect and provide a practical framework for developing efficient transgenesis in other non-traditional model organisms.

Keywords

CRISPR/Cas9; Transgenesis; *piggyBac*; Q-system; Reporter assay; *Oncopeltus fasciatus*

bioRxiv preprint doi: https://doi.org/10.64898/2026.07.30.741915; this version posted November 9, 2026. The copyright holder for this preprint (which was not certified by peer review) is the author/funder, who has granted bioRxiv a license to display the preprint in perpetuity. It is made available under a CC-BY 4.0 International license.

Summary statement

We developed an efficient *piggyBac* transgenesis system in the milkweed bug with a nuclear targeting approach, expanding genetic tools for non-model insects.

bioRxiv preprint doi: https://doi.org/10.64898/2026.07.30.741915; this version posted November 9, 2026. The copyright holder for this preprint (which was not certified by peer review) is the author/funder, who has granted bioRxiv a license to display the preprint in perpetuity. It is made available under a CC-BY 4.0 International license.

Introduction

Insects are one of the most diverse groups of animals on Earth (Stork, 2017). Their remarkable beauty, adaptations, and diversity have long fascinated biologists. Many biological questions about insect diversity and evolution cannot be addressed using the long-standing arthropod model *Drosophila melanogaster* alone (Clark et al., 2019; Kao et al., 2026; Truman et al., 2026). Beyond the *Drosophila melanogaster* paradigm, recent technological advancements have enabled us to use functional genetics to investigate many non-traditional model organisms, opening new avenues for studies of the evolution of developmental mechanisms (Gudmunds et al., 2022). Comparative studies are essential to understand the evolutionary history of insects. Establishing genomic and biological resources across multiple species has thus become a critical investment in cell and developmental biology.

The large milkweed bug, *Oncopeltus fasciatus* (Lygaeidae, Hemiptera) has a long history of comparative developmental studies (reviewed in Chipman, 2017; Feir, 1974). Hemiptera is a large and diverse order of insects that is phylogenetically important for understanding insect evolution, as it is an outgroup to Holometabola, the clade of insects that undergo complete metamorphosis (Misof et al., 2014). In the mid-twentieth century, *O. fasciatus* was widely used as a model organism across many different contexts, including embryology, physiology, and histology (e.g. Butt, 1949; Kelly and Telfer, 1979; Schreiner, 1977). However, the rise of *D. melanogaster* genetics largely displaced *O. fasciatus*, along with other insect species. Approximately two decades ago, taking advantage of its ease of rearing and high sensitivity to RNAi-mediated gene perturbation, *O. fasciatus* began to re-emerge as an evo-devo model, particularly for the study of segmentation and body patterning (Angelini and Kaufman, 2005; Angelini et al., 2005; Liu and Kaufman, 2004a; Liu and Kaufman, 2004b; Liu and Kaufman, 2005; Liu

bioRxiv preprint doi: https://doi.org/10.64898/2026.07.30.741915; this version posted November 9, 2026. The copyright holder for this preprint (which was not certified by peer review) is the author/funder, who has granted bioRxiv a license to display the preprint in perpetuity. It is made available under a CC-BY 4.0 International license.

and Patel, 2009; Liu and Patel, 2010). More recently, the development of CRISPR/Cas9-mediated targeted mutagenesis (Reding and Pick, 2020) and knock-in methods (Shirai et al., 2026) has further expanded its utility as a comparative model organism for functional genetics.

Since transgenesis is a powerful genetic tool for investigating gene function and *cis*-regulatory elements (Gregory et al., 2016; Handler, 2002), deploying this tool in *O. fasciatus* is essential for establishing it as a more versatile model organism. We focus here on a hyperactive variant of the *piggyBac* transposase called hyPBase (Yusa et al., 2011), which has been successfully applied across multiple insect species (Chen and Palli, 2021; Gonzalez-Sqalli et al., 2024; Hart et al., 2023; Heryanto et al., 2022; Inada et al., 2025; Kou et al., 2023; Ohde et al., 2025), consistently outperforming the original *piggyBac* transposase in overall efficiency (Eckermann et al., 2018; Ohde et al., 2025; Otte et al., 2018).

Here, we describe an efficient *piggyBac*-mediated transgenesis system in *O. fasciatus*. First, we generate a useful eye- and body-color mutant strain by crossing the *Of-vermilion* (*Of-v*) mutant (Reding et al., 2023) with a newly generated CRISPant strain carrying a mutation in *Of-xanthine dehydrogenase* (*Of-xdh1*), the ortholog of *D. melanogaster rosy*, enabling easier detection of fluorescent signals through the adult cuticle. Using this double mutant strain, we develop a highly efficient *piggyBac*-mediated transgenesis system by incorporating additional SV40 nuclear localization signals (NLSs) (Kalderon et al., 1984) into hyPBase. Furthermore, we provide evidence that Q system mediated-binary expression (Potter et al., 2010) is functional in *O. fasciatus*. Together, our results substantially expand the experimental possibilities of *O. fasciatus* as a comparative genetic model organism and provide a practical framework for implementing efficient transgenesis in other non-traditional model organisms.

bioRxiv preprint doi: https://doi.org/10.64898/2026.07.30.741915; this version posted November 9, 2026. The copyright holder for this preprint (which was not certified by peer review) is the author/funder, who has granted bioRxiv a license to display the preprint in perpetuity. It is made available under a CC-BY 4.0 International license.

Results

Establishment of a useful eye- and body-color mutant strain in *O. fasciatus*

Many successful insect transgenesis systems rely on detection of a dominant marker, often expression of a fluorescent protein, in the eye (Berghammer et al., 1999). However, detecting this marker expression can be challenging if the animal's eyes are darkly pigmented. In the case of *O. fasciatus*, the wild-type eye color is black. Therefore, we aimed to generate a mutant strain with a lighter eye color to facilitate the detection of fluorescent signal, such as GFP or RFP, derived from transgenesis. Previous studies have attempted to generate such a strain: one study reported that the *O. fasciatus white* (*Of-w*) gene, commonly used to provide a suitable background for detection of a dominant rescue construct in other insects, caused lethality when disrupted (Reding and Pick, 2020), while another study established strains mutant for *Of-v*, an ommochrome pathway gene, displaying dark red eye color (Reding et al., 2023). However, we were not certain whether the eyes of the *Of-v* mutants were light enough to detect fluorescent signal. In 1970, Peter Lawrence reported *O. fasciatus* mutants named "*red eye* (*re*)", "*white body* (*wb*)", and "*cream body* (*cb*)" (Lawrence, 1970). *re* mutants had red eyes, and the described phenotypes of *re* mutants are generally consistent with that of *Of-v* mutants (Reding et al., 2023), suggesting that *re* mutants lack ommochrome pigments. However, *re* was reported to be autosomal (Lawrence, 1970), whereas *Of-v* is located on the X-chromosome (Reding et al., 2023), indicating that the gene responsible the *re* phenotype is different from *Of-v*. By contrast, *wb* and *cb* mutants were both reported to have a whitish yellow body color, and these described phenotypes are comparable to the loss of orange body coloration observed upon systemic RNAi of pteridine pathway genes (Liu, 2016; Reding et al., 2023).

bioRxiv preprint doi: https://doi.org/10.64898/2026.07.30.741915; this version posted November 9, 2026. The copyright holder for this preprint (which was not certified by peer review) is the author/funder, who has granted bioRxiv a license to display the preprint in perpetuity. It is made available under a CC-BY 4.0 International license.

Importantly, double mutants of *re* and either *wb* or *cb* showed eye color distinct from that of the single mutants (Lawrence, 1970), and maternal RNAi of *punch*, a pteridine pathway gene, resulted in eye-color defects in embryos (Liu, 2016). Together, these results suggested that both ommochrome and pteridine pigments might contribute to eye color formation in *O. fasciatus*. Based on these findings, we decided to target the *O. fasciatus* ortholog of the pteridine pathway gene *xdh1* (*Of-xdh1*, Accession No. OFAS027123), whose *D. melanogaster* ortholog is the *rosy* gene (Keith et al., 1987). *Of-xdh1* has been implicated in body coloration in *O. fasciatus* based on systemic RNAi-mediated functional analysis (Reding et al., 2023).

Of-xdh1 is predicted to encode a 1341 amino acid pteridine pathway enzyme containing 2Fe-2S, flavin adenine dinucleotide (FAD) binding, and molybdopterin binding domains, as determined by InterProScan (Fig. 1A). To generate a homozygous mutant *Of-xdh1* strain (Fig. 1B), we designed a guide RNA targeting the region immediately downstream of the start codon (Fig. 1A), hoping to generate an indel and frameshift resulting in a premature stop codon and eliminating the functional domains of this enzyme. Following injection of Cas9/gRNA ribonucleoprotein complex into 54 eggs, 17 of 18 hatchlings (94.4%) showed a clear body color difference in the injected generation (G_0) compared to wild type (WT), enabling selection of potential mutants (Fig. 1C). After three rounds of crossing, we established a homozygous strain named *xdh1*$^{\Delta 2}$, carrying a two base pair deletion allele introducing a premature stop codon, and displaying orange body coloration (Fig. 1D–E and Supplementary Fig. 1).

To investigate the potential involvement of *xdh1* in eye-color formation, we crossed *xdh1*$^{\Delta 2}$ animals with those from the *Of-v* mutant strain *v*^{1} (Reding et al., 2023) (Supplementary Fig. 2) to generate a double homozygous mutant strain. We confirmed the mutations at both loci by sequencing. Comparison of eye color among four different

bioRxiv preprint doi: https://doi.org/10.64898/2026.07.30.741915; this version posted November 9, 2026. The copyright holder for this preprint (which was not certified by peer review) is the author/funder, who has granted bioRxiv a license to display the preprint in perpetuity. It is made available under a CC-BY 4.0 International license.

strains (wild type, v^1, $xdh1^{\Delta 2}$, and v^1 $xdh1^{\Delta 2}$), revealed that the v^1 $xdh1^{\Delta 2}$ double mutant strain displayed a brighter orange eye color than all the others (Fig. 1E–F and Supplementary Fig. 3). The double mutant strain also showed a brighter yellowish body color than the others, particularly at early nymphal stages (Fig. 1E, and Supplementary Fig. 3), indicating that both ommochrome and pteridine pigments contribute to eye and body color formation in *O. fasciatus*. Thus, we used this strain for the subsequent transgenesis experiments described in the following sections.

Nuclear targeting allows an efficient hyPBase-mediated transgenesis in *O. fasciatus*

To develop a transgenesis method in *O. fasciatus* using the v^1 $xdh1^{\Delta 2}$ strain (Fig. 2A), we first utilized the *piggyBac* vector *pXL[9×P3-mScarlet-I-SV40T]* (1,775 bp). In this vector, mScarlet-I is placed under the control of the 9×P3 promoter, consisting of nine copies of a Pax6 homeodomain binding site, which drives specific expression in the eyes in many insects (Berghammer et al., 1999; Horn and Wimmer, 2000; Horn et al., 2000; Inada et al., 2025; Ohde et al., 2025; Sheng et al., 1997) (Fig. 2B). We screened for mScarlet-I expression in the eyes of injected animals at both mid-nymphal and adult stages. In the first round of injection with *in vitro* transcribed *hyPBase* mRNA, 5/29 G_0 animals were mScarlet-I-positive at nymphal stages (G_0 somatic transformation rate (STR) = 17.2%), and 6/25 (STR = 24.0%) at adult stages (Fig. 2C–D and Table 1). However, no G_0 animals showed mScarlet-I expression at either stage in a second round of injection using the same batch of reagents (0/70 at nymphal stages and 0/62 at adult stages; STR = 0%) (Fig. 2D and Table 1), suggesting inconsistent transgenesis efficiency with unmodified hyPBase.

Given this inconsistency across technical replicate experiments, we hypothesized that incorporating additional SV40T nuclear localization signals (NLSs)

bioRxiv preprint doi: https://doi.org/10.64898/2026.07.30.741915; this version posted November 9, 2026. The copyright holder for this preprint (which was not certified by peer review) is the author/funder, who has granted bioRxiv a license to display the preprint in perpetuity. It is made available under a CC-BY 4.0 International license.

into hyPBase would improve transgenesis efficiency (Fig. 2B). To test this hypothesis, we compared STR values across 0×, 1×, 3× and 5×NLS *hyPBase* mRNA conditions using the same donor vector. We found that 1× and 3×NLS *hyPBase* mRNA yielded higher and more consistent STR values than 0×NLS. Across two experimental replicates, STR values for 1×NLS ranged from 15.7% (11/70) to 23.1% (18/78) at nymphal stages and from 17.5% (10/57) to 31.8% (20/63) at adult stages; 3×NLS ranged from 15.2% (7/46) to 34.1% (15/44) at nymphal stages and from 20.0% (8/41) to 38.5% (15/40) at adult stages (Fig. 2D and Table 1). By contrast, with 5×NLS we recovered no positive G_0 animals (0/68 at nymphal stages) (Fig. 2D and Table 1). We also noted that screening at nymphal stages underestimates STR values (Fig. 2D and Table 1), possibly because the eye color of the v^1 $xdh1^{\Delta 12}$ strain becomes progressively lighter with development (Fig. 1E–F and Supplementary Fig. 3).

To investigate whether this trend was conserved in another insect species, we injected the same series of *hyPBase* mRNAs with the same donor vector *pXL[9xP3-mScarlet-I-SV40T]* into embryos of the cricket *Gryllus bimaculatus* (Supplementary Fig. 4 and Supplementary Table 1). In contrast to our results from *O. fasciatus* (Fig. 2D and Table 1), we found no differences in efficiency across NLS copy number in *G. bimaculatus* (Supplementary Fig. 4 and Supplementary Table 1), although overall efficiency in *G. bimaculatus* was generally higher than in *O. fasciatus* (Table 1 and Supplementary Table 1). Together, these results indicate that incorporating 1× and 3×NLS into *hyPBase* mRNA may be a practical strategy to improve transgenesis efficiency in species where standard methods are inefficient.

To assess germ line transmission, we backcrossed mScarlet-I-positive G_0 *O. fasciatus* adults with v^1 $xdh1^{\Delta 12}$ adults of the opposite sex and counted the number of mScarlet-I-positive G_1 animals emerging from single pair matings (see Supplementary

bioRxiv preprint doi: https://doi.org/10.64898/2026.07.30.741915; this version posted November 9, 2026. The copyright holder for this preprint (which was not certified by peer review) is the author/funder, who has granted bioRxiv a license to display the preprint in perpetuity. It is made available under a CC-BY 4.0 International license.

Tables 2–4 for detailed results of individual crosses). In positive G_1 animals we detected mScarlet-I expression throughout the compound eyes and in the ocelli (Fig. 2E). G_1 germ line transformation efficiency (GTE) with 0×NLS *hyPBase* mRNA was 16.7% (1/6 crosses), whereas 1× and 3×NLS conditions provided approximate twofold enhancement, yielding 33.3% (9/27 crosses) and 35.0% (7/20 crosses) GTE, respectively (Fig. 2F and Supplementary Tables 2–4).

To determine whether the v^1 $xdh1^{\Delta 2}$ mutant background indeed facilitates the detection of mScarlet-I expression in the eyes, we compared mScarlet-I visibility between wild type and v^1 $xdh1^{\Delta 2}$ backgrounds. We found that mScarlet-I expression was visible throughout the eye in the v^1 $xdh1^{\Delta 2}$ background, whereas in the wild-type background the visible signal was restricted to a small, dot-like area at the center of the eye (Supplementary Fig. 5). These results confirm that the v^1 $xdh1^{\Delta 2}$ background enhances marker visibility.

Evaluation of a 9×P3-EGFP transgenesis marker in *O. fasciatus*

To expand the transgenesis toolkit in *O. fasciatus*, we next tested the donor plasmid *pXL[9×P3-EGFP-SV40T, attP]* (1,838 bp) carrying an EGFP transformation marker driven by the 9×P3 promoter and an attP site for future application of phiC31-mediated site-specific integration (Fig. 3A) (Groth et al., 2004). Two experimental replicates of injection with 3×NLS *hyPBase* mRNA resulted in 15.4% (10/65) and 9.3% (5/54) G_0 STR when screened at nymphal stages (Table 2). As with mScarlet-I expression, we observed EGFP expression in the compound eyes and in the ocelli (Fig. 3B). Among successful backcrosses (12 of 15 EGFP-positive G_0 animals) with animals of the opposite sex from the v^1 $xdh1^{\Delta 2}$ strain, we recovered EGFP-positive G_1 animals from each of five independent G_0 crosses (5/12 crosses; GTE = 41.7%) (Fig. 3C–D; see Supplementary

bioRxiv preprint doi: https://doi.org/10.64898/2026.07.30.741915; this version posted November 9, 2026. The copyright holder for this preprint (which was not certified by peer review) is the author/funder, who has granted bioRxiv a license to display the preprint in perpetuity. It is made available under a CC-BY 4.0 International license.

Table 5 for detailed results of individual crosses). We then crossed four G_1 adults with animals of the opposite sex of the *v*^{1} *xdh1*$^{\Delta 2}$ strain and found that three of these crosses showed >72.5% G_2 transgene inheritance rates, suggesting that the parent G_1 animals were likely to have more than one transgene (Supplementary Table 5). Using two G_2 animals from one of the crosses which showed a 50% inheritance rate, consistent with one insertion, we performed splinkerette PCR (Potter and Luo, 2010) and determined the transgene insertion site by sequencing the resulting PCR products, confirming genomic integration of the transgene (Supplementary Fig. 6).

Attempt to generate a histone-labelled and a membrane-labelled transgenic milkweed bug

Nuclear and plasma membrane markers are practical and useful tools for developmental biology (e.g. Benton et al., 2013; Karapidaki et al., 2026; Nakamura et al., 2010). To try to generate a transgenic strain with ubiquitously constitutively fluorescently labelled histones, we prepared the donor plasmid *pXL[Gbact-H2B-mScarlet3-SV40T]* (2,974 bp), in which H2B-mScarlet3 is driven by the previously characterized *Gryllus bimaculatus* actin promoter (*Gbact*) (Supplementary Fig. 7). This promoter can drive ubiquitous constitutive expression and has been widely used in the cricket community (Nakamura et al., 2010; Ohde et al., 2025; Zhang et al., 2002). We reasoned that, just as some *D. melanogaster* promoters retain their function in transgenic insects of other species (Bottino-Rojas and James, 2022), the cricket promoter might retain its function in another hemimetabolous insect. We injected the donor plasmid with 1×NLS *hyPBase* mRNA and screened approximately 100 hatched G_0 animals for mScarlet3 expression (Table 2). We obtained one animal displaying clear mScarlet3 expression through the integument across the whole body and backcrossed it with the *v*^{1} *xdh1*$^{\Delta 2}$ strain to

bioRxiv preprint doi: https://doi.org/10.64898/2026.07.30.741915; this version posted November 9, 2026. The copyright holder for this preprint (which was not certified by peer review) is the author/funder, who has granted bioRxiv a license to display the preprint in perpetuity. It is made available under a CC-BY 4.0 International license.

generate G_1 progeny. We found that 42.4% of G_1 animals (14/33) displayed the same mScarlet3 expression pattern as the G_0 parent (Supplementary Fig. 7 and Supplementary Table 6). We observed that nuclei with detectable mScarlet3 expression were located underneath epidermal cells, whereas nuclei in overlying epidermal cells did not express detectable mScarlet3 (Supplementary Fig. 7). When we dissected ovaries from G_1 adult females, we detected nuclear mScarlet3 expression in the ovariole muscle sheath but not in the tropharium or follicle cells (Supplementary Fig. 7). Similarly, we observed mScarlet3 expression in the testis muscle sheath, but not in sperm cells (Supplementary Fig. 7). These expression patterns suggest that the transgene may have integrated in the vicinity of a muscle-specific enhancer, resulting in enhancer trap-like expression driven by an endogenous regulatory element, rather than the ubiquitous constitutive expression driven by this *Gbact* promoter in other transgenic contexts (Nakamura et al., 2010). Importantly, this result also suggests that the *Gbact* promoter retains basal promoter activity in *O. fasciatus*, as it appears sufficient to support enhancer trap-mediated expression. We used splinkerette PCR to identify the transgene insertion site as being within an intron of an uncharacterized gene locus encoding a protein with a predicted transmembrane domain (Accession No. OFAS019046-RA; Supplementary Fig. 7).

We next aimed to generate a membrane-labelled transgenic strain using the GAP43 membrane localization tag, which has recently been shown to be broadly applicable across a wide variety of animals (Karapidaki et al., 2026). We prepared the donor plasmid *pXL[Gbact-GAP43-mScarlet3-SV40T, 9×P3-EGFP-SV40T]* (3,635 bp), in which membrane-tagged mScarlet3 and EGFP are driven by the *Gbact* and 9×P3 promoters, respectively (Supplementary Fig. 8). We injected this donor plasmid together with 1×NLS *hyPBase* mRNA and screened for EGFP expression in the eyes at

bioRxiv preprint doi: https://doi.org/10.64898/2026.07.30.741915; this version posted November 9, 2026. The copyright holder for this preprint (which was not certified by peer review) is the author/funder, who has granted bioRxiv a license to display the preprint in perpetuity. It is made available under a CC-BY 4.0 International license.

nymphal stages. Of 113 screened G_0 nymphs, 15 showed EGFP expression (STR = 13.3%) (Table 2). We backcrossed these 15 EGFP-positive G_0 animals with animals of the opposite sex from the *v*^{1} *xdh1*$^{\Delta 12}$ strain, and seven of the crosses successfully yielded G_1 progeny. Of these, three yielded EGFP-positive G_1 animals (GTE = 42.9%) (Supplementary Fig. 8 and Supplementary Table 7). However, we could not detect clear membrane-labelled expression of mScarlet3 in the ovary or testis of any G_1 progeny. We did, however, detect mScarlet3 expression in the eyes of G_1 adults (Supplementary Fig. 8), which we speculate is due to 9×P3 enhancer trapping within the transgene. Together, these results suggest that the *Gbact* promoter is active in *O. fasciatus* but may not be sufficient to drive ubiquitous expression.

Identification of a constitutive and ubiquitous promoter in *O. fasciatus*

To identify a promoter that would drive stable, constitutive, and ubiquitous expression in *O. fasciatus*, we focused on an endogenous actin promoter. Based on a BLAST search using *D. melanogaster* Actin 5c (Act5c; NP_001284915.1), we identified two orthologs in *O. fasciatus*, *Of-act5ca* (Accession No. OFAS010390-RA) and *Of-act5cb* (Accession No. OFAS010391-RA), which are annotated as tandem loci in the genome (Panfilio et al., 2019). We prepared the donor plasmid *pXL[Ofact-H2B-mScarlet3-SV40T]* (4,650 bp), in which H2B-mScarlet3 is driven by the 2.5 kb upstream of the *Of-act5ca* gene (Fig. 4A). Three experimental replicates of injection with 3×NLS *hyPBase* mRNA resulted in 73.8% (31/42), 82.2% (37/45), and 70.0% (56/80) G_0 STR respectively when screened at nymphal stages (Table 2). Some mScarlet3-positive G_0 animals showed mScarlet3 expression only as dots or patches on their bodies. However, a subset of G_0 animals exhibited mScarlet3 expression across more than 50% of their bodies from embryonic stages (Fig. 4B), which was maintained through nymphal stages. Specifically, 9.5%

bioRxiv preprint doi: https://doi.org/10.64898/2026.07.30.741915; this version posted November 9, 2026. The copyright holder for this preprint (which was not certified by peer review) is the author/funder, who has granted bioRxiv a license to display the preprint in perpetuity. It is made available under a CC-BY 4.0 International license.

(4/42), 15.5% (7/45), and 5.0% (4/80) of screened nymphs displayed mScarlet3 expression across more than 50% of their bodies (Table 2). We selected nine of these strongly expressing G_0 animals for backcrossing with animals of the opposite sex from the *v*^{1} *xdh1*$^{\Delta 2}$ strain, and seven of the crosses yielded G_1 progeny. Of these, three yielded mScarlet3-positive G_1 animals (GTE = 42.9%) (Supplementary Table 8) displaying ubiquitous mScarlet3 expression throughout the body (a representative image at the fifth nymphal stage is shown in Fig. 4C).

Having successfully established a ubiquitously expressing histone-labelled transgenic *O. fasciatus*, we asked whether the fluorescent signal could be visualized through the eggshell in live embryos. Visualizing embryogenesis in living animals through the thick, semi-opaque eggshell and optically occlusive yolk has been a challenge in previous studies of *O. fasciatus* (Auman and Chipman, 2018; Panfilio, 2009; Panfilio et al., 2006). We focused specifically on katatrepsis, an essential embryonic movement (Panfilio, 2008). We found that all nuclei of the developing embryo were easily visualized through the eggshell, allowing us to capture the entire process of katatrepsis and appendage elongation over 36 hours (Fig. 4D and Supplementary Videos 1–3).

Evidence for functionality of the Q system in *O. fasciatus*

To investigate whether this transgenesis method enables integration of large DNA payloads, we prepared the donor plasmid *pXL[Ofinv-QF2, 15×QUAS-mScarlet3, 9×P3-EGFP-SV40T]* (7,161 bp). This construct employs the Q system, a binary expression system composed of the transcriptional activator QF2 (a modified version of QF) and its binding site 15×QUAS (Potter et al., 2010; Riabinina et al., 2015) together with a 2.4 kb region upstream of the segment polarity gene *Of-invected* (*Of-inv*) (Accession No. OFAS025056), and the 9×P3 promoter-driven EGFP transformation

bioRxiv preprint doi: https://doi.org/10.64898/2026.07.30.741915; this version posted November 9, 2026. The copyright holder for this preprint (which was not certified by peer review) is the author/funder, who has granted bioRxiv a license to display the preprint in perpetuity. It is made available under a CC-BY 4.0 International license.

marker (Fig. 6A). We performed three independent injections of the donor plasmid together with 1×NLS *hyPBase* mRNA. Among the surviving G_0 nymphs, 50.0% (24/48), 26.1% (29/111), and 16.4% (18/110) showed mScarlet3 expression on their bodies at the nymphal instar stage (Table 2, Fig. 5B–F, and Supplementary Fig. 9). Notably, one of these 24 individuals displayed intense expression that partly appeared to align with thoracic segment boundaries. This individual also exhibited a segmental fusion phenotype (#1; Fig. 5B), which we speculate could be due to the strong activity of the *Of-inv* 2.4 kb regulatory region. At later nymphal stages, we observed strong mScarlet3 expression along the lateral edge of thoracic segments in a second individual (#2; Fig. 5C), broad mScarlet3 expression across the dorsal abdomen in a third (#3; Fig. 5D), and small patches and dots of expression in others (Supplementary Fig. 9). In individual #3 (Fig. 5D), clear segmental stripes of mScarlet3 expression were detected in the ventral abdomen (Fig. 5D), suggesting that *Of-inv* is expressed in post-embryonic development. Unfortunately, we did not achieve germ line transmission to the next generation, because animals with intense mScarlet3 expression died early and without producing progeny. To obtain information about whether the transgene had integrated into the genome despite this limitation, we performed splinkerette PCR on two G_0 individuals (#4; Fig. 5E; #5; Fig. 5F-G) . We detected multiple integration events in these individuals, indicating that our approach can mediate genomic integration of a large payload at least in G_0 animals.

bioRxiv preprint doi: https://doi.org/10.64898/2026.07.30.741915; this version posted November 9, 2026. The copyright holder for this preprint (which was not certified by peer review) is the author/funder, who has granted bioRxiv a license to display the preprint in perpetuity. It is made available under a CC-BY 4.0 International license.

Discussion

We have established a system for efficient *piggyBac*-mediated transgenesis in the milkweed bug *O. fasciatus*. We show that efficiency is improved by the incorporation of NLS sequences into the hyPBase transposase. We also created a double mutant strain that facilitates more efficient screening with fluorescent 9×P3-driven transformation markers. This efficient and practical system enabled us to introduce multiple transgenic constructs carrying expression cassettes ranging from 1.8 to 7.2 kb in size into the *O. fasciatus* genome. Furthermore, we demonstrated proof of principle feasibility of the Q system-mediated binary expression system, expanding the genetic toolkit available in *O. fasciatus*.

CRISPR-mediated mutagenesis enabled us to revisit a classic study for the first time in half a century. Lawrence (1970) reported eye- and body-color mutants induced by ethyl methanesulfonate (EMS) treatment during the golden age of *O. fasciatus* research. Based on the descriptions of the phenotypes of these mutants (1970) and other studies (Liu, 2016; Reding et al., 2023), we focused on manipulating genes belonging to the pteridine pathway to generate a body-color mutant, and successfully established the v^{1} $xdh1^{\Delta 12}$ double mutant strain showing body- and eye-color defects (Fig. 1). Although a recent study using RNAi-mediated functional analysis did not reveal a role for *xdh1* in eye-color formation (Reding et al., 2023), our results provide evidence that *xdh1* is involved in both body- and eye-color formation (Fig. 1). This discrepancy may be attributable to the often transient and incomplete nature of RNAi-mediated knockdown compared to a genomic loss-of-function allele. We further showed that both mScarlet-I and EGFP expressions can be detected through the eyes of the v^{1} $xdh1^{\Delta 12}$ strain (Figs. 2, 3). Importantly, we have maintained this strain for over two years under the same conditions as the wild type strain and have observed no obvious developmental defects.

bioRxiv preprint doi: https://doi.org/10.64898/2026.07.30.741915; this version posted November 9, 2026. The copyright holder for this preprint (which was not certified by peer review) is the author/funder, who has granted bioRxiv a license to display the preprint in perpetuity. It is made available under a CC-BY 4.0 International license.

As we have shown here, this strain is also used routinely for microinjection without noticeable problems. Together, these properties make the *v*^{1} *xdh1*$^{\Delta 12}$ strain useful for developing future methods for transgenesis and targeted genomic integration, including CRISPR/Cas9-based knock-in (Matsuoka et al., 2025).

Another key finding is that we enhanced the overall efficiency of *piggyBac*-mediated transgenesis in *O. fasciatus* by incorporating SV40T NLS sequences into hyPBase. We found that 1× and 3×NLS (but not 5×NLS) increased both average STR and GTE compared to 0×NLS in *O. fasciatus* (Fig. 2), even though *piggyBac* transposase itself carries an intrinsic nuclear localization signal (Keith et al., 2008). We therefore used 1× and 3×NLS *hyPBase* mRNA for the subsequent transgenesis experiments. Copy-number estimates from G_1 crossing experiments suggested that most transgenic lines generated with either 1× or 3×NLS *hyPBase* carried a single insertion (Supplementary Tables 5 and 7–8). The exception was the minimal donor plasmid *pXL[9×P3-EGFP-SV40T, attP]*, which led to multiple insertions (Supplementary Table 5). Since this plasmid is considerably smaller than the other transgenes and was tested only with 3×NLS *hyPBase*, we cannot distinguish the effect of NLS number from that of cargo size. Based on these results, either 1× or 3×NLS *hyPBase* can be used. We recommend 1×NLS *hyPBase* as a starting point, particularly when single-copy integration is desirable, with 3×NLS *hyPBase* as an alternative. A similar nuclear targeting approach may also be usefully applied to future phiC31-mediated site-specific integration in *O. fasciatus*, as a previous study demonstrated that the efficiency of phiC31 integrase is markedly improved by C-terminal incorporation of NLS in cultured mammalian cells (Andreas et al., 2002).

Interestingly, our results showed that 5×NLS completely abolished the transgenesis activity with no positive animals recovered, suggesting that an excessive

bioRxiv preprint doi: https://doi.org/10.64898/2026.07.30.741915; this version posted November 9, 2026. The copyright holder for this preprint (which was not certified by peer review) is the author/funder, who has granted bioRxiv a license to display the preprint in perpetuity. It is made available under a CC-BY 4.0 International license.

number of NLS may be detrimental to transposase function in *O. fasciatus*. By contrast, all NLS-tagged *hyPBase* mRNAs functioned equally efficiently in *G. bimaculatus* (Supplementary Fig. 4), indicating that this nuclear targeting approach did not provide additional benefit in this species. We speculate that this species-specific difference may reflect differences in the timing of cellularization and/or biochemical properties between the two species. It would be interesting for future studies to investigate species-specific activity profiles of NLS-tagged *hyPBase* mRNAs across a broad range of insect species.

Identifying a suitable endogenous promoter driving ubiquitous and constitutive expression can be challenging in non-traditional insect models. Here we found that a promoter (*Gbact*) that drives ubiquitous, constitutive expression in a cricket species (Nakamura et al., 2010) did not drive such expression in *O. fasciatus*. Instead, the cricket promoter appeared to drive tissue-specific expression patterns, possibly due to capture by an endogenous *O. fasciatus* enhancer (Supplementary Fig. 7). In this case, the *Gbact* promoter appeared to function as a basal promoter. Similarly, in the case of GAP43-mScarlet3 driven by *Gbact*, we observed no clear membrane signals in ovaries or testes across multiple insertions (Supplementary Fig. 7). Although we cannot formally exclude the possibility that these expression patterns reflect position effects at the specific insertion sites, the consistent absence of ubiquitous expression across multiple independent insertions suggests that the *Gbact* promoter itself may not drive sufficiently strong ubiquitous expression in *O. fasciatus* to overcome the influence of nearby *O. fasciatus* enhancers. This observation is similar to one reported previously for the beetle *Tribolium castaneum*, wherein species-specific promoters were required to drive the desired expression patterns in transgenic animals (Schinko et al., 2010). To address this challenge, we identified the endogenous *O. fasciatus Act5c* promoter as one able to drive ubiquitous, constitutive expression and used it to successfully establish multiple

bioRxiv preprint doi: https://doi.org/10.64898/2026.07.30.741915; this version posted November 9, 2026. The copyright holder for this preprint (which was not certified by peer review) is the author/funder, who has granted bioRxiv a license to display the preprint in perpetuity. It is made available under a CC-BY 4.0 International license.

422 histone-labelled transgenic strains (Fig. 4). Together, these transgenic strains and our
423 exploration of heterologous and endogenous promoters provide valuable genetic and
424 experimental resources for future work, facilitating comparative developmental studies in
425 *O. fasciatus*.

426 Finally, we tested the feasibility of the Q system, a binary expression system,
427 in *O. fasciatus* using a single-vector design, in which QF2 is driven by the 2.4-kb *Of-inv*
428 upstream region and 15×QUAS-mScarlet3 is placed downstream of a transcriptional
429 terminator (Fig. 5A). Across three independent injections, 16.4–50.0% of surviving G_0
430 nymphs showed mScarlet3 expression, including segmentally patterned signal consistent
431 with the expression of a segment polarity gene (Fig. 5B–F). Together with the detection
432 of integration events in G_0 individuals, these results indicate that a Q system-based
433 transgene cassette exceeding 7 kb can be integrated and can drive reporter expression in
434 *O. fasciatus*. This may provide a platform for amplifying and visualizing cis-regulatory
435 element activity in future studies. However, although the terminator is expected to
436 minimize transcriptional readthrough from the QF2 cassette, our single-vector design
437 cannot formally exclude the possibility that mScarlet3 expression arises from
438 transcriptional readthrough, or from direct activation of the reporter's minimal promoter
439 by the *Of-inv* regulatory region. Future work, including crossing QF2 driver and QUAS
440 reporter lines, will be needed to provide definitive validation. Notably, one of the G_0
441 nymphs we obtained with strong transgene expression exhibited a segmental fusion
442 phenotype (Fig. 5), which we speculate could be due to excessive *Of-inv* promoter
443 activity; this animal died before late nymphal stages. This could mean that maintaining
444 moderate transcriptional expression levels of some constructs may be important for
445 viability.

bioRxiv preprint doi: https://doi.org/10.64898/2026.07.30.741915; this version posted November 9, 2026. The copyright holder for this preprint (which was not certified by peer review) is the author/funder, who has granted bioRxiv a license to display the preprint in perpetuity. It is made available under a CC-BY 4.0 International license.

Taken together, our results have substantially expanded the functional genetic toolkit of *O. fasciatus* as a comparative model insect for Evo-Devo research. By combining a visibly light-colored mutant background, NLS-tagged hyPBase activity, and the Q system-based binary expression platform, we have established a versatile and practical framework for functional genetics in this species. These technological advances position *O. fasciatus* as an increasingly powerful system for addressing fundamental biological questions in development and evolution. Moreover, the nuclear targeting approach for improving overall transgenesis efficiency will offer a scalable framework that may benefit other non-model organisms, broadening the scope of comparative genetics in Evo-Devo studies beyond established model species.

bioRxiv preprint doi: https://doi.org/10.64898/2026.07.30.741915; this version posted November 9, 2026. The copyright holder for this preprint (which was not certified by peer review) is the author/funder, who has granted bioRxiv a license to display the preprint in perpetuity. It is made available under a CC-BY 4.0 International license.

Materials and Methods

Animal husbandry

Oncopeltus fasciatus was maintained on sunflower seeds at 28–30 °C and 60% relative humidity with 12L:12D as described previously (Ewen-Campen et al., 2011). v^1 mutant *O. fasciatus* were kindly provided by Katie Reding and Leslie Pick (University of Maryland, College Park, MD, USA). A *Gryllus bimaculatus* colony derived from the *gwhite* strain at Tokushima University (Niwa et al., 1997) was maintained on cat food (Purina) under identical environmental conditions.

Embryo microinjection

Injection needles were prepared by pulling glass capillaries (Cat#1B100-4, World Precision Instruments) with a Sutter P-97 Flaming/Brown micropipette puller. In *O. fasciatus*, eggs were collected within four hours after egg laying and injections were completed within two hours after egg collection. Two glass microscope slides were taped together with double-sided tape to create a ledge with exposed double-sided tape, against which embryos were aligned. Eggs were submerged in tap water for 20-40 minutes to reduce the inner pressure for ease of injection. Injected eggs were kept at 28 ℃. In *G. bimaculatus*, eggs were collected within two hours after egg laying and injection procedures were completed within two hours after egg collection. Eggs were aligned in injection plates with wells made of 2% agarose dissolved in MilliQ water. Injected eggs were kept at 28℃ until the desired stage.

CRISPR-Cas9-mediated targeted mutagenesis

bioRxiv preprint doi: https://doi.org/10.64898/2026.07.30.741915; this version posted November 9, 2026. The copyright holder for this preprint (which was not certified by peer review) is the author/funder, who has granted bioRxiv a license to display the preprint in perpetuity. It is made available under a CC-BY 4.0 International license.

Alt-R S.p. Cas9 Nuclease V3 (Cat# 1081059) and tracrRNA (Cat# 1072533) were chemically synthesized by Integrated DNA Technologies (IDT). *Of-xdh1* crRNA was designed to target the coding sequence using CRISPR Optimal Target Finder (Gratz et al., 2014). Synthetic crRNA was provided by IDT. Cas9 ribonucleoprotein complex (RNP) was prepared according to IDT instructions. Briefly, tracrRNA and crRNA were resuspended to 100 μM in Nuclease-Free Duplex Buffer (Cat# 11-01-03-01). 5 μl of each RNA were mixed, heated to 95℃ for five minutes, and allowed to cool to room temperature to form 50 μM gRNA duplex. 3 μl gRNA duplex and 2 μl Cas9 protein were mixed and incubated at room temperature for ten minutes to form Cas9/gRNA RNP at roughly 25 μM. Finally, RNP was diluted tenfold in 1×PBS with 0.05% phenol red.

Donor plasmid construction

The *pXL[Gbact-H2B-EGFP]* vector was kindly provided by Taro Nakamura (National Institute of Basic Biology, Okazaki, Japan) and used as a backbone vector for all *piggyBac*-mediated transgenesis in this study. The H2B CDS, derived from *G. bimaculatus*, was used as a nuclear marker. The plasmid encoding an insect codon-optimized variant of mScarlet-I, *pUC[9×P3-mScarlet-I-SV40T]*, was kindly provided by Takaaki Daimon (Kyoto University, Kyoto, Japan). Using these constructs, the donor plasmids *pXL[9×P3-mScarlet-I-SV40T]* and *pXL[9×P3-EGFP-SV40T, attP]* were assembled. To generate *pXL[Gbact-H2B-mScarlet3-SV40T]* and *pXL[Gbact-GAP43-mScarlet3-SV40T, 9×P3-EGFP-SV40T]*, the plasmid *5_T7-GAP43-mScarlet3* (Addgene #225932) was used in addition to the plasmids described above. To generate *pXL[Ofact-H2B-mScarlet3-SV40T]*, the 2.5 kb region upstream of *Of-act5ca* was amplified from *O. fasciatus* genomic DNA, and other

bioRxiv preprint doi: https://doi.org/10.64898/2026.07.30.741915; this version posted November 9, 2026. The copyright holder for this preprint (which was not certified by peer review) is the author/funder, who has granted bioRxiv a license to display the preprint in perpetuity. It is made available under a CC-BY 4.0 International license.

506 sequences were obtained from *pXL[Gbact-H2B-mScarlet3-SV40T]*. To generate
507 *pXL[Ofinv-QF2, 15×QUAS, 9×P3-EGFP]*, the 2.4 kb region upstream of *Of-inv* was
508 amplified from *O. fasciatus* genomic DNA, and QF2 and QUAS sequences were
509 obtained from plasmids *pBAC-DsRed-QF2-hsp70* (Addgene #104876) and
510 *PBAC-ECFP-15×QUAS_TATA-SV40* (Addgene #104875), respectively. Nucleotide
511 sequences of all donor plasmids are provided in Supplementary Data 1. For
512 microinjection, donor plasmids were diluted to 200 ng/ μ L in nuclease-free water.
513
514 **mRNA preparation**
515 The expression vector for mammalian codon-optimized hyPBase (*pCMV-hyPBase*)
516 (Yusa et al., 2011) was kindly provided by Takahiro Ohde (Kyoto University, Kyoto,
517 Japan). To generate *pCMV-3×NLS-hyPBase*, the backbone of *pCMV-hyPBase* was
518 linearized by inverse PCR using primers partially encoding the SV40 NLS. The
519 remaining NLS sequences were provided as annealed oligonucleotides, and the fragments
520 were assembled using the Gibson Assembly Cloning Kit (New England Biolabs,
521 Cat#E5510S), so that three tandem SV40 NLS repeats were fused to the N-terminus of
522 hyPBase. *pCMV-1×NLS-hyPBase* and *pCMV-5×NLS-hyPBase* were generated from
523 *pCMV-3×NLS-hyPBase* using the Q5 Site-Directed Mutagenesis Kit (New England
524 Biolabs, Cat#E0554S) according to the manufacturer's protocol. Amino acid sequences
525 of all hyPBase variants are provided in Supplementary Data 2, and the primers and
526 oligonucleotides used are listed in Supplementary Table 9. For *hyPBase* mRNA
527 synthesis, the plasmids were linearized with BbsI (New England Biolabs, Cat#R0539S),
528 and capped mRNA was transcribed using the mMESSAGE mMACHINE T7
529 Transcription kit (Thermo Fisher Scientific, Cat#AM1344), followed by lithium
530 chloride purification. The concentration of purified mRNA was determined by

bioRxiv preprint doi: https://doi.org/10.64898/2026.07.30.741915; this version posted November 9, 2026. The copyright holder for this preprint (which was not certified by peer review) is the author/funder, who has granted bioRxiv a license to display the preprint in perpetuity. It is made available under a CC-BY 4.0 International license.

measuring absorbance at 260 nm using a NanoDrop Eight spectrophotometer (Thermo Fisher Scientific). For microinjection, purified mRNAs were diluted to 400 ng/μL in nuclease-free water.

Genomic DNA extraction and genotyping

For genotyping, genomic DNA was extracted from a single leg of animals. Legs were homogenized in squish buffer (10 mM Tris-HCl pH 7.5, 1 mM EDTA, 25 mM NaCl, 200 μg/ml Proteinase K), incubated at 60℃ for two hours, and then at 95℃ for three minutes to inactivate Proteinase K. Genomic PCR was performed using Phusion HF DNA polymerase (New England Biolabs Cat#M0530L). Targeted mutagenesis was detected using the Alt-R Genome Editing Detection Kit (IDT, Cat#1075932), and fixed alleles were confirmed by Sanger sequencing. For splinkerette PCR, genomic DNA was prepared using the DNeasy & Tissue kit (QIAGEN, Cat#69506).

Splinkerette PCR

Genomic DNA was extracted from two G_2 animals carrying *9×P3-EGFP-SV40T*, *attP*, two G_2 animals carrying *Gbact-H2B-mScarlet3-SV40T*, and two G_0 animals showing mScarlet3 expression from *Ofinv-QF2, 15×QUAS-mScarlet3*, *9×P3-EGFP-SV40T*. Extracted genomic DNA was digested with BstYI (New England Biolabs, Cat#R0523S), followed by self-ligations. Two rounds of splinkerette PCR were performed using KOD-One (TOYOBO, Cat#KMM-101NV). All procedures for splinkerette PCR were performed as described previously (Potter and Luo, 2010). For G_2 animals, the PCR products were purified and directly sequenced by Sanger sequencing. For G_0 animals, since the PCR products yielded faint, smeared bands, they

bioRxiv preprint doi: https://doi.org/10.64898/2026.07.30.741915; this version posted November 9, 2026. The copyright holder for this preprint (which was not certified by peer review) is the author/funder, who has granted bioRxiv a license to display the preprint in perpetuity. It is made available under a CC-BY 4.0 International license.

were cloned into the pGEM-T easy Vector (Promega, Cat#A1360). Primers are listed in Supplementary Table S9.

Screening transgenic animals

Animals were anesthetized with CO_2 and screened for fluorescence using a Zeiss Axio Zoom V16 stereomicroscope. Images were captured using a Zeiss Axical 512 color camera or HAMAMATSU C11440-22CU digital camera.

Nuclear and F-actin staining

Ovaries were dissected from transgenic G_1 adults and fixed with 4% formaldehyde in 1× PBS for 30 minutes at room temperature, followed by three washes with PBT (1× PBS with 0.1% Triton X-100). Samples were incubated with 5 ng/µl Hoechst 33342 and Alexa Fluor 488-phalloidin (1:200; Thermo Fisher Scientific, Cat#A12379) in PBT at room temperature for one hour or at 4℃ overnight. Samples were washed four times over one hour with PBT. After washing, samples were mounted in 100% glycerol. Images were taken using a Nikon CSU-W1 spinning disk inverted confocal microscope.

Live imaging

Appropriately staged eggs were collected under a Zeiss Axio Zoom V16 stereomicroscope and attached to a standard 90 mm polystyrene Petri dish using heptane glue. Live imaging was performed on a Nikon CSU-W1 spinning disk inverted confocal microscope with 10× air objective at 29□. Image stacks comprising approximately 40 optical sections (4 µm z-steps) were taken at 10 minute intervals.

Use of artificial intelligence tools

bioRxiv preprint doi: https://doi.org/10.64898/2026.07.30.741915; this version posted November 9, 2026. The copyright holder for this preprint (which was not certified by peer review) is the author/funder, who has granted bioRxiv a license to display the preprint in perpetuity. It is made available under a CC-BY 4.0 International license.

The authors used ChatGPT (OpenAI) and Claude (Anthropic) to improve the clarity and readability of the text. All authors reviewed and edited all output and take responsibility for all content. No AI tools were used to generate original data, results, or scientific content.

Acknowledgements

We thank Tarun Kumar and Daniella Haber for helping with animal husbandry, Suhrid Ghosh for assistance with live imaging, and all members of the Extavour lab for discussion. Y.S. is supported by the Human Frontier Science Program (HFSP) Fellowship LT0048/2025-L (DOI: https://doi.org/10.52044/HFSP.LT00482025-L.pc.gr.231571). Y.S. was a Japan Society for the Promotion of Science (JSPS) Overseas Research Fellow. This study was supported by NSF award IOS-2220747, NIH award 1R01GM143611, and funds from the Howard Hughes Medical Institute (HHMI) to C.G.E., who is an HHMI investigator.

Author contributions

Conceptualization: Y.S.; Methodology: Y.S.; Validation: Y.S.; Formal analysis: Y.S.; Investigation: Y.S., Y.H., A.W., J.A.K.; Resources: Y.S., Y.H., A.W., J.A.K.; Data curation: Y.S.; Writing - original draft: Y.S.; Writing - review & editing: Y.S., Y.H., A.W., J.A.K., C.G.E.; Visualization: Y.S.: Supervision: Y.S., C.G.E.; Project administration: Y.S., C.G.E.; Funding acquisition: Y.S., C.G.E.

Data and resource availability

All data and resources in this paper will be shared upon request.

bioRxiv preprint doi: https://doi.org/10.64898/2026.07.30.741915; this version posted November 9, 2026. The copyright holder for this preprint (which was not certified by peer review) is the author/funder, who has granted bioRxiv a license to display the preprint in perpetuity. It is made available under a CC-BY 4.0 International license.

Disclosures

The authors declare no competing or financial interests.

bioRxiv preprint doi: https://doi.org/10.64898/2026.07.30.741915; this version posted November 9, 2026. The copyright holder for this preprint (which was not certified by peer review) is the author/funder, who has granted bioRxiv a license to display the preprint in perpetuity. It is made available under a CC-BY 4.0 International license.

References

Andreas, S., Schwenk, F., Küter-Luks, B., Faust, N. and Kühn, R. (2002). Enhanced efficiency through nuclear localization signal fusion on phage phiC31-integrase: activity comparison with Cre and FLPe recombinase in mammalian cells. *Nucleic Acids Res.* **30**, 2299–2306.

Angelini, D. R. and Kaufman, T. C. (2005). Functional analyses in the milkweed bug Oncopeltus fasciatus (Hemiptera) support a role for Wnt signaling in body segmentation but not appendage development. *Dev Biol* **283**, 409–423.

Angelini, D. R., Liu, P. Z., Hughes, C. L. and Kaufman, T. C. (2005). Hox gene function and interaction in the milkweed bug Oncopeltus fasciatus (Hemiptera). *Dev Biol* **287**, 440–455.

Auman, T. and Chipman, A. D. (2018). Growth zone segmentation in the milkweed bug Oncopeltus fasciatus sheds light on the evolution of insect segmentation. *BMC Evol. Biol.* **18**, 178.

Benton, M. A., Akam, M. and Pavlopoulos, A. (2013). Cell and tissue dynamics during Tribolium embryogenesis revealed by versatile fluorescence labeling approaches. *Development* **140**, 3210–3220.

Berghammer, A. J., Klingler, M. and Wimmer, E. A. (1999). A universal marker for transgenic insects. *Nature* **402**, 370–371.

bioRxiv preprint doi: https://doi.org/10.64898/2026.07.30.741915; this version posted November 9, 2026. The copyright holder for this preprint (which was not certified by peer review) is the author/funder, who has granted bioRxiv a license to display the preprint in perpetuity. It is made available under a CC-BY 4.0 International license.

628 **Bottino-Rojas, V. and James, A. A.** (2022). Use of Insect Promoters in Genetic
629 Engineering to Control Mosquito-Borne Diseases. *Biomolecules* **13**, 16.

630 **Butt, F. H.** (1949). Embryology of the Milkweed Bug, Oncopeltus fasciatus
631 (Hemiptera). *Cornell Experiment Station Memoir* 3–43.

632 **Chen, X. and Palli, S. R.** (2021). Hyperactive piggyBac Transposase-mediated
633 Germline Transformation in the Fall Armyworm, Spodoptera frugiperda. *J. Vis.*
634 *Exp. : JoVE.*

635 **Chipman, A. D.** (2017). Oncopeltus fasciatus as an evo devo research organism.
636 *genesis* **55**, e23020.

637 **Clark, E., Peel, A. D. and Akam, M.** (2019). Arthropod segmentation. *Development*
638 **146**, dev170480.

639 **Donoughe, S. and Extavour, C. G.** (2016). Embryonic development of the cricket
640 Gryllus bimaculatus. *Dev. Biol.* **411**, 140–156.

641 **Eckermann, K. N., Ahmed, H. M. M., KaramiNejadRanjbar, M., Dippel, S.,**
642 **Ogaugwu, C. E., Kitzmann, P., Isah, M. D. and Wimmer, E. A.** (2018).
643 Hyperactive piggyBac transposase improves transformation efficiency in diverse
644 insect species. *Insect Biochem. Mol. Biol.* **98**, 16–24.

645 **Ewen-Campen, B., Shaner, N., Panfilio, K. A., Suzuki, Y., Roth, S. and Extavour,**
646 **C. G.** (2011). The maternal and early embryonic transcriptome of the milkweed bug
647 Oncopeltus fasciatus. *BMC Genomics* **12**, 61.

bioRxiv preprint doi: https://doi.org/10.64898/2026.07.30.741915; this version posted November 9, 2026. The copyright holder for this preprint (which was not certified by peer review) is the author/funder, who has granted bioRxiv a license to display the preprint in perpetuity. It is made available under a CC-BY 4.0 International license.

Feir, D. (1974). Oncopeltus Fasciatus: A Research Animal. *Annu. Rev. Èntomol.* **19**, 81–96.

Gonzalez-Sqalli, E., Caron, M. and Loppin, B. (2024). The white gene as a transgenesis marker for the cricket Gryllus bimaculatus. *G3: Genes, Genomes, Genet.* **14**, jkae235.

Gratz, S. J., Ukken, F. P., Rubinstein, C. D., Thiede, G., Donohue, L. K., Cummings, A. M. and O'Connor-Giles, K. M. (2014). Highly Specific and Efficient CRISPR/Cas9-Catalyzed Homology-Directed Repair in Drosophila. *Genetics* **196**, 961–971.

Gregory, M., Alphey, L., Morrison, N. I. and Shimeld, S. M. (2016). Insect transformation with piggyBac: getting the number of injections just right. *Insect Mol Biol* **25**, 259–271.

Groth, A. C., Fish, M., Nusse, R. and Calos, M. P. (2004). Construction of Transgenic Drosophila by Using the Site-Specific Integrase From Phage φC31. *Genetics* **166**, 1775–1782.

Gudmunds, E., Wheat, C. W., Khila, A. and Husby, A. (2022). Functional genomic tools for emerging model species. *Trends Ecol Evol* **37**, 1104–1115.

Handler, A. M. (2002). Use of the piggyBac transposon for germ-line transformation of insects. *Insect Biochem Molec* **32**, 1211–1220.

Hart, T., Frank, D. D., Lopes, L. E., Olivos-Cisneros, L., Lacy, K. D., Trible, W., Ritger, A., Valdés-Rodríguez, S. and Kronauer, D. J. C. (2023). Sparse and

bioRxiv preprint doi: https://doi.org/10.64898/2026.07.30.741915; this version posted November 9, 2026. The copyright holder for this preprint (which was not certified by peer review) is the author/funder, who has granted bioRxiv a license to display the preprint in perpetuity. It is made available under a CC-BY 4.0 International license.

669 stereotyped encoding implicates a core glomerulus for ant alarm behavior. *Cell* **186**,
670 3079-3094.e17.

671 **Heryanto, C., Mazo-Vargas, A. and Martin, A.** (2022). Efficient hyperactive
672 piggyBac transgenesis in Plodia pantry moths. *Front. Genome Ed.* **4**, 1074888.

673 **Horn, C. and Wimmer, E. A.** (2000). A versatile vector set for animal transgenesis.
674 *Dev Genes Evol* **210**, 630–637.

675 **Horn, C., Jaunich, B. and Wimmer, E. A.** (2000). Highly sensitive, fluorescent
676 transformation marker for Drosophila transgenesis. *Dev. Genes Evol.* **210**, 623–629.

677 **Inada, K., Ohde, T. and Daimon, T.** (2025). Efficient transgenic system for the
678 firebrat Thermobia domestica utilizing hyPBase and G0 founder prescreening. *Gene*
679 **955**, 149449.

680 **Kalderon, D., Roberts, B. L., Richardson, W. D. and Smith, A. E.** (1984). A short
681 amino acid sequence able to specify nuclear location. *Cell* **39**, 499–509.

682 **Kao, J. A., Rivard, E. L., Kapoor, R. R. and Extavour, C. G.** (2026). The dynamic
683 evolution of panarthropod germ cell specification mechanisms. *Development* **153**,
684 dev205168.

685 **Karapidaki, I., Handberg-Thorsager, M., Momose, T., Yasuo, H., Genikhovich, G.,**
686 **Assaf, S., Deleau, C., Pang, Y., Pavlich, C., Lohmann, B., et al.** (2026). Targeting
687 the cell membrane in established and emerging model organisms. *Development* **153**,.

bioRxiv preprint doi: https://doi.org/10.64898/2026.07.30.741915; this version posted November 9, 2026. The copyright holder for this preprint (which was not certified by peer review) is the author/funder, who has granted bioRxiv a license to display the preprint in perpetuity. It is made available under a CC-BY 4.0 International license.

688 **Keith, T. P., Riley, M. A., Kreitman, M., Lewontin, R. C., Curtis, D. and**
689 **Chambers, G.** (1987). Sequence of the Structural Gene for Xanthine Dehydrogenase
690 (rosy Locus) in Drosophila melanogaster. *Genetics* **116**, 67–73.

691 **Keith, J. H., Fraser, T. S. and Fraser, M. J.** (2008). Analysis of the piggyBac
692 transposase reveals a functional nuclear targeting signal in the 94 c-terminal
693 residues. *BMC Mol. Biol.* **9**, 72–72.

694 **Kelly, T. J. and Telfer, W. H.** (1979). The function of the follicular epithelium in
695 vitellogenic Oncopeltus follicles. *Tissue Cell* **11**, 663–672.

696 **Kou, Z., Luo, X., Jiang, Y., Chen, B., Song, Y., Wang, Y., Xu, J., Tomberlin, J. K.**
697 **and Huang, Y.** (2023). Establishment of highly efficient transgenic system for black
698 soldier fly (Hermetia illucens). *Insect Sci.* **30**, 888–900.

699 **Lawrence, P. A.** (1970). Some new mutants of the Large Milkweed Bug Oncopeltus
700 fasciatus Dall. *Genet. Res.* **15**, 347–350.

701 **Liu, J.** (2016). Unraveling the molecular mechanisms of aposematic pigmentation in
702 Oncopeltus fasciatus.

703 **Liu, P. Z. and Kaufman, T. C.** (2004a). hunchback is required for suppression of
704 abdominal identity, and for proper germband growth and segmentation in the
705 intermediate germband insect Oncopeltus fasciatus. *Development* **131**, 1515–1527.

706 **Liu, P. Z. and Kaufman, T. C.** (2004b). Kru□ppel is a gap gene in the intermediate
707 germband insect Oncopeltus fasciatus and is required for development of both
708 blastoderm and germband-derived segments. *Development* **131**, 4567–4579.

bioRxiv preprint doi: https://doi.org/10.64898/2026.07.30.741915; this version posted November 9, 2026. The copyright holder for this preprint (which was not certified by peer review) is the author/funder, who has granted bioRxiv a license to display the preprint in perpetuity. It is made available under a CC-BY 4.0 International license.

Liu, P. Z. and Kaufman, T. C. (2005). even-skipped is not a pair-rule gene but has segmental and gap-like functions in Oncopeltus fasciatus, an intermediate germband insect. *Development* **132**, 2081–2092.

Liu, P. Z. and Patel, N. H. (2009). Segmentation in the intermediate germband insect, Oncopeltus fasciatus. *Dev Biol* **331**, 456–457.

Liu, P. Z. and Patel, N. H. (2010). giant is a bona fide gap gene in the intermediate germband insect, Oncopeltus fasciatus. *Development* **137**, 835–844.

Matsuoka, Y., Nakamura, T., Watanabe, T., Barnett, A. A., Tomonari, S., Ylla, G., Whittle, C. A., Noji, S., Mito, T. and Extavour, C. G. (2025). Establishment of CRISPR/Cas9-based knock-in in a hemimetabolous insect: targeted gene tagging in the cricket Gryllus bimaculatus. *Dev. (Camb., Engl.)* **152**, dev199746.

Misof, B., Liu, S., Meusemann, K., Peters, R. S., Donath, A., Mayer, C., Frandsen, P. B., Ware, J., Flouri, T., Beutel, R. G., et al. (2014). Phylogenomics resolves the timing and pattern of insect evolution. *Science* **346**, 763–767.

Nakamura, T., Yoshizaki, M., Ogawa, S., Okamoto, H., Shinmyo, Y., Bando, T., Ohuchi, H., Noji, S. and Mito, T. (2010). Imaging of Transgenic Cricket Embryos Reveals Cell Movements Consistent with a Syncytial Patterning Mechanism. *Curr Biol* **20**, 1641–1647.

Niwa, N., Saitoh, M., Ohuchi, H., Yoshioka, H. and Noji, S. (1997). Correlation between Distal-less Expression Patterns and Structures of Appendages in Development of the Two-Spotted Cricket, Gryllus bimaculatus. *Zool Sci* **14**, 115–125.

bioRxiv preprint doi: https://doi.org/10.64898/2026.07.30.741915; this version posted November 9, 2026. The copyright holder for this preprint (which was not certified by peer review) is the author/funder, who has granted bioRxiv a license to display the preprint in perpetuity. It is made available under a CC-BY 4.0 International license.

Ohde, T., Nakamura, T., Mito, T. and Daimon, T. (2025). Highly efficient hyPBase-mediated transgenesis facilitates gain-of-function analysis in the cricket Gryllus bimaculatus. *Insect Biochem. Mol. Biol.* **184**, 104405.

Otte, M., Netschitailo, O., Kaftanoglu, O., Wang, Y., Page, R. E. and Beye, M. (2018). Improving genetic transformation rates in honeybees. *Sci. Rep.* **8**, 16534.

Panfilio, K. A. (2008). Extraembryonic development in insects and the acrobatics of blastokinesis. *Dev. Biol.* **313**, 471–491.

Panfilio, K. A. (2009). Late extraembryonic morphogenesis and its zen RNAi -induced failure in the milkweed bug Oncopeltus fasciatus. *Dev Biol* **333**, 297–311.

Panfilio, K. A., Liu, P. Z., Akam, M. and Kaufman, T. C. (2006). Oncopeltus fasciatus zen is essential for serosal tissue function in katatrepsis. *Dev. Biol.* **292**, 226–243.

Panfilio, K. A., Jentzsch, I. M. V., Benoit, J. B., Erezyilmaz, D., Suzuki, Y., Colella, S., Robertson, H. M., Poelchau, M. F., Waterhouse, R. M., Ioannidis, P., et al. (2019). Molecular evolutionary trends and feeding ecology diversification in the Hemiptera, anchored by the milkweed bug genome. *Genome Biol.* **20**, 64.

Potter, C. J. and Luo, L. (2010). Splinkerette PCR for mapping transposable elements in Drosophila. *PloS one* **5**, e10168.

Potter, C. J., Tasic, B., Russler, E. V., Liang, L. and Luo, L. (2010). The Q System: A Repressible Binary System for Transgene Expression, Lineage Tracing, and Mosaic Analysis. *Cell* **141**, 536–548.

bioRxiv preprint doi: https://doi.org/10.64898/2026.07.30.741915; this version posted November 9, 2026. The copyright holder for this preprint (which was not certified by peer review) is the author/funder, who has granted bioRxiv a license to display the preprint in perpetuity. It is made available under a CC-BY 4.0 International license.

Reding, K. and Pick, L. (2020). High-Efficiency CRISPR/Cas9 Mutagenesis of the white Gene in the Milkweed Bug Oncopeltus fasciatus. *Genetics* **215**, 1027–1037.

Reding, K., Lê, M. and Pick, L. (2023). Genome editing of the vermilion locus generates a visible eye color marker for Oncopeltus fasciatus. *Sci. Rep.* **13**, 4188.

Riabinina, O., Luginbuhl, D., Marr, E., Liu, S., Wu, M. N., Luo, L. and Potter, C. J. (2015). Improved and expanded Q-system reagents for genetic manipulations. *Nat. Methods* **12**, 219–222.

Schindelin, J., Arganda-Carreras, I., Frise, E., Kaynig, V., Longair, M., Pietzsch, T., Preibisch, S., Rueden, C., Saalfeld, S., Schmid, B., et al. (2012). Fiji: an open-source platform for biological-image analysis. *Nat. Methods* **9**, 676–82.

Schinko, J. B., Weber, M., Viktorinova, I., Kiupakis, A., Averof, M., Klingler, M., Wimmer, E. A. and Bucher, G. (2010). Functionality of the GAL4/UAS system in Tribolium requires the use of endogenous core promoters. *Bmc Dev Biol* **10**, 53.

Schreiner, B. (1977). Vitellogenesis in the milkweed bug, Oncopeltus fasciatus Dallas (Hemiptera). A light and electron microscopic investigation. *J Morphol* **151**, 35–79.

Sheng, G., Thouvenot, E., Schmucker, D., Wilson, D. S. and Desplan, C. (1997). Direct regulation of rhodopsin 1 by Pax-6/eyeless in Drosophila: evidence for a conserved function in photoreceptors. *Genes Dev.* **11**, 1122–1131.

Shirai, Y., Kao, J. A., Kumar, T., Matsuda, N., Nakagawa, R., Nureki, O., Extavour, C. G. and Daimon, T. (2026). HUH-tagged Cas9 as a platform for

bioRxiv preprint doi: https://doi.org/10.64898/2026.07.30.741915; this version posted November 9, 2026. The copyright holder for this preprint (which was not certified by peer review) is the author/funder, who has granted bioRxiv a license to display the preprint in perpetuity. It is made available under a CC-BY 4.0 International license.

efficient ssODN-mediated knock-in via embryo and adult injection in insects. *Commun. Biol.* **9**, 514.

Stork, N. E. (2017). How Many Species of Insects and Other Terrestrial Arthropods Are There on Earth? *Annu. Rev. Entomol.* **63**, 1–15.

Truman, J. W., Suzuki, Y. and Riddiford, L. M. (2026). Juvenile Hormone and the Evolution of Insect Metamorphosis. *Integr. Comp. Biol.* **66**, icag053.

Yusa, K., Zhou, L., Li, M. A., Bradley, A. and Craig, N. L. (2011). A hyperactive piggyBac transposase for mammalian applications. *Proc. Natl. Acad. Sci.* **108**, 1531–1536.

Zhang, H., Shinmyo, Y., Hirose, A., Mito, T., Inoue, Y., Ohuchi, H., Loukeris, T. G., Eggleston, P. and Noji, S. (2002). Extrachromosomal transposition of the transposable element Minos in embryos of the cricket Gryllus bimaculatus. *Dev Growth Differ* **44**, 409–417.

bioRxiv preprint doi: https://doi.org/10.64898/2026.07.30.741915; this version posted November 9, 2026. The copyright holder for this preprint (which was not certified by peer review) is the author/funder, who has granted bioRxiv a license to display the preprint in perpetuity. It is made available under a CC-BY 4.0 International license.

Figure Legends

Figure 1. Establishment of a useful double mutant strain in *O. fasciatus*. (A) *Of*-xdh1 predicted protein structure. The N-terminal orange square indicates the gRNA target site. Protein domains were predicted using InterProScan. FAD, flavin adenine dinucleotide. (B) Schematic of the experimental workflow and genetic crosses performed to establish the homozygous *xdh1* mutant strain. (C) Representative images of wild type (WT) and *xdh1* G_0 mutant hatchlings (dorsal view). Scale bar, 500 μm. (D) gRNA target site and mutant allele of *xdh1*. (E) Representative images of nymphs (dorsal view) and close-up views of eye coloration (dorsal view) in WT, v^1, $xdh1^{\Delta 2}$, and v^1 $xdh1^{\Delta 2}$. Arrowheads indicate eye color. Black scale bar, 3 mm; white scale bar, 1 mm. (F) Representative images of adults (lateral view) and close-up views of eye coloration (ventral view) in WT, v^1, $xdh1^{\Delta 2}$, and v^1 $xdh1^{\Delta 2}$. Arrowheads indicate eye color. Black scale bar, 3 mm; white scale bar, 1 mm. Anterior is up in (C), (E), and (F).

Figure 2. Investigation of a nuclear targeting approach for hyPBase-mediated transgenesis in *O. fasciatus*. (A) Schematic of the experiments to identify G_0 mScarlet-I-positive animals and establish stable transgenic lines. (B) Schematic of the *piggyBac* donor vector *pXL[9×P3-mScarlet-I-SV40T]* and *hyPBase* mRNA carrying 0×, 1×, 3×, or 5×NLS. (C) Representative images of G_0 mScarlet-I-positive adults. Scale bar, 1 mm. (D) Mean G_0 somatic transformation rate (STR) across *hyPBase* mRNA carrying 0×, 1×, 3×, or 5×NLS. Each dot represents an independent injection experiment. (E) Representative images of G_1 mScarlet-I-positive nymphs and adults. Arrowheads indicate eyes. Scale bar, 1 mm. (F) Mean G_1 germ line transformation efficiency (GTE). The height of each bar represents the mean proportion of mScarlet-I-positive animals

bioRxiv preprint doi: https://doi.org/10.64898/2026.07.30.741915; this version posted November 9, 2026. The copyright holder for this preprint (which was not certified by peer review) is the author/funder, who has granted bioRxiv a license to display the preprint in perpetuity. It is made available under a CC-BY 4.0 International license.

among G_1 progeny from an individual cross. Each dot represents an individual backcross that yielded G_1 progeny. Red numbers indicate the number of crosses yielding heritable mutant alleles and the corresponding percentages.

Figure 3. Establishment of multiple attP strains using 3×NLS *hyPBase* in *O. fasciatus*. (A) Schematic of the *piggyBac* donor vector *pXL[9×P3-EGFP-SV40T, attP]* and *hyPBase* mRNA carrying 3×NLS. (B) Representative images of G_0 EGFP-positive adults. Arrowheads indicate eyes. Scale bar, 1 mm. (C) Representative images of G_1 EGFP-positive adults. Arrowheads indicate eyes. Scale bar, 1 mm. (D) G_1 germ line transformation efficiency (GTE). Each bar represents the proportion of EGFP-positive animals among G_1 progeny from an individual cross. Each dot represents an individual backcross that yielded G_1 progeny. Green numbers indicate the number of crosses yielding heritable transgenes and the corresponding percentages.

Figure 4. Establishment of the ubiquitous histone-labelled strain using 3×NLS *hyPBase* in *O. fasciatus*. (A) Schematic of the *piggyBac* donor vector *pXL[Ofact-H2B-mScarlet3-SV40T]* and *hyPBase* mRNA carrying 3×NLS. (B) Representative images of G_0 mScarlet3-positive adults (lateral view). Anterior is to the right. Scale bar, 300 μm. (C) Representative images of G_1 mScarlet3-positive nymphs (dorsal view). Anterior is up. Scale bar, 3 mm. (D) Time series of embryonic development of mScarlet3-positive G_2 animal (ventral view), visualized with the "Green Fire Blue" relative intensity lookup table in Fiji (Schindelin et al., 2012). Maximum-intensity projections of a ventro-lateral view of the same embryo are timed relative to the first time point shown at the far left (0 min). Anterior is up. Scale bar, 100 μm.

bioRxiv preprint doi: https://doi.org/10.64898/2026.07.30.741915; this version posted November 9, 2026. The copyright holder for this preprint (which was not certified by peer review) is the author/funder, who has granted bioRxiv a license to display the preprint in perpetuity. It is made available under a CC-BY 4.0 International license.

Figure 5. Proof of principle of the Q system using 1×NLS *hyPBase* in *O. fasciatus*.

(A) Schematic of the *piggyBac* donor vector *pXL[Ofinv-QF2, 15×QUAS-mScarlet3-SV40T, 9×P3-EGFP-SV40T]* and *hyPBase* mRNA carrying 1×NLS. (B–F) Representative images of G_0 mScarlet3-positive nymphs. Yellow arrow indicates the putative segmentation defect. Yellow arrowheads indicate the segmentally iterated abdominal expression of mScarlet3. Scale bars, 500 μm (B) and 1 mm (C–F). Anterior is up in (B–F). White asterisks in (E) indicate where legs were removed to improvevisibility of mScarlet3 expression. (G) Schematic of the splinkerette PCR procedure in G_0 individuals. (H) Sequences of the junctions between the transgene and the flanking genomic DNA, determined by splinkerette PCR in G_0 individuals.

bioRxiv preprint doi: https://doi.org/10.64898/2026.07.30.741915; this version posted November 9, 2026. The copyright holder for this preprint (which was not certified by peer review) is the author/funder, who has granted bioRxiv a license to display the preprint in perpetuity. It is made available under a CC-BY 4.0 International license.

Figures

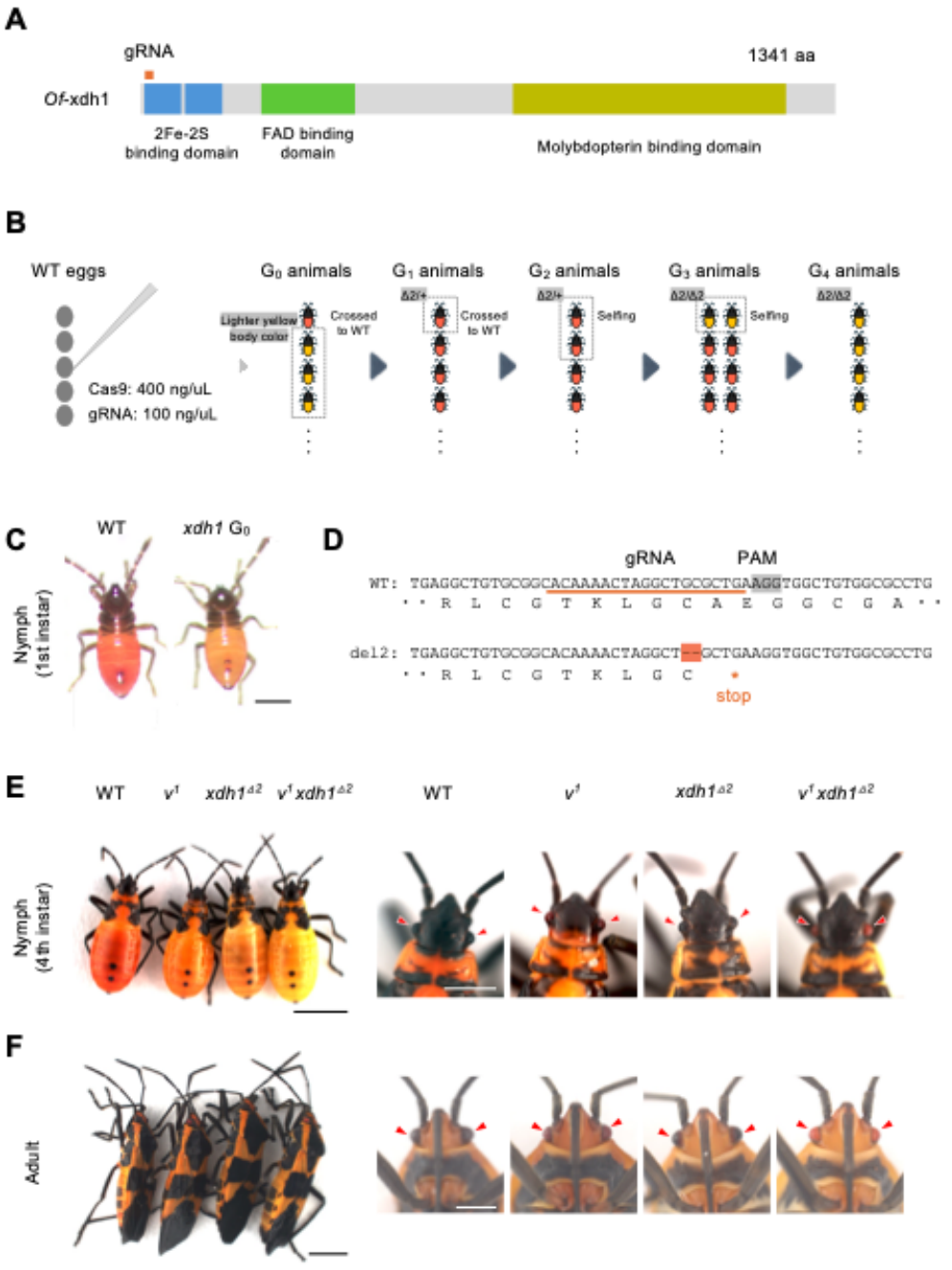
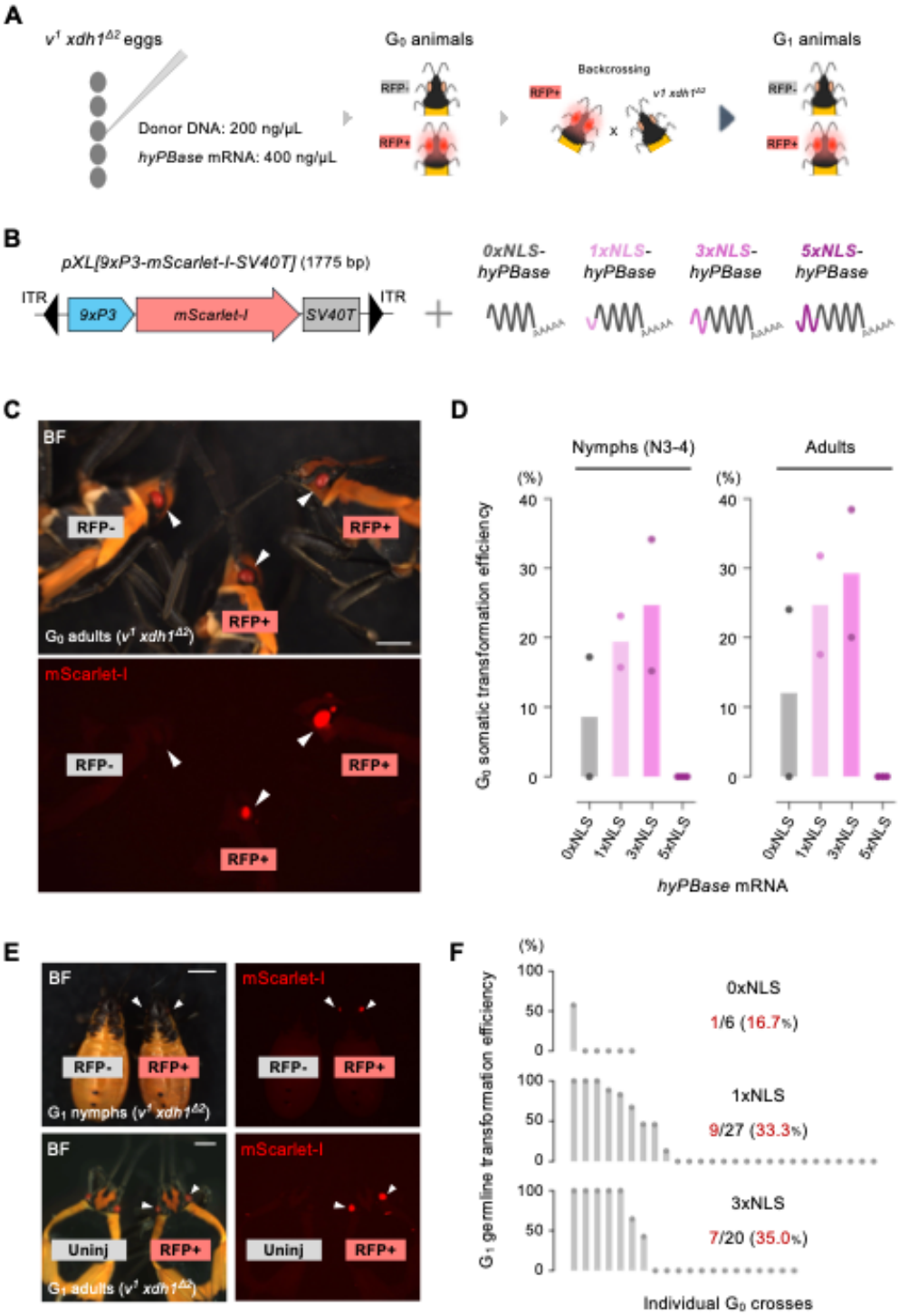


Figure 1. Establishment of a useful double mutant strain in *O. fasciatus*.

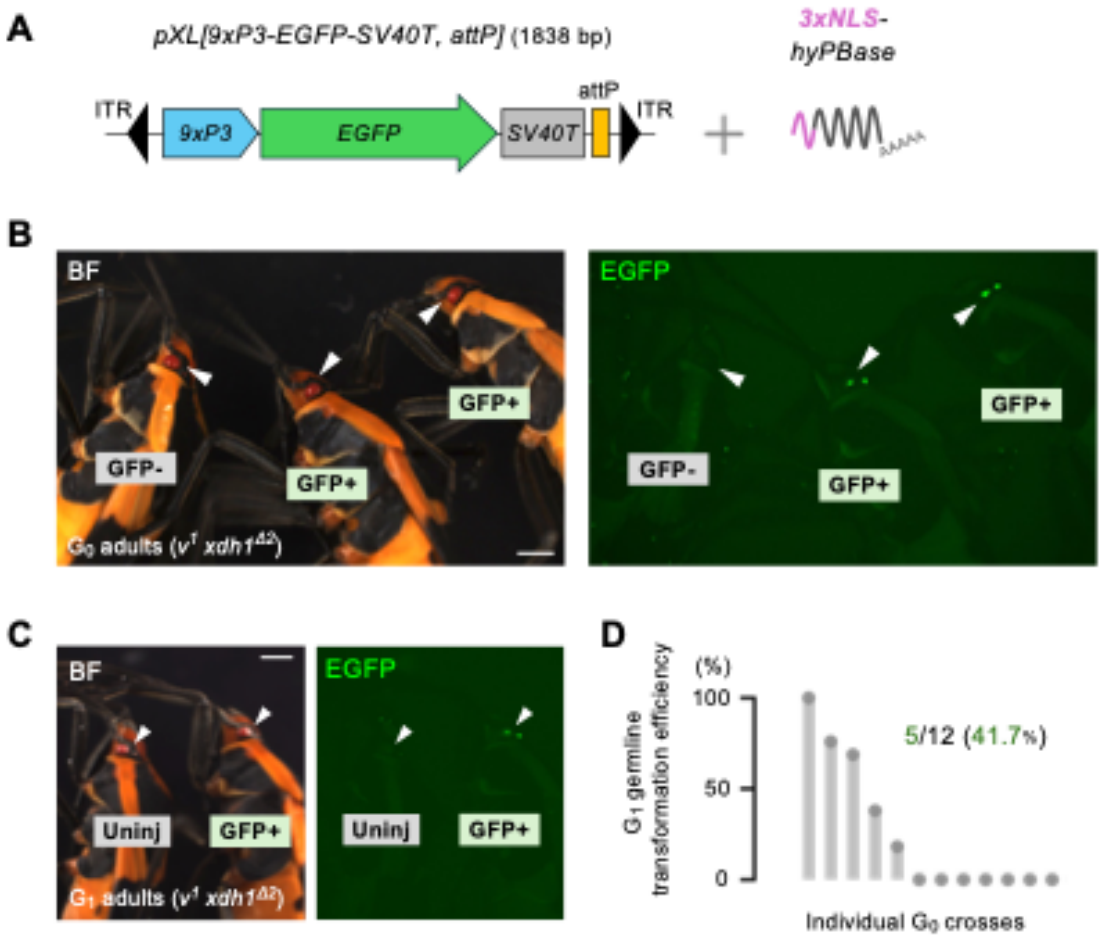
bioRxiv preprint doi: https://doi.org/10.64898/2026.07.30.741915; this version posted November 9, 2026. The copyright holder for this preprint (which was not certified by peer review) is the author/funder, who has granted bioRxiv a license to display the preprint in perpetuity. It is made available under a CC-BY 4.0 International license.



854 **Figure 2. Investigation of a nuclear targeting approach for hyPBase-mediated**

855 **transgenesis in *O. fasciatus*.**

bioRxiv preprint doi: https://doi.org/10.64898/2026.07.30.741915; this version posted November 9, 2026. The copyright holder for this preprint (which was not certified by peer review) is the author/funder, who has granted bioRxiv a license to display the preprint in perpetuity. It is made available under a CC-BY 4.0 International license.



856

857 **Figure 3. Establishment of multiple attP strains using 3×NLS *hyPBase* in *O.***

858 ***fasciatus.***

859

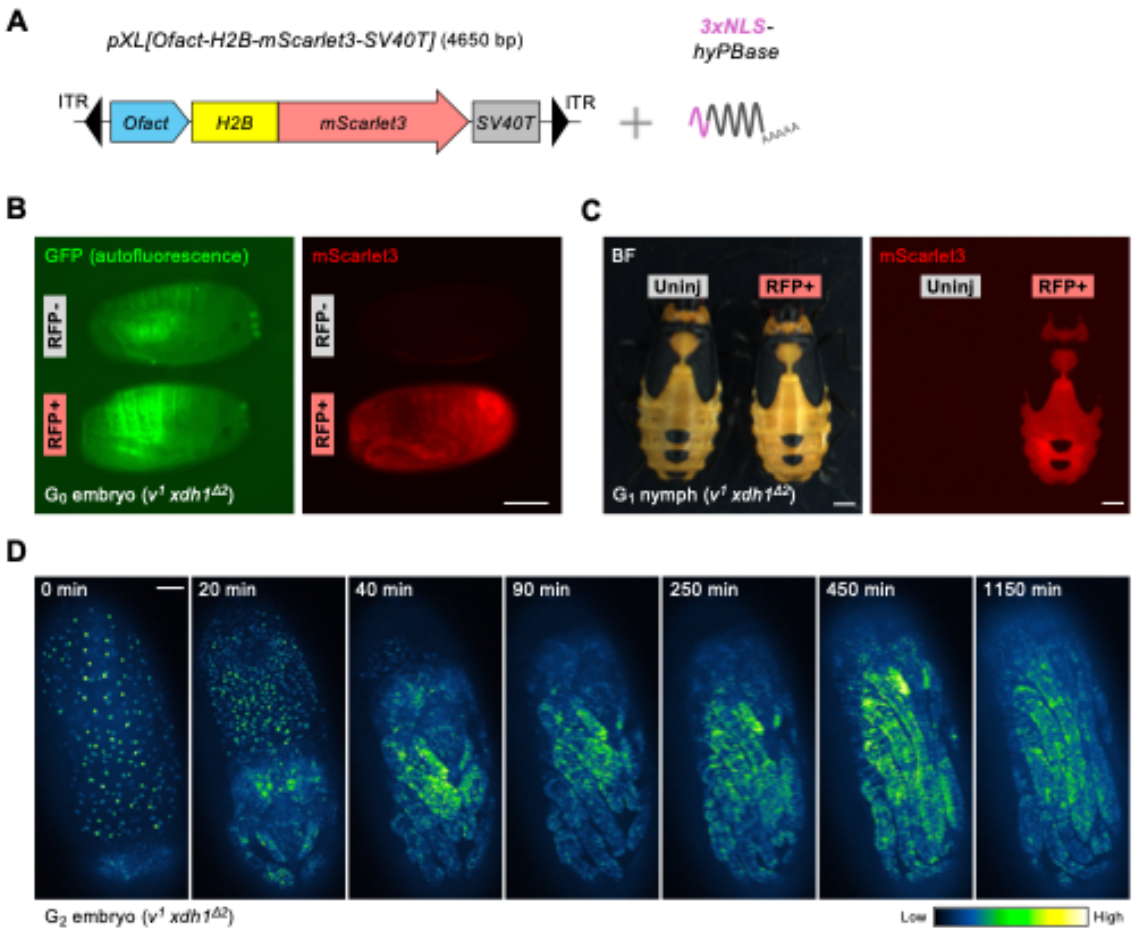
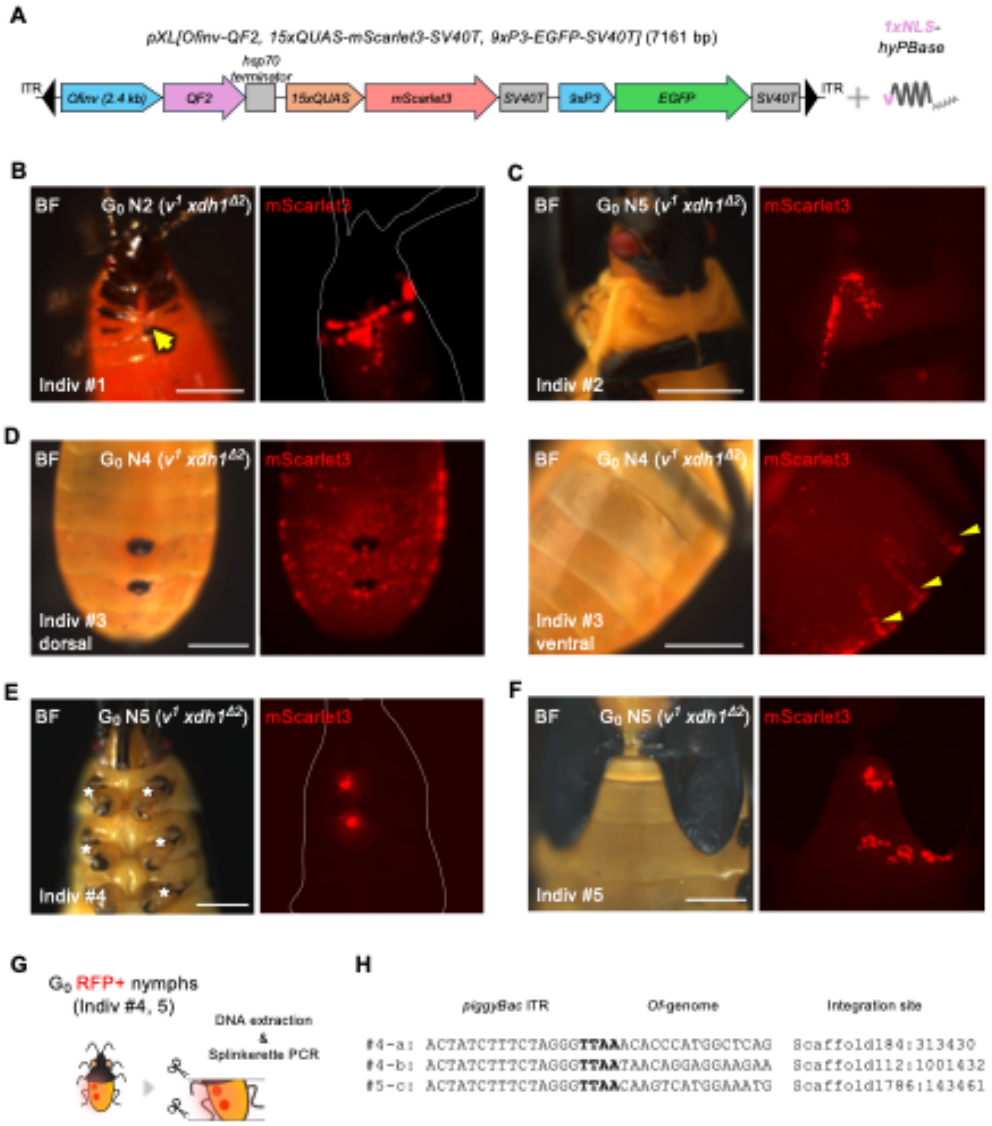


Figure 4. Establishment of the ubiquitous histone-labelled strain using 3×NLS *hyPBase* in *O. fasciatus*.

bioRxiv preprint doi: https://doi.org/10.64898/2026.07.30.741915; this version posted November 9, 2026. The copyright holder for this preprint (which was not certified by peer review) is the author/funder, who has granted bioRxiv a license to display the preprint in perpetuity. It is made available under a CC-BY 4.0 International license.

bioRxiv preprint doi: https://doi.org/10.64898/2026.07.30.741915; this version posted November 9, 2026. The copyright holder for this preprint (which was not certified by peer review) is the author/funder, who has granted bioRxiv a license to display the preprint in perpetuity. It is made available under a CC-BY 4.0 International license.



886
887
888 **Figure 5. Proof of principle of the Q system using 1×NLS *hyPBase* in *O. fasciatus*.**

Tables

Table 1. Detailed results of *piggyBac*-mediated transgenesis experiments with *hyPBase* mRNA carrying 0×, 1×, 3×, or 5×NLS in *O. fasciatus*. Each row shows the results of an independent experiment. All G_0 nymphs and adults reached each respective stage were screened. Percentages shown in parentheses indicate somatic transformation rates (STR). Nymphs were screened at stages 3 to 5.

Donor plasmid	Transposase (mRNA)	Injected eggs	% injected eggs survived to nymphal screening	Screened G0 nymphs	mScarlet-I + nymphs	mScarlet-I - nymphs	% screened nymphs survived to adult screening	Screened G0 adults	mScarlet-I + adults	mScarlet-I - adults
pXL[9xP3-mScarlet-I-SV40T]	0xNLS-hyPBase	135	21.5%	29	5 (17.2%)	24	86.2%	25	6 (24.0%)	19
pXL[9xP3-mScarlet-I-SV40T]	0xNLS-hyPBase	246	28.5%	70	0	70	88.6%	62	0	62
pXL[9xP3-mScarlet-I-SV40T]	1xNLS-hyPBase	170	45.9%	78	18 (23.1%)	60	80.8%	63	20 (31.8%)	43
pXL[9xP3-mScarlet-I-SV40T]	1xNLS-hyPBase	185	37.8%	70	11 (15.7%)	59	81.4%	57	10 (17.5%)	47
pXL[9xP3-mScarlet-I-SV40T]	3xNLS-hyPBase	161	28.6%	46	7 (15.2%)	39	89.1%	41	8 (20.0%)	33
pXL[9xP3-mScarlet-I-SV40T]	3xNLS-hyPBase	218	20.1%	44	15 (34.1%)	29	90.8%	40	15 (38.5%)	25
pXL[9xP3-mScarlet-I-SV40T]	5xNLS-hyPBase	130	34.6%	45	0	45	86.7%	39	0	39
pXL[9xP3-mScarlet-I-SV40T]	5xNLS-hyPBase	80	7.5%	6	0	6	83.3%	5	0	5
pXL[9xP3-mScarlet-I-SV40T]	5xNLS-hyPBase	73	23.3%	17	0	17	94.1%	16	0	16

bioRxiv preprint doi: https://doi.org/10.64898/2026.07.30.741915; this version posted November 9, 2026. The copyright holder for this preprint (which was not certified by peer review) is the author/funder, who has granted bioRxiv a license to display the preprint in perpetuity. It is made available under a CC-BY 4.0 International license.

Table 2. Detailed results of *piggyBac*-mediated transgenesis experiments with NLS-tagged hyPBase in *O. fasciatus*. Each row shows the results of an independent experiment. All G_0 nymphs and adults reached each respective stage were screened. Percentages shown in parentheses indicate somatic transformation rates (STR). FP, fluorescent protein. For experiments using donor plasmid pXL[Ofact-H2B-mScarlet3-SV40T], numbers in bold indicate FP + nymphs that had detectable fluorescence in >50% of their body area. Nymphs were screened at nymphal stages 3 to 5, except for the experiment using donor plasmid pXL[Ofinv-QF2, 15xQUAS-mScarlet3-SV40T, 9xP3-mScarlet-I-SV40T], which were screened at nymphal stages 2 to 5.

Donor plasmid	Transposase (mRNA)	Injected eggs	% of injected eggs survived to nymphal screening	Screened G0 nymphs	FP + nymphs	FP - nymphs
pXL[9xP3-EGFP-SV40T,attP]	3xNLS-hyPBase	245	26.5%	65	10 (15.4%)	55
pXL[9xP3-EGFP-SV40T,attP]	3xNLS-hyPBase	122	44.3%	54	5 (9.3%)	51
pXL[Gbact-H2B-mScarlet3-SV40T]	1xNLS-hyPBase	~300	~33.3%	~100	1	~100
pXL[Gbact-GAP43-mScarlet3-SV40T, 9xP3-mScarlet-I-SV40T]	1xNLS-hyPBase	341	33.1%	113	15 (13.3%)	98
pXL[Ofact-H2B-mScarlet3-SV40T]	3xNLS-hyPBase	104	40.4%	42	31, **4** (73.8%, **9.5%**)	11

bioRxiv preprint doi: https://doi.org/10.64898/2026.07.30.741915; this version posted November 9, 2026. The copyright holder for this preprint (which was not certified by peer review) is the author/funder, who has granted bioRxiv a license to display the preprint in perpetuity. It is made available under a CC-BY 4.0 International license.

pXL[Ofact-H2B-mScarlet3-SV40T]	3xNLS-hyPBase	175	25.7%	45	37, **7** (82.2%, **15.5%**)	8
pXL[Ofact-H2B-mScarlet3-SV40T]	3xNLS-hyPBase	179	44.7%	80	56, **4** (70.0%, **5.0%**)	24
pXL[Ofinv-QF2, 15xQUAS-mScarlet3-SV40T, 9xP3-mScarlet-I-SV40T]	1xNLS-hyPBase	192	25.0%	48	24 (50.0%)	24
pXL[Ofinv-QF2, 15xQUAS-mScarlet3-SV40T, 9xP3-mScarlet-I-SV40T]	1xNLS-hyPBase	242	45.9%	111	29 (26.1%)	82
pXL[Ofinv-QF2, 15xQUAS-mScarlet3-SV40T, 9xP3-mScarlet-I-SV40T]	1xNLS-hyPBase	283	38.9%	110	18 (16.4%)	92

bioRxiv preprint doi: https://doi.org/10.64898/2026.07.30.741915; this version posted November 9, 2026. The copyright holder for this preprint (which was not certified by peer review) is the author/funder, who has granted bioRxiv a license to display the preprint in perpetuity. It is made available under a CC-BY 4.0 International license.

Supporting Information for

A nuclear targeting approach enables efficient transgenesis in the milkweed bug *Oncopeltus fasciatus*

Yu Shirai, Yousuf Hashm, Ashley Watts, Jonchee A. Kao, Cassandra G. Extavour

This file contains:

SI Figures S1-S9

SI Tables S1-S9

SI Data 1 and Data 2

SI Video Legends

SI References



Supplementary Figures

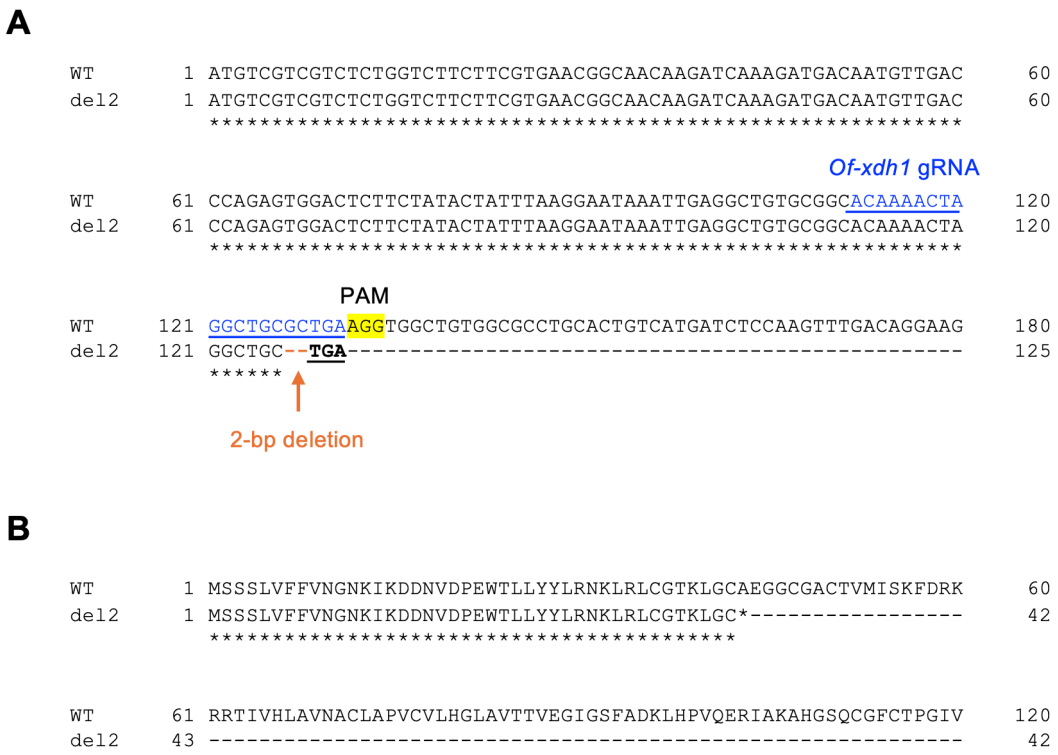


Figure S1. Nucleotide and amino acid sequence of *Of-xdh1* in the *xdh1*$^{\Delta 2}$ mutant. (A) Alignment of the nucleotide sequences of *Of-xdh1* around the gRNA target site of WT and *xdh*$^{\Delta 2}$ strains. Note the presence of a 2-bp deletion in the *xdh1*$^{\Delta 2}$ allele (shown in orange). The premature stop codon induced by this deletion is indicated in bold black. (B) Alignment of the amino acid sequences of *Of-xdh1* of the WT and *xdh1*$^{\Delta 2}$ strains. The 2-bp deletion caused a frameshift mutation in the *xdh1*$^{\Delta 2}$ allele.

A

```
WT      1 ATGGAGCCCGACAGCAATTGCAGATCTTCCGAGATCCAGAA-ATGTGGAGAGCAAAGTGG     59
v1      1 ATGGAGCCCGACAGCAATTGCAGATCTTCCGAGATCCAGAAGATGTGGAGAGCAAAGTGG     60
          ****************************************.******************
                                                  ↑
                                                  1-bp insertion

WT     60 AATGCTGTATGGGGATTACCTCCAACTTGACAAAATACTGAAGGCCCAAAGATTGCTGAG    119
v1     61 AATGCTGTATGGGGATTACCTCCAACTTGA------------------------------     90
          ****************************
```

B

```
WT      1 MEPDSNCRSSEIQKCGEQSGMLYGDYLQLDKILKAQRLLSESNNATVMDEHLFIVTHQGN     60
v1      1 MEPDSNCRSSEIQKMWRAKWNAVWGLPPT*------------------------------     29
          **************

WT     61 KLNSTQEMTNEGLNERQTLDVVKRLNRIVLILKLLVEQVMILETMTPLDFMEFRDYLCPA    120
v1     29 ------------------------------------------------------------     29

WT    121 SGFQSAQFRLIENKLGVKTEHRVRSFQHYSTVFERDKEALNEIKKSETEQSLADLIEQWL    180
v1     29 ------------------------------------------------------------     29

WT    181 ERTPGLDENGFDFWGKYIKNVEFLLQHYYEKAMKSNSETEKTTKLAEYEKKKTIFNSVLN    240
v1     29 ------------------------------------------------------------     29

WT    241 KDMHDLFVQRGERRFTHKAFQGAIMITFYRDEPRFSQPHQILTLLMDIDSLVTKWRLCSK    300
v1     29 ------------------------------------------------------------     29

WT    301 TWINYYNDKYKVLLISDRYKCFLDLFNLSSFLLPRNFIPPLSSSVRNQINIHTWNTKKQT    360
v1     29 ------------------------------------------------------------     29

WT    361 EDHEED*                                                          366
v1     29 ------                                                          29
```

Figure S2. Nucleotide and amino acid sequence of *Of-v* in the v^1 mutant. (A) Alignment of the nucleotide sequences of *Of-v* around the gRNA target site of wild type (WT) and v^1 strains. Note the presence of a 1-bp insertion in the v^1 allele (shown in red). The premature stop codon induced by this insertion is indicated in bold black. Further details are described in (Reding and Pick, 2023). (B) Alignment of the amino acid sequences of *Of-v* of the WT and v^1 strains. The 1-bp insertion caused a frameshift mutation in the v^1 allele (shown in red).

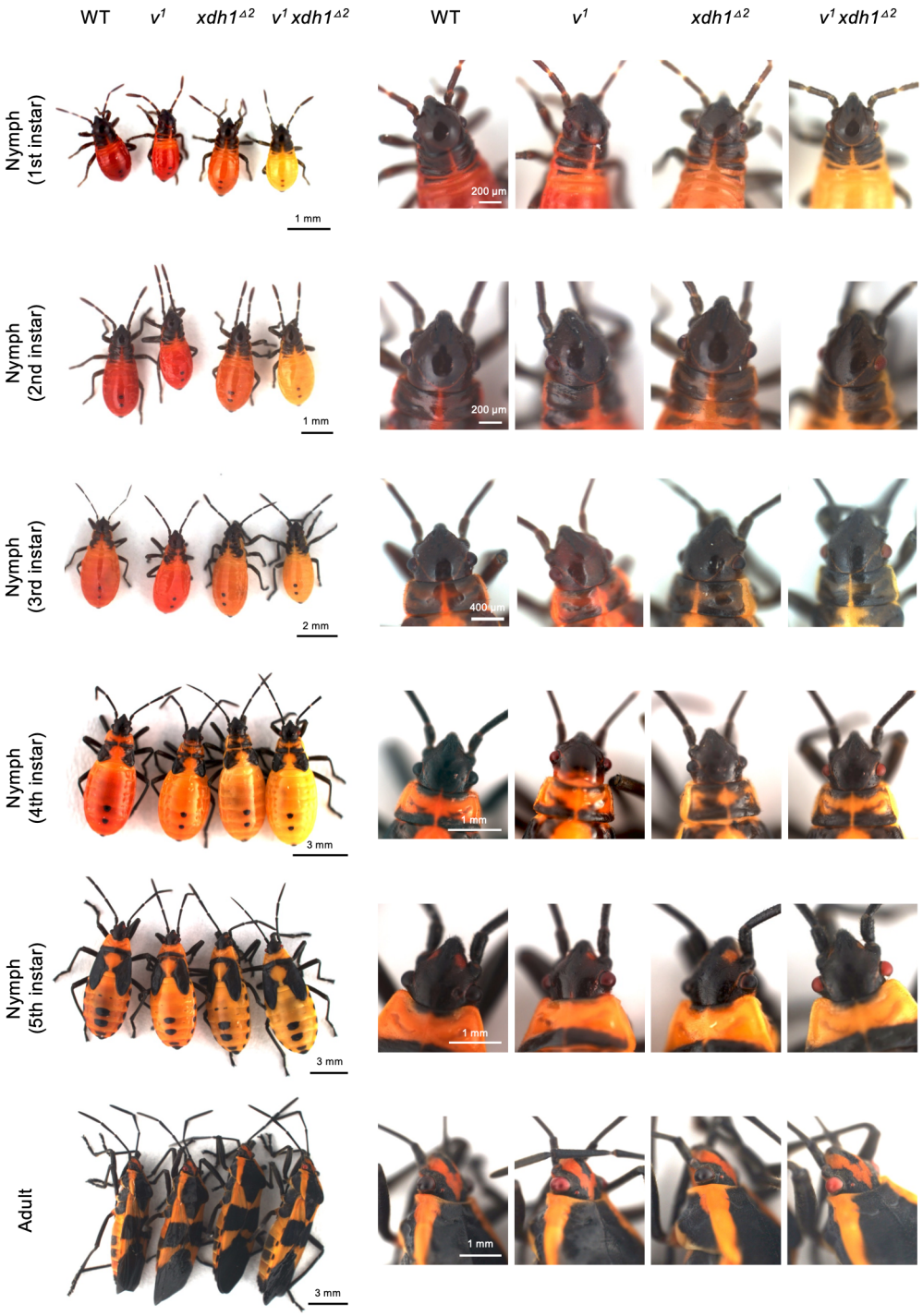


Figure S3. Comparisons of phenotypes of wild type (WT), *v*^{1}, *xdh1*$^{\Delta 2}$, and *v*^{1} *xdh1*$^{\Delta 2}$ throughout postembryonic development. All images of nymphs and close-up views (bottom right) are shown in dorsal view; low-magnification adult image (bottom left) is shown in lateral view. Anterior is up in all images.

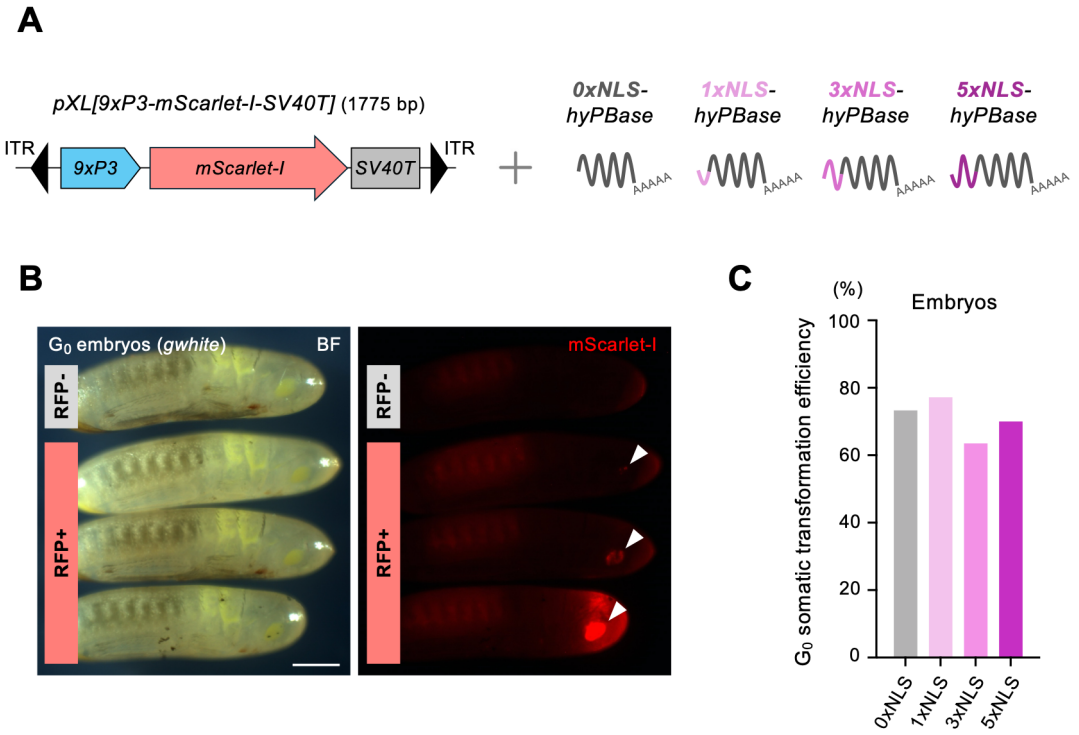


Figure S4. Investigation of a nuclear targeting approach for *piggyBac*-mediated transgenesis in *G. bimaculatus*. (A) Schematic of the *piggyBac* donor vector *pXL[9×P3-mScarlet-I-SV40T]* and *hyPBase* mRNA carrying 0×, 1×, 3×, or 5× NLS. (B) Representative images of G_0 RFP-positive embryos (embryonic stage >13) (Donoughe and Extavour, 2016). Scale bar, 500 µm. Arrowheads indicate eyes. Anterior is to the right. (C) G_0 somatic transformation rate (STR) across 0×, 1×, 3×, or 5×NLS *hyPBase* conditions.

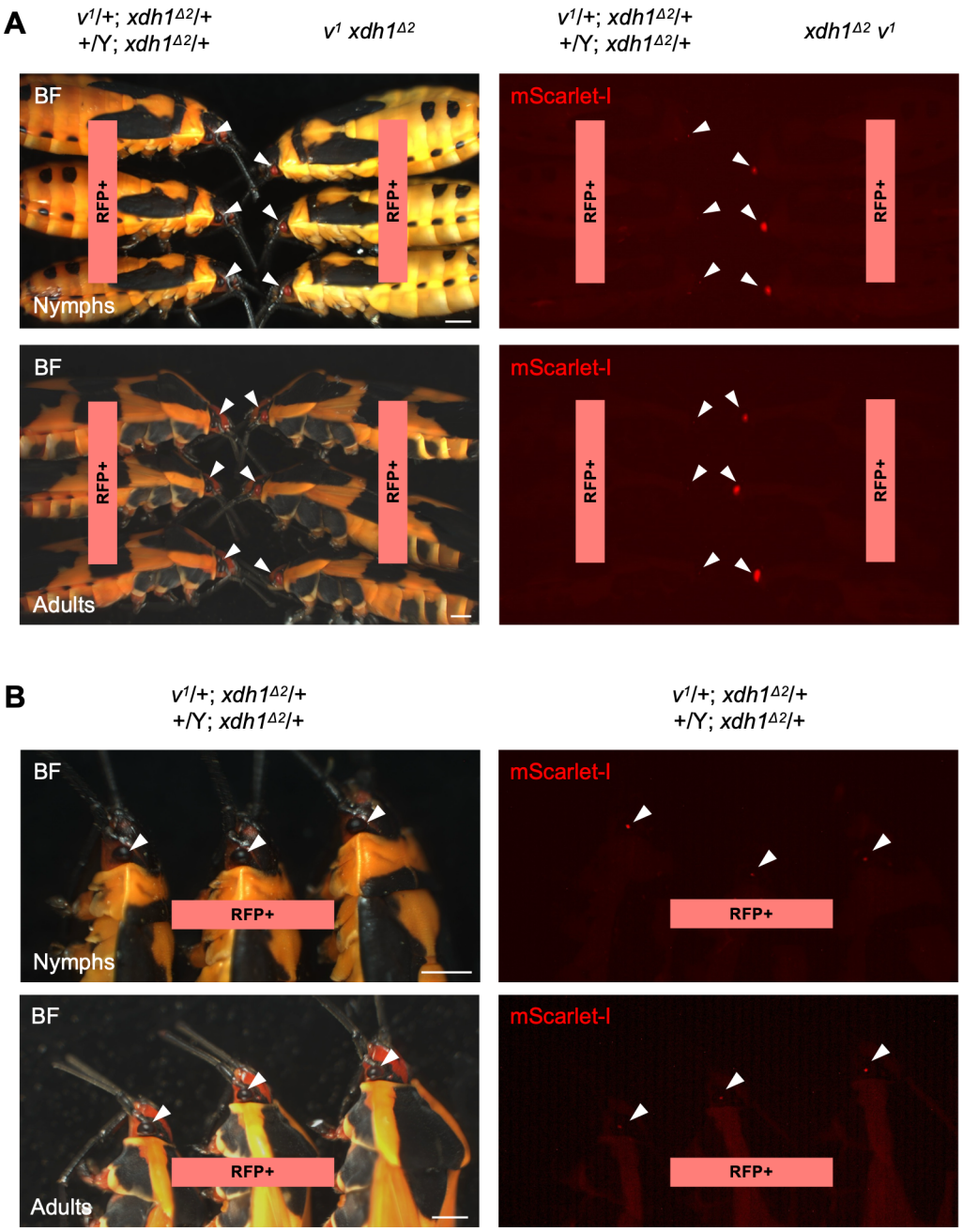


Figure S5. Comparison of mScarlet-I detection between wild type and *v*^{1} *xdh1*$^{\Delta 2}$ backgrounds in *O. fasciatus*. (A) Representative images of mScarlet-I-positive nymphs and adults in phenotypically wild-type backgrounds (*v*^{1}/+; *xdh1*$^{\Delta 2}$/+ or +/Y; *xdh1*$^{\Delta 2}$/+) and the *xdh1*$^{\Delta 2}$ *v*^{1} mutant background. Arrowheads indicate eyes. (B) Enlarged images of mScarlet-I-positive nymphs and adults in the wild type background (*xdh1*$^{\Delta 2}$/+ *v*^{1}/+ or *xdh1*$^{\Delta 2}$/+ +/Y). Scale bar, 1 mm. Transgene copy number was not controlled, as this comparison was intended to assess the visibility of the eye marker.

Integration site in 9xP3-EGFP, attP strain 5A

TATTTCAAGAATGCATGCGTCAATTTTACGCAGACTATCTTTCTAGGC**TTAA**TTAAAATTGCGTGGTACGATTTG
TAATCTACAGTTTACCCGGACACTAAATTACAATTTTACGTTTTATTGGCCGAAAATAGTTGTTTTTCTAGACAA
AA

Scaffold407: 476763-476862 (pident = 100%)

*The transgene was inserted into an intron of OfasTmpM006116-RA

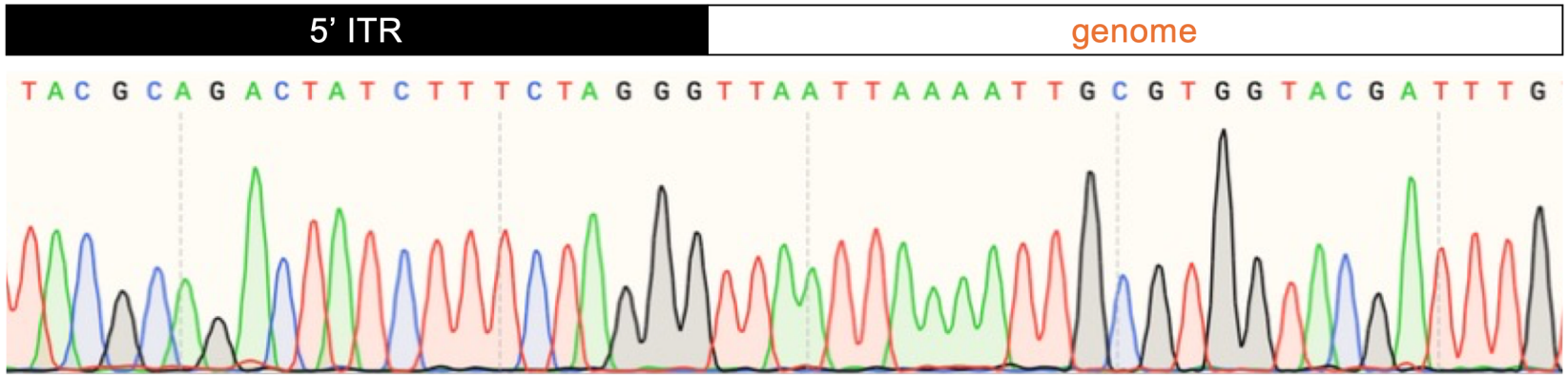
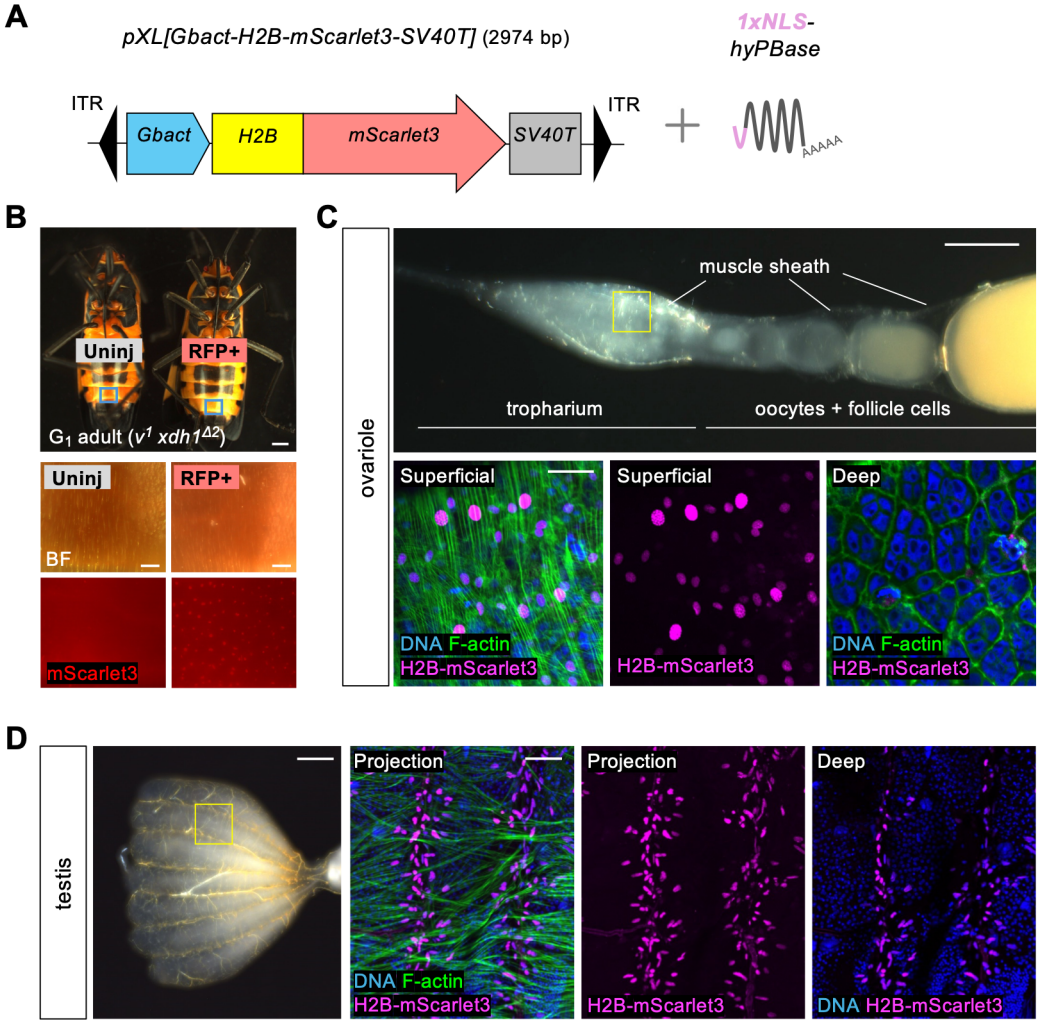


Figure S6. Nucleotide sequences around the transgene integration site in the *9×P3-EGFP*, *attP* strain in *O. fasciatus* as determine by splinkerette PCR.


A
pXL[Gbact-H2B-mScarlet3-SV40T] (2974 bp)
1xNLS-hyPBase
ITR
Gbact
H2B
mScarlet3
SV40T
ITR
AAAAA
B
Uninj
RFP+
G1 adult (v1 xdh1Δ2)
Uninj
RFP+
BF
mScarlet3
C
ovariole
muscle sheath
tropharium
oocytes + follicle cells
Superficial
DNA F-actin
H2B-mScarlet3
Superficial
H2B-mScarlet3
Deep
DNA F-actin
H2B-mScarlet3
D
testis
Projection
DNA F-actin
H2B-mScarlet3
Projection
H2B-mScarlet3
Deep
DNA H2B-mScarlet3

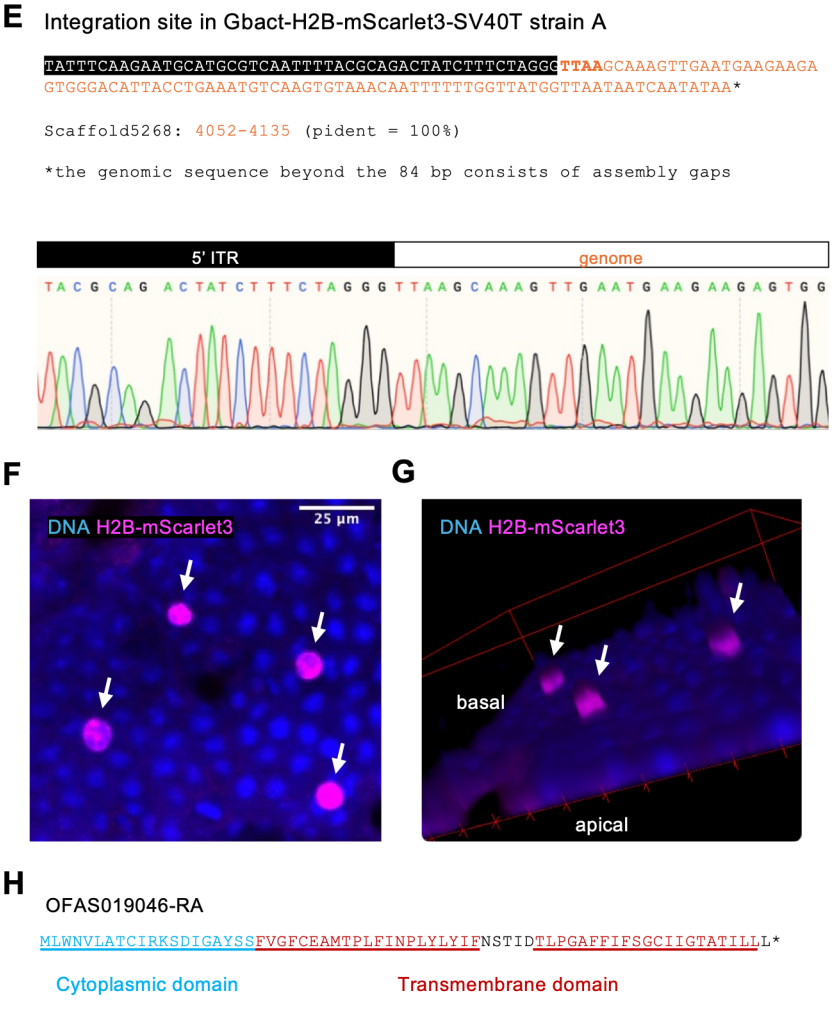

E
Integration site in Gbact-H2B-mScarlet3-SV40T strain A
TATTTCAAGAATGCATGCGTCAATTTTACGCAGACTATCTTTCTAGGGTTAAGCAAAGTTGAATGAAGAAGA
GTGGGACATTACCTGAAATGTCAAGTGTAAACAATTTTTTGGTTATGGTTAATAATCAATATAA*
Scaffold5268: 4052-4135 (pident = 100%)
*the genomic sequence beyond the 84 bp consists of assembly gaps
5' ITR
genome
F
DNA H2B-mScarlet3
25 µm
G
DNA H2B-mScarlet3
basal
apical
H
OFAS019046-RA
MLWNVLATCIRKSDIGAYSSFVGFCEAMTPLFINPLYLYIFNSTIDTLPGAFFIFSGCIIGTATILLL*
Cytoplasmic domain
Transmembrane domain

Fig S7 (previous page). Establishment of the tissue-specific histone-labelled strain using 1×NLS *hyPBase* in *O. fasciatus*. (A) Schematic of the *piggyBac* donor vector *pXL[Gbact-H2B-mScarlet3-SV40T]* and *hyPBase* mRNA carrying 1×NLS. (B) Representative images of G_1 mScarlet3-positive adults (ventral view). Anterior is up. Scale bars, 1 mm (whole-body image) and 100 μm (close-up images). (C) Representative brightfield image (top) and confocal images (bottom) of an ovariole from a G_1 transgenic adult, co-stained for DNA (blue) and F-actin (green). The yellow box in the brightfield image indicates the approximate region shown in the confocal images. Confocal images are single optical sections. In the superficial focal plane, H2B-mScarlet3 expression (magenta) is detectable in muscle sheath nuclei. In the deep focal plane, H2B-mScarlet3 expression is not detectable in the tropharium nuclei. Scale bars, 300 μm (brightfield image) and 50 μm (confocal images) (D) Representative brightfield image (left) and confocal images (right three panels) of a testis of G_1 transgenic adult testis co-stained for DNA (blue) and F-actin (green). H2B-mScarlet3 expression (magenta) was detected in muscle sheath nuclei, but not in sperm cells. Scale bars, 300 μm (brightfield image) and 50 μm (confocal images). Anterior is to the left in (C) and (D). (E) Nucleotide sequences around the transgene integration site in the *H2B-mScarlet3-SV40T* strain as determined by splinkerette PCR. (F) Confocal image of the abdominal integument of the *H2B-mScarlet3-SV40T* strain co-stained for DNA. Epidermal nuclei were labelled with blue, but not labelled with magenta (H2B-mScarlet3). Arrows indicate cells labelled with H2B-mScarlet3. (G) 3D reconstruction of the abdominal integument of the H2B-mScarlet3 strain co-stained for DNA, showing that the histone-labelled nuclei with H2B-mScarlet3 were located underneath the epidermal nuclei. Arrows indicate cells labelled with H2B-mScarlet3. (H) Amino acid sequences of the uncharacterized protein (OFAS019046-RA) encoded by the locus containing the transgene insertion site.

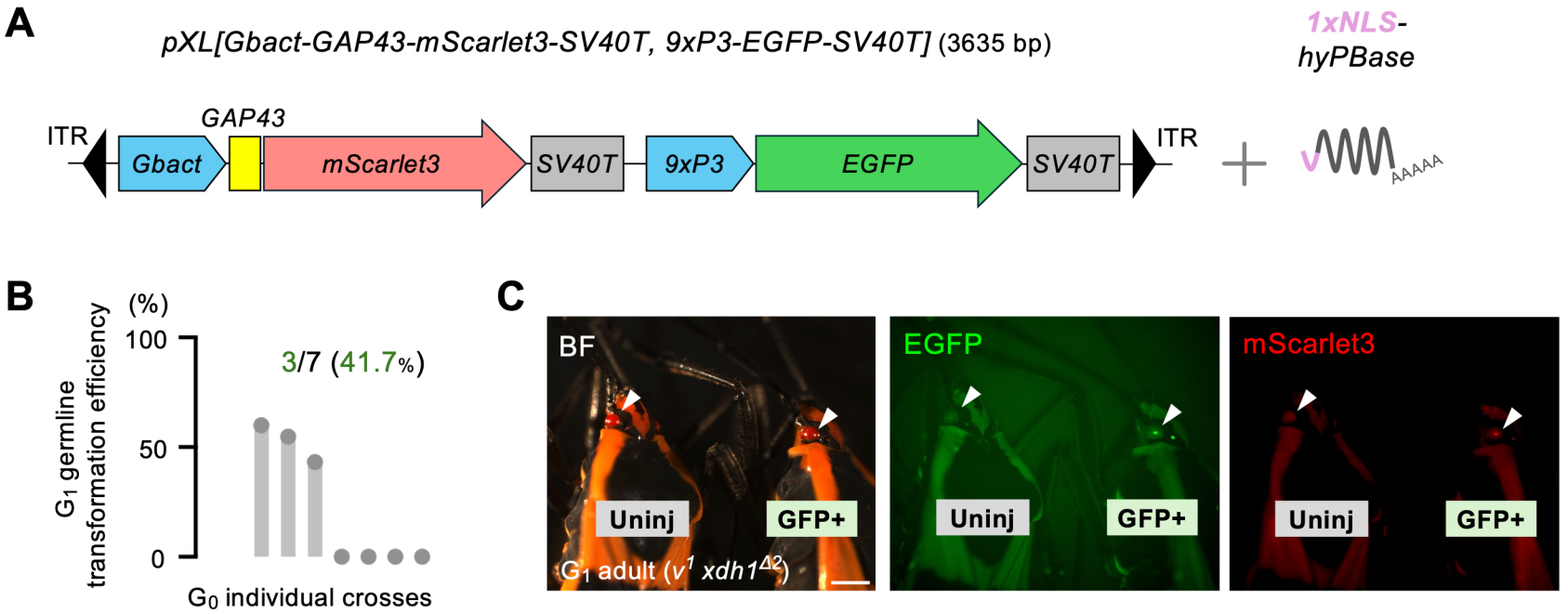
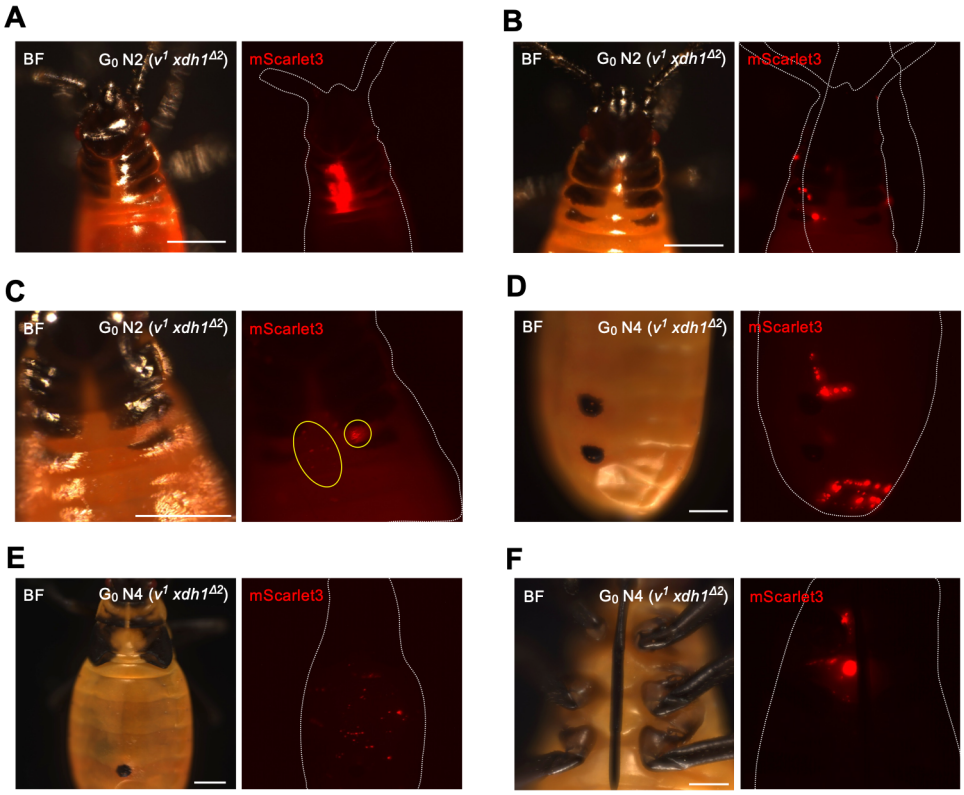


Figure S8. Attempt to generate a membrane-labelled strain using 1×NLS *hyPBase* in *O. fasciatus*. (A) Schematic of the *piggyBac* donor vector *pXL[Gbact-GAP43-mScarlet3-SV40T, 9xP3-EGFP-SV40T]* and *hyPBase* mRNA carrying 1×NLS. (B) G_1 germ line transformation efficiency (GTE). Each bar represents the proportion of EGFP-positive animals among G_1 progeny from an individual cross. Each dot represents an individual backcross that yielded G_1 progeny. Green numbers indicate the number of crosses yielding heritable transgenes and the corresponding percentages. (C) Representative images of G_1 EGFP-positive adults. Weak mScarlet3 expression in their eyes was also observed.



G

Integration sites in Ofinv-QF2, 15×QUAS-mScarlet3-SV40T, 9×P3-EGFP-SV40T, G_0 indiv#4

```
TATTTCAAGAATGCATGCGTCAATTTTACGCAGACTATCTTTCTAGGGTTAAACACCCATGGCTCAGGACAAGCTTC
TATATTATAAATAAAAGATTGACCTGGGCGGGATTAGAACCCGCGGCGTCAGGATTGCGAGACCTGTACGGATCC

Scaffold184: 313430-313529 (pident = 100%)

TATTTCAAGAATGCATGCGTCAATTTTACGCAGACTATCTTTCTAGGGTTAATAACAGGAGGAAGAATGAGAGAGTA
GTCAACACTCACAAACACACAAAATAGAAATAACGCAAAGTATTGCGAATATTTAGTTTTCTTTTTATATATATT

Scaffold112: 1001432-1001531 (pident = 100%)
```

H

Integration sites in Ofinv-QF2, 15×QUAS-mScarlet3-SV40T, 9×P3-EGFP-SV40T, G_0 indiv#5

```
TATTTCAAGAATGCATGCGTCAATTTTACGCAGACTATCTTTCTAGGGTTAACAAGTCATGGAAATGTGAACTTAGG
GACAGGACGTCCTCTCTCATCTTCATGATAGCCCTGAAGATGGCTTGCAATGTAAGCCGAAACGTTGGCAGATAA

Scaffold1786: 143362-143461 (pident = 99%)
```

Figure S9. Additional data on Q system application using 1×NLS *hyPBase* in *O. fasciatus*. (A–F) Representative images of G_0 mScarlet3-positive nymphs. White dotted lines indicate animal boundaries. Yellow dotted circles indicate mScarlet3 expression. Scale bars, 500 μm. Anterior is up in (A–F). (G-H) Nucleotide sequences around the transgene integration site of animals in the injected generation as determined by splinkerette PCR.

Supplementary Tables

Table S1. Detailed results of piggyBac-mediated transgenesis experiments with hyPBase mRNA carrying 0×, 1×, 3×, or 5×NLS in *G. bimaculatus*. Each row shows the results of an independent experiment. Percentages shown in parentheses indicate somatic transformation rates (STR).

Donor plasmid	Transposase (mRNA)	Injected eggs	% of injected eggs survived to screening	Screened G0 embryos	mScarlet-I **+** nymphs	mScarlet-I **-** nymphs
pXL[9xP3-mScarlet-I-SV40T]	0xNLS-hyPBase	194	69.6%	135	99 (73.3%)	36
pXL[9xP3-mScarlet-I-SV40T]	1xNLS-hyPBase	194	70.1%	136	105 (77.2%)	31
pXL[9xP3-mScarlet-I-SV40T]	3xNLS-hyPBase	190	72.1%	137	87 (63.5%)	50
pXL[9xP3-mScarlet-I-SV40T]	5xNLS-hyPBase	192	67.7%	130	91 (70.0%)	39

Table S2. Results of crossing experiments with 0×NLS-hyPBase. F, female. M, male. GTR, germ line transformation rate.

mRNA	donor plasmid
0xNLS-hyPBase	9xP3-mScarlet-I-SV40T

G0 indiv#	mScarlet-I expression	sex	crossed with	Screened G1 animals	RFP+	RFP-	GTR (%)
1	+	M	*v*^{1} *xdh1*$^{\Delta}$	60	0	60	0
2	+	F	*v*^{1} *xdh1*$^{\Delta}$	57	0	57	0
3	+	M	*v*^{1} *xdh1*$^{\Delta}$	57	0	57	0
4	+	F	*v*^{1} *xdh1*$^{\Delta}$	54	31	23	57.4
5	+	F	*v*^{1} *xdh1*$^{\Delta}$	57	0	57	0
6	+	F	*v*^{1} *xdh1*$^{\Delta}$	13	0	13	0

Table S3. Results of crossing experiments with 1×NLS-hyPBase. F, female. M, male. GTR, germ line transformation rate. Data from two independent injection experiments are shown.

mRNA	donor plasmid						
1xNLS-hyPBase	9xP3-mScarlet-I-SV40T						
G0 indiv#	mScarlet-I expression	sex	crossed with	Screened G1 animals	RFP+	RFP-	GTR (%)
1	+	F	*v*^{1} *xdh1*$^{\Delta 2}$	55	0	55	0
2	+	F	*v*^{1} *xdh1*$^{\Delta 2}$	45	0	45	0
3	+	F	*v*^{1} *xdh1*$^{\Delta 2}$	64	0	64	0
4	+	F	*v*^{1} *xdh1*$^{\Delta 2}$	52	0	52	0
5	+	F	*v*^{1} *xdh1*$^{\Delta 2}$	53	44	9	83.0
6	+	M	*v*^{1} *xdh1*$^{\Delta 2}$	sterile	0	0	NA
7	+	M	*v*^{1} *xdh1*$^{\Delta 2}$	24	11	13	45.8
8	+	M	*v*^{1} *xdh1*$^{\Delta 2}$	50	0	50	0
9	+	F	*v*^{1} *xdh1*$^{\Delta 2}$	34	0	34	0
10	+	F	*v*^{1} *xdh1*$^{\Delta 2}$	43	0	43	0
11	+	F	*v*^{1} *xdh1*$^{\Delta 2}$	61	54	7	88.5
12	+	M	*v*^{1} *xdh1*$^{\Delta 2}$	39	18	21	46.2
13	+	M	*v*^{1} *xdh1*$^{\Delta 2}$	51	0	51	0
14	+	M	*v*^{1} *xdh1*$^{\Delta 2}$	52	35	17	67.3
15	+	M	*v*^{1} *xdh1*$^{\Delta 2}$	48	0	48	0
16	+	M	*v*^{1} *xdh1*$^{\Delta 2}$	26	0	26	0
17	+	M	*v*^{1} *xdh1*$^{\Delta 2}$	62	0	62	0
18	+	M	*v*^{1} *xdh1*$^{\Delta 2}$	46	6	40	13.0
19	+	M	*v*^{1} *xdh1*$^{\Delta 2}$	50	0	50	0
20	+	M	*v*^{1} *xdh1*$^{\Delta 2}$	sterile	0	0	NA

mRNA	donor plasmid

1xNLS-hyPBase	9xP3-mScarlet-I-SV40T						
G0 indiv#	mScarlet-I expression	sex	crossed with	Screened G1 animals	RFP+	RFP-	GTR (%)
1	+	M	*v*^{1} *xdh1*$^{\Delta 2}$	51	0	51	0
2	+	F	*v*^{1} *xdh1*$^{\Delta 2}$	55	0	55	0
3	+	F	*v*^{1} *xdh1*$^{\Delta 2}$	60	60	0	100.0
4	+	F	*v*^{1} *xdh1*$^{\Delta 2}$	56	0	56	0
5	+	F	*v*^{1} *xdh1*$^{\Delta 2}$	52	0	52	0
6	+	M	*v*^{1} *xdh1*$^{\Delta 2}$	50	0	50	0
7	+	F	*v*^{1} *xdh1*$^{\Delta 2}$	sterile	0	0	NA
8	+	F	*v*^{1} *xdh1*$^{\Delta 2}$	50	50	0	100.0
9	+	M	*v*^{1} *xdh1*$^{\Delta 2}$	53	53	0	100.0
10	+	M	*v*^{1} *xdh1*$^{\Delta 2}$	51	0	51	0

Table S4. Results of crossing experiments with 3×NLS-hyPBase. F, female. M, male. GTR, germ line transformation rate. Data from two independent injection experiments are shown.

mRNA	donor plasmid						
3xNLS-hyPBase	9xP3-mScarlet-I-SV40T						
G0 indiv#	mScarlet-I expression	sex	crossed with	Screened G1 animals	RFP+	RFP-	GTR (%)
1	+	M	*v*^{1} *xdh1*$^{\Delta 2}$	60	0	60	0
2	+	M	*v*^{1} *xdh1*$^{\Delta 2}$	55	0	55	0
3	+	M	*v*^{1} *xdh1*$^{\Delta 2}$	3	3	0	100.0
4	+	F	*v*^{1} *xdh1*$^{\Delta 2}$	51	33	18	64.7
18	+	M	*v*^{1} *xdh1*$^{\Delta 2}$	61	0	61	0
19	+	M	*v*^{1} *xdh1*$^{\Delta 2}$	1	0	1	0
20	+	M	*v*^{1} *xdh1*$^{\Delta 2}$	57	0	57	0
41	+	M	*v*^{1} *xdh1*$^{\Delta 2}$	30	0	30	0

mRNA	donor plasmid						
3xNLS-hyPBase	9xP3-mScarlet-I-SV40T						
G0 indiv#	mScarlet-I expression	sex	crossed with	Screened G1 animals	RFP+	RFP-	GTR (%)
18	+	M	*v*^{1} *xdh1*$^{\Delta 2}$	51	0	51	0
19	+	M	*v*^{1} *xdh1*$^{\Delta 2}$	sterile	0	0	NA
20	+	M	*v*^{1} *xdh1*$^{\Delta 2}$	57	0	57	0
21	+	M	*v*^{1} *xdh1*$^{\Delta 2}$	68	0	68	0
22	+	M	*v*^{1} *xdh1*$^{\Delta 2}$	64	64	0	100.0
23	+	M	*v*^{1} *xdh1*$^{\Delta 2}$	36	0	36	0
24	+	F	*v*^{1} *xdh1*$^{\Delta 2}$	34	0	34	0
25	+	F	*v*^{1} *xdh1*$^{\Delta 2}$	23	0	23	0
26	+	F	*v*^{1} *xdh1*$^{\Delta 2}$	died	0	0	NA
27	+	M	*v*^{1} *xdh1*$^{\Delta 2}$	45	0	45	0
28	+	M	*v*^{1} *xdh1*$^{\Delta 2}$	sterile	0	0	NA
29	+	F	*v*^{1} *xdh1*$^{\Delta 2}$	50	50	0	100.0
30	+	F	*v*^{1} *xdh1*$^{\Delta 2}$	54	23	31	42.6
31	+	F	*v*^{1} *xdh1*$^{\Delta 2}$	51	51	0	100.0
40	+	F	*v*^{1} *xdh1*$^{\Delta 2}$	11	11	0	100.0

Table S5. Results of crossing experiments for attP strains. The integration site was determined for the line derived from G1 individual 8A. F, female. M, male. GTR, germ line transformation rate. Data from two independent injection experiments are shown.

mRNA	donor plasmid						
3xNLS-hyPBase	9xP3-EGFP-SV40T;attP						
G0 indiv#	EGFP expression	sex	crossed with	Screened G1 animals	GFP+	GFP-	GTR (%)
1	+	F	*v*^{1} *xdh1*$^{\Delta 2}$	49	0	49	0
2	+	F	*v*^{1} *xdh1*$^{\Delta 2}$	41	0	41	0
3	+	F	*v*^{1} *xdh1*$^{\Delta 2}$	died	0	0	NA
4	+	F	*v*^{1} *xdh1*$^{\Delta 2}$	died	0	0	NA
5	+	F	*v*^{1} *xdh1*$^{\Delta 2}$	25	19	6	76.0
6	+	M	*v*^{1} *xdh1*$^{\Delta 2}$	26	0	26	0
7	+	M	*v*^{1} *xdh1*$^{\Delta 2}$	44	0	44	0
8	+	F	*v*^{1} *xdh1*$^{\Delta 2}$	42	16	26	38.1
9	+	M	*v*^{1} *xdh1*$^{\Delta 2}$	sterile	0	0	NA
10	+	M	*v*^{1} *xdh1*$^{\Delta 2}$	5	5	0	100.0
G1 indiv#	EGFP expression	sex	crossed with	Screened G2 animals	GFP+	GFP-	G2 inheritance rate (%)
5A	+	F	*v*^{1} *xdh1*$^{\Delta 2}$	33	27	6	81.8
8A	+	F	*v*^{1} *xdh1*$^{\Delta 2}$	64	32	32	50.0

mRNA	donor plasmid						
3xNLS-hyPBase	9xP3-EGFP-SV40T;attP						
G0 indiv#	EGFP expression	sex	crossed with	Screened G1 animals	GFP**+**	GFP**-**	GTR (%)
1	+	F	*v*^{1} *xdh1*$^{\Delta 2}$	48	0	48	0
2	+	M	*v*^{1} *xdh1*$^{\Delta 2}$	31	0	31	0
3	+	F	*v*^{1} *xdh1*$^{\Delta 2}$	45	31	14	68.9
4	+	M	*v*^{1} *xdh1*$^{\Delta 2}$	39	0	39	0
5	+	M	*v*^{1} *xdh1*$^{\Delta 2}$	33	6	27	18.2
G1 indiv#	EGFP expression	sex	crossed with	Screened G2 animals	GFP**+**	GF**P-**	G2 inheritance rate (%)
3A	+	M	*v*^{1} *xdh1*$^{\Delta 2}$	44	37	7	84.1
3B	+	F	*v*^{1} *xdh1*$^{\Delta 2}$	51	37	14	72.5

Table S6. Results of crossing experiments for Gbact-H2B-mScarlet3 strain. F, female. GTR, germ line transformation rate.

mRNA	donor plasmid						
1xNLS-hyPBase	Gbact-H2B-mScarlet3-SV40T						
G0 indiv#	mScarlet-I expression	sex	crossed with	Screened G1 animals	RFP**+**	RF**P-**	GTR (%)
1	+	F	v^{1} $xdh1^{\Delta 2}$	30	14	16	46.7%

Table S7. Results of crossing experiments for Gbact-GAP43-mScarlet3;9xP3-EGFP strains. F, female. M, male. GTR, germ line transformation rate.

mRNA	donor plasmid
1xNLS-hyPBase	Gbact-GAP43-mScarlet3-SV40T;9xP3-EGFP-SV40T

G0 indiv#	EGFP expression	sex	crossed with	Screened G1 animals	GFP+	GFP-	GTR (%)
1	+	M	*v*^{1} *xdh1*$^{\Delta 2}$	45	27	18	60.0
2	+	M	*v*^{1} *xdh1*$^{\Delta 2}$	died	0	0	NA
3	+	M	*v*^{1} *xdh1*$^{\Delta 2}$	died	0	0	NA
4	+	M	*v*^{1} *xdh1*$^{\Delta 2}$	died	0	0	NA
5	+	M	*v*^{1} *xdh1*$^{\Delta 2}$	35	0	35	
6	+	M	*v*^{1} *xdh1*$^{\Delta 2}$	36	0	36	
7	+	M	*v*^{1} *xdh1*$^{\Delta 2}$	33	0	33	
8	+	F	*v*^{1} *xdh1*$^{\Delta 2}$	42	23	19	54.8
9	+	F	*v*^{1} *xdh1*$^{\Delta 2}$	35	0	35	
10	+	F	*v*^{1} *xdh1*$^{\Delta 2}$	died	0	0	NA
11	+	F	*v*^{1} *xdh1*$^{\Delta 2}$	44	19	25	43.2

G1 indiv#	EGFP expression	sex	crossing with	Screened G2 animals	GFP+	GFP-	G2 inheritance rate (%)
1A	+	M	*v*^{1} *xdh1*$^{\Delta 2}$	56	28	28	50.0
1B	+	M	*v*^{1} *xdh1*$^{\Delta 2}$	46	21	25	45.7
8A	+	M	*v*^{1} *xdh1*$^{\Delta 2}$	45	23	22	51.1

Table S8. Results of crossing experiments for Ofact-H2B-mScarlet3 strain. F, female. M, male. GTR, germ line transformation rate. Data from three independent injection experiments are shown.

mRNA	donor plasmid						
3xNLS-hyPBase	Ofact-H2B-mScarlet3-SV40T						
G0 indiv#	RFP expression	sex	crossed with	Screened G1 animals	RFP+	RFP-	GTR (%)
1	+	F	*v*^{1} *xdh1*$^{\Delta 2}$	20	0	20	0
2	+	F	*v*^{1} *xdh1*$^{\Delta 2}$	32	17	15	53.1
3	+	F	*v*^{1} *xdh1*$^{\Delta 2}$	20	0	20	0
4	+	F	*v*^{1} *xdh1*$^{\Delta 2}$	49	0	49	0
G1 indiv#	RFP expression	sex	crossed with	Screened G2 animals	RFP+	RFP-	G2 inheritance rate (%)
1A	+	F	*v*^{1} *xdh1*$^{\Delta 2}$	50	32	18	64.0
1B	+	M	*v*^{1} *xdh1*$^{\Delta 2}$	sterile	0	0	NA
1C	+	M	*v*^{1} *xdh1*$^{\Delta 2}$	sterile	0	0	NA
1D	+	M	*v*^{1} *xdh1*$^{\Delta 2}$	31	14	17	45.2
1E	+	F	*v*^{1} *xdh1*$^{\Delta 2}$	sterile	0	0	NA
1F	+	F	*v*^{1} *xdh1*$^{\Delta 2}$	46	24	22	52.2

mRNA	donor plasmid
3xNLS-hyPBase	Ofact-H2B-mScarlet3-SV40T

G0 indiv#	RFP expression	sex	crossed with	Screened G1 animals	RFP+	RFP-	GTR (%)
1	+	F	*v*[1] *xdh1*[Δ2]	30	0	30	0.0
2	+	M	*v*[1] *xdh1*[Δ2]	51	10	41	19.6
G1 indiv#	**RFP expression**	**sex**	**crossed with**	**Screened G2 animals**	**RFP+**	**RFP-**	**G2 inheritance rate (%)**
1A	+	F	*v*[1] *xdh1*[Δ2]	53	26	27	49.1
1B	+	M	*v*[1] *xdh1*[Δ2]	sterile	0	0	NA
1C	+	M	*v*[1] *xdh1*[Δ2]	55	33	22	60.0

mRNA	donor plasmid
3xNLS-hyPBase	Ofact-H2B-mScarlet3-SV40T

G0 indiv#	RFP expression	sex	crossed with	Screened G1 animals	RFP+	RFP-	GTR (%)
1	+	M	*v*[1] *xdh1*[Δ2]	died	0	0	NA
2	+	M	*v*[1] *xdh1*[Δ2]	died	0	0	NA
3	+	M	*v*[1] *xdh1*[Δ2]	no data	3	no data	no data
G1 indiv#	**RFP expression**	**sex**	**crossed with**	**Screened G2 animals**	**RFP+**	**RFP-**	**G2 inheritance rate (%)**
3A, 3B, 3C	+	F (3)	*v*[1] *xdh1*[Δ2]	63	32	31	50.8

Table S9. Primers used in the study.

Name	Sequence (5'- to -3')	Purpose
Of-xdh1-F1	GGCTAACTTCCTAATGGTGGGTT	Genotyping of *Of-xdh1*
Of-xdh1-R1	CTGCCATAGCAGAAAGAAAGGT	Genotyping of *Of-xdh1*
hyPBase-Nterm3NLS-F	CCAAAAAAAAGCGCAAGGTTCCGAGATCTCCTGAATTCGC	inverse PCR for pCMV-3xNLS-hyPBase construction
hyPBase-Nterm3NLS-R	ACTTTGCGTTTCTTCTTCGGCATGGTGGATCCCATGGTGG	inverse PCR for pCMV-3xNLS-hyPBase construction
3NLS-top	CCGAAGAAGAAACGCAAAGTTCCGAAAAAGAAACGCAAAGTGCCCAAAAAAAAGCGCAAG	Oligonucleotides annealing for pCMV-3xNLS-hyPBase construction
3NLS-bottom	CTTGCGCTTTTTTTTGGGCACTTTGCGTTTCTTTTTCGGAACTTTGCGTTTCTTCTTCGG	Oligonucleotides annealing for pCMV-3xNLS-hyPBase construction
SDM-1NLS-F	CCGAGATCTCCTGAATTCGC	Site-directed mutagenesis for pCMV-1xNLS-hyPBase construction
SDM-1NLS-R	ACTTTGCGTTTCTTCTTCGG	Site-directed mutagenesis for pCMV-1xNLS-hyPBase construction
SDM-5NLS-F	CCTAAGAAAAAGCGTAAAGTCCCGAGATCTCCTGAATTCGC	Site-directed mutagenesis for pCMV-5xNLS-hyPBase construction

SDM-5NLS-R	TACCTTTCGCTTCTTTTTTGGAACCTTGCGCTTTTTTTTGG	Site-directed mutagenesis for pCMV-5xNLS-hyPBase construction
SPLNK-BOT	CGAAGAGTAACCGTTGCTAGGAGAGACCGTGGCTGAATGAGACTGGTGTCGACACTAGTGG	Annealing of splinkerrette PCR
SPLNK-GATC-TOP	GATCCCACTAGTGTCGACACCAGTCTCTAATTTTTTTTTTCAAAAAAA	Annealing of splinbkerrette PCR
SPLNK#1	CGAAGAGTAACCGTTGCTAGGAGAGACC	1st PCR of splinbkerrette PCR
SPLNK#2	GTGGCTGAATGAGACTGGTGTCGAC	2nd PCR of splinbkerrette PCR
5'SPLNK-PB#1	ACCGCATTGACAAGCACG	1st PCR of splinbkerrette PCR
5'SPLNK-PB#2	CTCCAAGCGGCGACTGAG	2nd PCR of splinbkerrette PCR
5'SPLNK-PB-SEQ	CGACTGAGATGTCCTAAATGC	Sequencing for splinbkerrette PCR

141

Data S1. plasmid constructs_260728_V4

pXL[9xP3-mScarlet-I-SV40T] = 1775 bp

TTAACCCTAGAAAGATAATCATATTGTGACGTACGTTAAAGATAATCATGTGTAAAATTGACGC

ATGTGTTTTATCGGTCTGTATATCGAGGTTTATTTATTAATTTGAATAGATATTAAGTTTTATT

ATATTTACACTTACATACTAATAATAAATTCAACAAACAATTTATTTATGTTTATTTATTTATT

AAAAAAAACAAAAACTCAAAATTTCTTCTATAAAGTAACAAAACTTTTATCGAATTCCTGCAGC

CCGGGGGATCCACTAGTTCTGTGAATTCAGATCTCCGGGGATCTAATTCAATTAGAGACTAATT

CAATTAGAGCTAATTCAATTAGGATTAATTCAATTAGAGACTAATTCAATTAGAGCTAATTCAA

TTAGGATTAATTCAATTAGAGACTAATTCAATTAGAGCTAATTCAATTAGGATCCAAGCTTATC

GATTTCGAACCCTCGACCGCCGGAGTATAAATAGAGGCGCTTCGTCTACGGAGCGACAATTCAA

TTCAAACAAGCAAAGTGAACACGTCGCTAAGCGAAAGCTAAGCAAATAAACAAGCGCAGCTGAA

CAAGCTAAACAATCGAAGAATCAAAATGGTGTCTAAGGGAGAGGCTGTCATCAAGGAATTCATG

CGCTTCAAGGTGCACATGGAGGGATCAATGAACGGTCACGAGTTCGAAATCGAGGGAGAAGGAG

AGGGCCGTCCTTACGAAGGTACCCAGACTGCCAAGCTGAAGGTCACCAAGGGTGGCCCACTGCC

TTTCTCCTGGGACATCCTGAGCCCCCAGTTCATGTACGGATCCCGCGCTTTCACTAAGCACCCC

GCCGACATCCCAGACTACTACAAGCAGAGCTTCCCAGAGGGTTTCAAGTGGGAACGTGTGATGA

ACTTCGAGGACGGAGGTGCTGTGACCGTCACTCAGGACACCTCCCTGGAAGACGGCACTCTGAT

CTACAAGGTGAAGCTGAGGGGTACCAACTTCCCTCCCGACGGCCCAGTCATGCAGAAGAAGACC

ATGGGATGGGAGGCTAGCACTGAAAGACTGTACCCTGAGGACGGCGTCCTGAAGGGAGACATCA

AGATGGCCCTGAGGCTGAAGGACGGCGGAAGATACCTGGCTGACTTCAAGACCACTTACAAGGC

CAAGAAGCCTGTGCAGATGCCCGGTGCCTACAACGTCGACAGGAAGCTGGACATCACCTCCCAC

AACGAGGACTACACTGTGGTCGAACAGTACGAGCGCTCTGAAGGCCGTCACTCAACTGGTGGCA

TGGACGAACTGTACAAGTAAAACTTGTTTATTGCAGCTTATAATGGTTACAAATAAAGCAATAG

CATCACAAATTTCACAAATAAAGCATTTTTTTCACTGCATTCTAGTTGTGGTTTGTCCAAACTC

ATCAATGTATCTTAAGATCTTCTAGATATCGGATCCCGGGGGTCGACGGTATCGATAAGCTTGA

TATCTATAACAAGAAAATATATATATAATAAGTTATCACGTAAGTAGAACATGAAATAACAATA

TAATTATCGTATGAGTTAAATCTTAAAAGTCACGTAAAAGATAATCATGCGTCATTTTGACTCA

CGCGGTCGTTATAGTTCAAAATCAGTGACACTTACCGCATTGACAAGCACGCCTCACGGGAGCT

CCAAGCGGCGACTGAGATGTCCTAAATGCACAGCGACGGATTCGCGCTATTTAGAAAGAGAGAG

CAATATTTCAAGAATGCATGCGTCAATTTTACGCAGACTATCTTTCTAGGGTTAA

piggybac ITR: 237* bp(L), 306 bp(R)

* 1 adenine deletion

Pax-6 homeodomain binding site: 11 bp x 9

Drosophila hsp70 promoter (minimal): 125 bp

mScarlet-I: 696 bp

SV40 polyadenylation signal: 122 bp

185 pXL[9xP3-EGFP-SV40T;attP] = 1838 bp

186 TTAACCCTAGAAAGATAATCATATTGTGACGTACGTTAAAGATAATCATGTGTAAAATTGACGC

187 ATGTGTTTTATCGGTCTGTATATCGAGGTTTATTTATTAATTTGAATAGATATTAAGTTTTATT

188 ATATTTACACTTACATACTAATAATAAATTCAACAAACAATTTATTTATGTTTATTTATTTATT

189 AAAAAAAACAAAAACTCAAAATTTCTTCTATAAAGTAACAAAACTTTTATCGAATTCCTGCAGC

190 CCGGGGGATCCACTAGTTCTGTGAATTCAGATCTCCGGGGATCTAATTCAATTAGAGACTAATT

191 CAATTAGAGCTAATTCAATTAGGATTAATTCAATTAGAGACTAATTCAATTAGAGCTAATTCAA

192 TTAGGATTAATTCAATTAGAGACTAATTCAATTAGAGCTAATTCAATTAGGATCCAAGCTTATC

193 GATTTCGAACCCTCGACCGCCGGAGTATAAATAGAGGCGCTTCGTCTACGGAGCGACAATTCAA

194 TTCAAACAAGCAAAGTGAACACGTCGCTAAGCGAAAGCTAAGCAAATAAACAAGCGCAGCTGAA

195 CAAGCTAAACAATCGAAGAATCAAAATGGTGAGCAAGGGCGAGGAGCTGTTCACCGGGGTGGTG

196 CCCATCCTGGTCGAGCTGGACGGCGACGTAAACGGCCACAAGTTCAGCGTGTCCGGCGAGGGCG

197 AGGGCGATGCCACCTACGGCAAGCTGACCCTGAAGTTCATCTGCACCACCGGCAAGCTGCCCGT

198 GCCCTGGCCCACCCTCGTGACCACCCTGACCTACGGCGTGCAGTGCTTCAGCCGCTACCCCGAC

199 CACATGAAGCAGCACGACTTCTTCAAGTCCGCCATGCCCGAAGGCTACGTCCAGGAGCGCACCA

200 TCTTCTTCAAGGACGACGGCAACTACAAGACCCGCGCCGAGGTGAAGTTCGAGGGCGACACCCT

201 GGTGAACCGCATCGAGCTGAAGGGCATCGACTTCAAGGAGGACGGCAACATCCTGGGGCACAAG

202 CTGGAGTACAACTACAACAGCCACAACGTCTATATCATGGCCGACAAGCAGAAGAACGGCATCA

203 AGGTGAACTTCAAGATCCGCCACAACATCGAGGACGGCAGCGTGCAGCTCGCCGACCACTACCA

204 GCAGAACACCCCCATCGGCGACGGCCCCGTGCTGCTGCCCGACAACCACTACCTGAGCACCCAG

205 TCCGCCCTGAGCAAAGACCCCAACGAGAAGCGCGATCACATGGTCCTGCTGGAGTTCGTGACCG

206 CCGCCGGGATCACTCTCGGCATGGACGAGCTGTACAAGTAAAACTTGTTTATTGCAGCTTATAA

207 TGGTTACAAATAAAGCAATAGCATCACAAATTTCACAAATAAAGCATTTTTTTCACTGCATTCT

208 AGTTGTGGTTTGTCCAAACTCATCAATGTATCTTAAGATCTTCTAGATATCGGATCCCGGTGCC

209 CCAACTGGGGTAACCTTTGAGTTCTCTCAGTTGGGGGGGGGTCGACGGTATCGATAAGCTTGAT

ATCTATAACAAGAAAATATATATATAATAAGTTATCACGTAAGTAGAACATGAAATAACAATAT

AATTATCGTATGAGTTAAATCTTAAAAGTCACGTAAAAGATAATCATGCGTCATTTTGACTCAC

GCGGTCGTTATAGTTCAAAATCAGTGACACTTACCGCATTGACAAGCACGCCTCACGGGAGCTC

CAAGCGGCGACTGAGATGTCCTAAATGCACAGCGACGGATTCGCGCTATTTAGAAAGAGAGAGC

AATATTTCAAGAATGCATGCGTCAATTTTACGCAGACTATCTTTCTAGGGTTAA

piggybac ITR: 237* bp(L), 305 bp(R)

* 1 adenine deletion

Pax-6 homeodomain binding site: 11 bp x 9

Drosophila hsp70 promoter (minimal): 125 bp

EGFP: 717 bp

SV40 polyadenylation signal: 122 bp

phage φC31 attP: 42 bp

pXL[Gbact-H2B-mScarlet3-SV40T] = 2974 bp

TTAACCCTAGAAAGATAATCATATTGTGACGTACGTTAAAGATAATCATGTGTAAAATTGACGC

ATGTGTTTTATCGGTCTGTATATCGAGGTTTATTTATTAATTTGAATAGATATTAAGTTTTATT

ATATTTACACTTACATACTAATAATAAATTCAACAAACAATTTATTTATGTTTATTTATTTATT

AAAAAAAAACAAAAACTCAAAATTTCTTCTATAAAGTAACAAAACTTTTATCGAATTCCTGCAG

CCCGGGGGATCCACTAGCGCTACCGGACTCAGATCTCGAGCAGTTCCTTCAAATGTTCAAAATA

GTATTAGTTTTTGTTACGCCTAAATTTCTTGAGAATGTTGTTTAAACTTTTATTTTCTGACAAA

TGTTAAAATCATTGCTGTTTTTTTTAGCAGACACTTTTCGAAGCTTGTGTTTTGATATCTCGTTG

TAAAGTAAATTCATTTATAAGTTCTCATTGACTTTTAACCGTTTTTAGCCGGCATGTTCCGGTA

GGGAGCGTTGGTTCCACGCTGCTGGCTCGATACCATATATGGTAAAGAAAGCTGCCATTGGATG

AGAAGCATGCCCTTATTAGTTGGTGGTGGGGGTAGGGTAGGCATGGGAGGGGCAGGGCCTCCGT

AGTATATTACTCATAGGCCGGCTCCCGGCTTGAATCAGTCTGGTGCTAGTTCTCGTACTGTGAA

GATAGCAGTGTTGCGCTGCTGCGTTTTTGTACATATTACATTGTAAGTTTCTAGTGCTTCTCGA

AGATACTTTGTGAATTTGTGTTACGAGCATTTGTGCCATGTGGGATATCAGCACAATTTTTCGT

GTGGATTTTCGCGTATGTGCTTGTGAGCAGTTAGGGCGGGGCAACCGGCTTCGTCCACACTCCC

AAGGATTTCGCCTTATTTGGCGGGTGTTTGCTTAGGGTCTAGCCACTGAATATGGGCGGTGCCT

GTGTAGTGGTTGCCGGTGTGGGGCTTAGTCTTGTCAATGGGCGGGAAACCGGTGTGGGGAAACT

AGTAGCGAATTGGATGGTTAACTAGTTTACTCGTGCTACGGTTCTCTTAATTTTTTTTTTATTT

CTTGCAGTACCCGTAAACTCAACTACTAACCGAATTCTGCAGGTCGACATGCCGCCCAAGACTA

GCGGAAAGGCCGCGAAGAAGGCCGGTAAGGCCCAGAAGAATATCTCCAAGGGAGACAAGAAGAA

GAAGCGCAAGAGGAAGGAAAGCTACGCCATCTACATCTACAAGGTGTTGAAGCAGGTCCATCCT

GACACCGGCATCTCCAGCAAGGCGATGAGCATCATGAACAGTTTTGTCAATGACATTTTCGAGC

GCATCGCCGCCGAGGCTTCCCGCCTGGCGCACTACAACAAGCGCTCTACCATCACCTCGCGGGA

GATCCAGACCGCTGTGCGTCTCCTTCTGCCCGGCGAGCTGGCGAAGCACGCTGTCAGCGAAGGC

ACTAAGGCTGTCACCAAGTACACCAGCTCCAAGAAGGATCCACCGGTCGCCACCATGGATAGCA

255 CCGAGGCAGTGATCAAGGAGTTCATGCGGTTCAAGGTGCACATGGAGGGCTCCATGAACGGCCA

256 CGAGTTCGAGATCGAGGGCGAGGGCGAGGGCCGCCCCTACGAGGGCACCCAGACCGCCAAGCTG

257 AGGGTGACCAAGGGTGGCCCCCTGCCCTTCTCCTGGGACATCCTGTCCCCTCAGTTCATGTACG

258 GCTCCAGGGCCTTCACGAAGCACCCCGCCGACATCCCCGACTACTGGAAGCAGTCCTTCCCCGA

259 GGGCTTCAAGTGGGAGCGCGTGATGAACTTCGAGGACGGCGGCGCTGTGTCCGTGGCCCAGGAC

260 ACCTCCCTGGAGGACGGCACCCTGATCTACAAGGTGAAGCTCCGCGGCACCAACTTCCCTCCTG

261 ACGGCCCCGTAATGCAGAAGAAGACAATGGGCTGGGAAGCATCCACCGAGCGGTTGTACCCCGA

262 GGACGTCGTGCTGAAGGGCGACATTAAGATGGCCCTGCGCCTGAAGGACGGCGGTCGCTACCTG

263 GCGGACTTCAAGACCACCTACAGGGCCAAGAAGCCCGTGCAGATGCCCGGCGCTTTCAACATCG

264 ACCGCAAGTTGGACATCACATCCCACAACGAGGACTACACCGTGGTGGAACAGTACGAACGCTC

265 CGTGGCCCGCCACTCCACCGGCTAAAGCGGCCGCGACTCTAGATCATAATCAGCCATACCACAT

266 TTGTAGAGGTTTTACTTGCTTTAAAAAACCTCCCACACCTCCCCCTGAACCTGAAACATAAAAT

267 GAATGCAATTGTTGTTGTTAACTTGTTTATTGCAGCTTATAATGGTTACAAATAAAGCAATAGC

268 ATCACAAATTTCACAAATAAAGCATTTTTTTCACTGCATTCTAGTTGTGGTTTGTCCAAACTCA

269 TCAATGTATCTTAAGGCGTAAATTGTAAGCGTTAATATTTTGTTAAAATTCGCGTTAAATTTTT

270 GTTAAATCAGCTCATTTTTTAACCAATAGGCCGAAATCGGCAAAATCCCTTATAAATCAAAAGA

271 ATAGACCGAGATAGGGTTGAGTGTTGTTCCAGTTAGATCTTAATACGACTCACTATAGGGCGAA

272 TTGGGTACCGGGCCCCCCCTCGAGGTCGACGGTATCGATAAGCTTGATATCTATAACAAGAAAA

273 TATATATATAATAAGTTATCACGTAAGTAGAACATGAAATAACAATATAATTATCGTATGAGTT

274 AAATCTTAAAAGTCACGTAAAAGATAATCATGCGTCATTTTGACTCACGCGGTCGTTATAGTTC

275 AAAATCAGTGACACTTACCGCATTGACAAGCACGCCTCACGGGAGCTCCAAGCGGCGACTGAGA

276 TGTCCTAAATGCACAGCGACGGATTCGCGCTATTTAGAAAGAGAGAGCAATATTTCAAGAATGC

277 ATGCGTCAATTTTACGCAGACTATCTTTCTAGGGTTAA

278

279 *piggybac* ITR: 238 bp(L), 305 bp(R)

Gryllus actin promoter: 826 bp

Gryllus H2B: 369 bp

mScarlet3: 672 bp

SV40 polyadenylation signal: 122 bp

289

290 pXL[Gbact-gap43-mScarlet3-SV40T;9xP3-EGFP-SV40T] = 3635 bp

291 TTAACCCTAGAAAGATAATCATATTGTGACGTACGTTAAAGATAATCATGTGTAAAATTGACGC

292 ATGTGTTTTATCGGTCTGTATATCGAGGTTTATTTATTAATTTGAATAGATATTAAGTTTTATT

293 ATATTTACACTTACATACTAATAATAAATTCAACAAACAATTTATTTATGTTTATTTATTTATT

294 AAAAAAAAACAAAAACTCAAAATTTCTTCTATAAAGTAACAAAACTTTTATCGAATTCCTGCAG

295 CCCGGGGGATCCACTAGCGCTACCGGACTCAGATCTCGAGCAGTTCCTTCAAATGTTCAAAATA

296 GTATTAGTTTTTGTTACGCCTAAATTTCTTGAGAATGTTGTTTAAACTTTTATTTTCTGACAAA

297 TGTTAAAATCATTGCTGTTTTTTTAGCAGACACTTTTCGAAGCTTGTGTTTTGATATCTCGTTG

298 TAAAGTAAATTCATTTATAAGTTCTCATTGACTTTTAACCGTTTTTAGCCGGCATGTTCCGGTA

299 GGGAGCGTTGGTTCCACGCTGCTGGCTCGATACCATATATGGTAAAGAAAGCTGCCATTGGATG

300 AGAAGCATGCCCTTATTAGTTGGTGGTGGGGGTAGGGTAGGCATGGGAGGGGCAGGGCCTCCGT

301 AGTATATTACTCATAGGCCGGCTCCCGGCTTGAATCAGTCTGGTGCTAGTTCTCGTACTGTGAA

302 GATAGCAGTGTTGCGCTGCTGCGTTTTTGTACATATTACATTGTAAGTTTCTAGTGCTTCTCGA

303 AGATACTTTGTGAATTTGTGTTACGAGCATTTGTGCCATGTGGGATATCAGCACAATTTTTCGT

304 GTGGATTTTCGCGTATGTGCTTGTGAGCAGTTAGGGCGGGGCAACCGGCTTCGTCCACACTCCC

305 AAGGATTTCGCCTTATTTGGCGGGTGTTTGCTTAGGGTCTAGCCACTGAATATGGGCGGTGCCT

306 GTGTAGTGGTTGCCGGTGTGGGGCTTAGTCTTGTCAATGGGCGGGAAACCGGTGTGGGGAAACT

307 AGTAGCGAATTGGATGGTTAACTAGTTTACTCGTGCTACGGTTCTCTTAATTTTTTTTTTATTT

308 CTTGCAGTACCCGTAAACTCAACTACTAACCGAATTCTGCAGGTCGACATGCTGTGCTGTATGA

309 GAAGAACCAAACAGGTTGAAAAGAATGATGAGGACCAAAAGATCATGGATAGCACCGAGGCAGT

310 GATCAAGGAGTTCATGCGGTTCAAGGTGCACATGGAGGGCTCCATGAACGGCCACGAGTTCGAG

311 ATCGAGGGCGAGGGCGAGGGCCGCCCCTACGAGGGCACCCAGACCGCCAAGCTGAGGGTGACCA

312 AGGGTGGCCCCCTGCCCTTCTCCTGGGACATCCTGTCCCCTCAGTTCATGTACGGCTCCAGGGC

313 CTTCACGAAGCACCCCGCCGACATCCCCGACTACTGGAAGCAGTCCTTCCCCGAGGGCTTCAAG

314 TGGGAGCGCGTGATGAACTTCGAGGACGGCGGCGCTGTGTCCGTGGCCCAGGACACCTCCCTGG

315 AGGACGGCACCCTGATCTACAAGGTGAAGCTCCGCGGCACCAACTTCCCTCCTGACGGCCCCGT

316 AATGCAGAAGAAGACAATGGGCTGGGAAGCATCCACCGAGCGGTTGTACCCCGAGGACGTCGTG

317 CTGAAGGGCGACATTAAGATGGCCCTGCGCCTGAAGGACGGCGGTCGCTACCTGGCGGACTTCA

318 AGACCACCTACAGGGCCAAGAAGCCCGTGCAGATGCCCGGCGCTTTCAACATCGACCGCAAGTT

319 GGACATCACATCCCACAACGAGGACTACACCGTGGTGGAACAGTACGAACGCTCCGTGGCCCGC

320 CACTCCACCGGCTAAAGCGGCCGCGACTCTAGATCATAATCAGCCATACCACATTTGTAGAGGT

321 TTTACTTGCTTTAAAAAACCTCCCACACCTCCCCCTGAACCTGAAACATAAAATGAATGCAATT

322 GTTGTTGTTAACTTGTTTATTGCAGCTTATAATGGTTACAAATAAAGCAATAGCATCACAAATT

323 TCACAAATAAAGCATTTTTTTCACTGCATTCTAGTTGTGGTTTGTCCAAACTCATCAATGTATC

324 TTAAGGTTCTGTGAATTCAGATCTCCGGGGATCTAATTCAATTAGAGACTAATTCAATTAGAGC

325 TAATTCAATTAGGATTAATTCAATTAGAGACTAATTCAATTAGAGCTAATTCAATTAGGATTAA

326 TTCAATTAGAGACTAATTCAATTAGAGCTAATTCAATTAGGATCCAAGCTTATCGATTTCGAAC

327 CCTCGACCGCCGGAGTATAAATAGAGGCGCTTCGTCTACGGAGCGACAATTCAATTCAAACAAG

328 CAAAGTGAACACGTCGCTAAGCGAAAGCTAAGCAAATAAACAAGCGCAGCTGAACAAGCTAAAC

329 AATCGAAGAATCAAAATGGTGAGCAAGGGCGAGGAGCTGTTCACCGGGGTGGTGCCCATCCTGG

330 TCGAGCTGGACGGCGACGTAAACGGCCACAAGTTCAGCGTGTCCGGCGAGGGCGAGGGCGATGC

331 CACCTACGGCAAGCTGACCCTGAAGTTCATCTGCACCACCGGCAAGCTGCCCGTGCCCTGGCCC

332 ACCCTCGTGACCACCCTGACCTACGGCGTGCAGTGCTTCAGCCGCTACCCCGACCACATGAAGC

333 AGCACGACTTCTTCAAGTCCGCCATGCCCGAAGGCTACGTCCAGGAGCGCACCATCTTCTTCAA

334 GGACGACGGCAACTACAAGACCCGCGCCGAGGTGAAGTTCGAGGGCGACACCCTGGTGAACCGC

335 ATCGAGCTGAAGGGCATCGACTTCAAGGAGGACGGCAACATCCTGGGGCACAAGCTGGAGTACA

336 ACTACAACAGCCACAACGTCTATATCATGGCCGACAAGCAGAAGAACGGCATCAAGGTGAACTT

337 CAAGATCCGCCACAACATCGAGGACGGCAGCGTGCAGCTCGCCGACCACTACCAGCAGAACACC

338 CCCATCGGCGACGGCCCCGTGCTGCTGCCCGACAACCACTACCTGAGCACCCAGTCCGCCCTGA

GCAAAGACCCCAACGAGAAGCGCGATCACATGGTCCTGCTGGAGTTCGTGACCGCCGCCGGGAT

CACTCTCGGCATGGACGAGCTGTACAAGTAAAACTTGTTTATTGCAGCTTATAATGGTTACAAA

TAAAGCAATAGCATCACAAATTTCACAAATAAAGCATTTTTTTCACTGCATTCTAGTTGTGGTT

TGTCCAAACTCATCAATGTATCTTGGTACCGGGCCCCCCCTCGAGGTCGACGGTATCGATAAGC

TTGATATCTATAACAAGAAAATATATATATAATAAGTTATCACGTAAGTAGAACATGAAATAAC

AATATAATTATCGTATGAGTTAAATCTTAAAAGTCACGTAAAAGATAATCATGCGTCATTTTGA

CTCACGCGGTCGTTATAGTTCAAAATCAGTGACACTTACCGCATTGACAAGCACGCCTCACGGG

AGCTCCAAGCGGCGACTGAGATGTCCTAAATGCACAGCGACGGATTCGCGCTATTTAGAAAGAG

AGAGCAATATTTCAAGAATGCATGCGTCAATTTTACGCAGACTATCTTTCTAGGGTTAA

piggybac ITR: 238 bp(L), 305 bp(R)

Gryllus actin promoter: 826 bp

GAP43 fragment (palmitoylation sites): 60 bp

mScarlet3: 672 bp

SV40 polyadenylation signal: 122 bp

Pax-6 homeodomain binding site: 11 bp x 9

Drosophila hsp70 promoter (minimal): 125 bp

EGFP: 717 bp

SV40 polyadenylation signal: 121 bp

pXL[Ofact-H2B-mScarlet3-SV40T] = 4650 bp

TTAACCCTAGAAAGATAATCATATTGTGACGTACGTTAAAGATAATCATGTGTAAAATTGACGC

ATGTGTTTTATCGGTCTGTATATCGAGGTTTATTTATTAATTTGAATAGATATTAAGTTTTATT

ATATTTACACTTACATACTAATAATAAATTCAACAAACAATTTATTTATGTTTATTTATTTATT

AAAAAAAAACAAAAACTCAAAATTTCTTCTATAAAGTAACAAAACTTTTATCGAATTCCTGCAG

CCCGGGGGATCCACTAGCGCTACCGGACTCAGATCTCGAGCGGGGAGATTTCTCGCCTTTCCTT

AGTGAGGAGTGGAGAGAGACTGTGGATATATATATATATATCCACACGTACACATTTATATATG

GTAGATAATATCTCTAAGAATTTGATTCTTTGACTGCACGCCACCGACATGCCAACCATCCAGA

GGTTAATTATATTTAGGAAATTTGGTTTAGGAATCCTTAAAAATAAACATTTGTTAAAACCTCG

ACATAGACTTCCTTCTTGATTCTTATACTTGACACTACATTGTGGTTAATTTAAGGTTGCTCGG

GGAAAATCATTCAGACATGTAATAAAATAGAAACGGATTTTGAACTTAATTTCTGTTTACAGTT

AGATAAAGAATTGTATTGCTATATAATGTACACACTGGACTGTCTGTGCCTGTGCTTATCCTAG

TAAATCGGCTTAACTAATAACCCTTCTTATAGAGGTAGATTGGTTGAGAAGATGACTTTCGTTT

CCAACATTAAAACAGAAACAAAATTACTTCTGTTTGGGTACTTATATAAAACCTGTAAGAAAGC

GAACCATAATAAGCTGTCAAGAAGAGCCCGGACCACAATGCCTAGGTCAGGTAGAAGCTGGTAG

AGAGATTTGGCAGAGGGCAGACCCATTGATGAGAGAATGGGCATGAATGGGAGTTTTAAAGGGA

ATCGGGAGAGTTTTAGAGCCTCAGGGATAGGGACTCTCGCGTCAGACGACATTTCGACAGGGGC

TTAACGGAATTGCACCAGGAATTAGGGATATTGTAGGGGACGGACGGGAGACTTGGAGGGACTC

TCAGCGCTACTAGGATTCGGAAATATTTCCAGTGACAGAACGGGAAATGGACTCCGCCTGCCTG

CAAATGCATGTTCAATAATAAAAACTGGCTGAGAGATATTTACAAAGGCGGCTCTTACTAAATG

CCGGCGAGCTGGAGGGATTTCTCCCTCGCCGCGGGCTCCGCCAATCAGCGGGCTCCATCCGTTT

TATGCCCATATATGGTAAGAGCGGCGGTCGAGGCCGCTGGTGGGGGAAGGCGGGTCCACCTCCC

TCCTCCCCCCCGACTCCCGGCTTTTCCCCCTCACAGCTATACCATACTTAACCCAATTGTTGTT

ATAATTTTTTTAATTACTCATTTTTTCCCATAAAAAAAACTGTATCGTGAAATCCGCTACCGGG

AAGGCGTATTATCAGCGGAATAGTGAAGTATTTGTGAGTGGCGGAGGAGGCGACACCCCCCGGA

391 TCGGGCGAGTCCACTCTCCTCCTGGAGACCAACGGCTCAATCCTCCTTCACTCCCGTCAATTGT

392 GTGATAGTGTACGCATTGGCTCTCGCCTCCTTCGTCCAGTAAAGGTAAGTCTTGCAGAGAAATC

393 TCACTATTTCCTACACTTACAGTAAATACTCTACATCCCTACTCTTCTAATAGTACTAACCGTT

394 TGTATATTGATATTTAAAGTGAAGGGGCCGGACTTTACTCCCGAATGAGTGCCGGTAGGACCTC

395 GCAAACGTGTTGCCTTCGTTTTCATTCTCTCGTCCTCTAAGTAAATTTAACTCCGGTATTTCGG

396 GACGTCCACAGCCAGAATTAAACTTGGATCTCTTCCAATATCTATGTTTAGGGAATGGTTTACT

397 ACGGTAGCGCCATTGACTGGAGCGCTATTTGTGTACTGATGAGAGTAGAGATGGCTCCTGGCCT

398 ATCTTGCCCTACCCCAAGTGTGGCGGTAAATCAGTTTTACCGGCTCTTTTAGGCCGGAATTGTG

399 TATTCCCTCGACCGTACTGCCATATAAGGAGATGTGCAGAGAGAGGGCGTGGAGGGGCGGGGGC

400 CGGTGGAGGGGGACGGCCTATATCACCCTCGGGACCCCTGCCCAAGCCACCAGTCCGACTTCAC

401 AGCTCAAACAGTACTCTGCGTACTATTTATTTATTTATTTTTAATAAGTAAGTGACTTCTCAAT

402 AACCTCTTAAAGAGTGGGTGTGGATTATAGTGCTACTTATATTAATCTATTAGTGCTCATCAGT

403 GAATCGTGTTTTATGTGATATGAGTGATTCAAAGTGAAACTTAATGGATTTACAATTAAATCTT

404 CAGGGTCAGATTATAGCATTTGGTCAAGCTTCCCGAGAGGTAAAATTTTTCCCTATTCCCTCTA

405 GGCCAATTGGATTTTAAATCAAGCATCCAATTGTCAAAATTAATTCATCTTATAGCTACTGGAA

406 ATATCTGGAATTATGTGAAACTCATTCAGTAAAACCCCCCATTTATTTAACATGTGTTATAACT

407 TAGTTGTATTTTAAATCACATGTACACTGACTTCAATTCACACAGGATGCCTGTAAAGTGATTT

408 ATTTAGTATTTTTTTTTTACAATATTTAGAATATTTTCAAATTATGTACTGTAAAATGCTTGAC

409 TATCTGTTGTTCTGAAACCCTTGAAGGCACTCTCTGATTTTATGGATACCTTCCATAGGATTTT

410 AATTTTAGTTTTTGTTTTTCAGCTTATTTAACTAACCCAAAACAAATTCTGCAGGTCGACATGC

411 CGCCCAAGACTAGCGGAAAGGCCGCGAAGAAGGCCGGTAAGGCCCAGAAGAATATCTCCAAGGG

412 AGACAAGAAGAAGAAGCGCAAGAGGAAGGAAAGCTACGCCATCTACATCTACAAGGTGTTGAAG

413 CAGGTCCATCCTGACACCGGCATCTCCAGCAAGGCGATGAGCATCATGAACAGTTTTGTCAATG

414 ACATTTTCGAGCGCATCGCCGCCGAGGCTTCCCGCCTGGCGCACTACAACAAGCGCTCTACCAT

415 CACCTCGCGGGAGATCCAGACCGCTGTGCGTCTCCTTCTGCCCGGCGAGCTGGCGAAGCACGCT

GTCAGCGAAGGCACTAAGGCTGTCACCAAGTACACCAGCTCCAAGAAGGATCCACCGGTCGCCA

CCATGGATAGCACCGAGGCAGTGATCAAGGAGTTCATGCGGTTCAAGGTGCACATGGAGGGCTC

CATGAACGGCCACGAGTTCGAGATCGAGGGCGAGGGCGAGGGCCGCCCCTACGAGGGCACCCAG

ACCGCCAAGCTGAGGGTGACCAAGGGTGGCCCCCTGCCCTTCTCCTGGGACATCCTGTCCCCTC

AGTTCATGTACGGCTCCAGGGCCTTCACGAAGCACCCCGCCGACATCCCCGACTACTGGAAGCA

GTCCTTCCCCGAGGGCTTCAAGTGGGAGCGCGTGATGAACTTCGAGGACGGCGGCGCTGTGTCC

GTGGCCCAGGACACCTCCCTGGAGGACGGCACCCTGATCTACAAGGTGAAGCTCCGCGGCACCA

ACTTCCCTCCTGACGGCCCCGTAATGCAGAAGAAGACAATGGGCTGGGAAGCATCCACCGAGCG

GTTGTACCCCGAGGACGTCGTGCTGAAGGGCGACATTAAGATGGCCCTGCGCCTGAAGGACGGC

GGTCGCTACCTGGCGGACTTCAAGACCACCTACAGGGCCAAGAAGCCCGTGCAGATGCCCGGCG

CTTTCAACATCGACCGCAAGTTGGACATCACATCCCACAACGAGGACTACACCGTGGTGGAACA

GTACGAACGCTCCGTGGCCCGCCACTCCACCGGCTAAAGCGGCCGCGACTCTAGATCATAATCA

GCCATACCACATTTGTAGAGGTTTTACTTGCTTTAAAAAACCTCCCACACCTCCCCCTGAACCT

GAAACATAAAATGAATGCAATTGTTGTTGTTAACTTGTTTATTGCAGCTTATAATGGTTACAAA

TAAAGCAATAGCATCACAAATTTCACAAATAAAGCATTTTTTTCACTGCATTCTAGTTGTGGTT

TGTCCAAACTCATCAATGTATCTTAAGGCGTAAATTGTAAGCGTTAATATTTTGTTAAAATTCG

CGTTAAATTTTTGTTAAATCAGCTCATTTTTTAACCAATAGGCCGAAATCGGCAAAATCCCTTA

TAAATCAAAAGAATAGACCGAGATAGGGTTGAGTGTTGTTCCAGTTAGATCTTAATACGACTCA

CTATAGGGCGAATTGGGTACCGGGCCCCCCCTCGAGGTCGACGGTATCGATAAGCTTGATATCT

ATAACAAGAAAATATATATATAATAAGTTATCACGTAAGTAGAACATGAAATAACAATATAATT

ATCGTATGAGTTAAATCTTAAAAGTCACGTAAAAGATAATCATGCGTCATTTTGACTCACGCGG

TCGTTATAGTTCAAAATCAGTGACACTTACCGCATTGACAAGCACGCCTCACGGGAGCTCCAAG

CGGCGACTGAGATGTCCTAAATGCACAGCGACGGATTCGCGCTATTTAGAAAGAGAGAGCAATA

TTTCAAGAATGCATGCGTCAATTTTACGCAGACTATCTTTCTAGGGTTAA

piggybac ITR: 238 bp(L), 305 bp(R)

Oncopeltus actin promoter: 2502 bp

Gryllus H2B: 369 bp

mScarlet3: 672 bp

SV40 polyadenylation signal: 122 bp

pXL[Ofinv2.4kb-QF2;15xQUAS-mScarlet3-SV40T;9xP3-EGFP-SV40T] =

7161 bp

TTAACCCTAGAAAGATAATCATATTGTGACGTACGTTAAAGATAATCATGTGTAAAATTGACGC

ATGTGTTTTATCGGTCTGTATATCGAGGTTTATTTATTAATTTGAATAGATATTAAGTTTTATT

ATATTTACACTTACATACTAATAATAAATTCAACAAACAATTTATTTATGTTTATTTATTTATT

AAAAAAAAACAAAAACTCAAAATTTCTTCTATAAAGTAACAAAACTTTTATCGAATTCCTGCAG

CCCGGGGGATCCACTAGCGCTACCGGACTCAGATCTCGAGATGATGAGGTGAAGTGTACTCGAA

GTAAGTGGACAGGGCGAGGGTGCTGTGGTCTTGTCAACAATTCTCTTTCTCACACCCACATTTC

ATCAGTTCTTCACTGTGTCTCATAAGATGCTTAATGCTTAAGTATGCTTAGGCCACATCAAAGC

TCTGTAAATAAATGTGCTTTGCGCTTTGTGATAAGGCTTTGCATGACTTAAAATACTAATATAT

ATAAAAAGAAAACTAAATATTCGCAATACTTTGCGTTATTTCTATTTTGTGTGTTTGTGAGTGT

TGACTACTCTCTCATTCTTCCTCCTGTTATTAATATATATATATTTAATATATGACTTTATATA

TTATATACATATAATTTCTAATTTCCGATTGCGTGATTAGACAAAATGTGAATCGCTAGCGTTA

GACAACTATTGCCGACTGCACCACGTATGCCGCCATGTGTATCCTTGGGAAGCGTGTTTCGCTC

CTTGGTCTTCCTAGCTCTTCCTTCCAGTTATCTTTATCTTCAGAGCTTCCTGTCTTATCAAACT

CAACATAATTTCAGCAAGACAACACACTAAATATTGGACTTTTCCATCTTTCACATTTGCAA

ATCTTCACTACCAATATGTCATACCAATGGCATCATAAATTAACCTGTTGTAAGACTCGATGCC

CCTCTGAAATTGTCAACTAATTTCCTGTGGTTTCCATTTTCCTTGATAGGAATAATACACCTTC

CACAATTAGATAATTATGGTATTATACATATAAACCTACACAGAGCTATCTATTGAAGTACAGA

TTATTTTAAGTTTAGTCTTTTGTGATGGGCTAATCCACGAGGCTGACTGACGTAATTTGGTTTC

ATATCCTACATAATTATCGGACGTGATTTGGGTAGGTCAATATTAGGAAAACCAATATTATATA

TAAATCATTTTTAACTTCTTTTTTTTTTTTTTAAGTCGTGGTACAAGCGTGAATATATTGATTT

CTTGTAGGAAATGTACTAAAATCGAATAATCGTATTTATAACAGTTGCCATAAAGTTGAAGTAA

CTGAATAAGTGTAAAATTCAATTCATTACATTTAATGTATAATAACATTTTTAGAGAGTAAGGC

477 ACTAAAAATTGTAGCTGTGCGGTTGAGCGAACCAACTAACAGGTAAAATTCAAATAAAGCACTT

478 CATTGCAAAATAGGGGGAGGGGGAGGGGGGAGAGATTTACAGGAGAAACAAATAGAATGCTCGC

479 AGGAATCGTGGTTATTATGGTAGGTGTATAGGACTAAAATCTTATCTACAAAAGTGCATTATAT

480 TGTAACAGTTTAATATCCACTGACTTCCAGGACCTCCTTGAGTCATCGGAATGATACAGCTTTA

481 TTTTATTTCATTTTAGAAAATATTTATGGGAAAAATAAATTGTTTCCAGACAGGATAGCTTGCA

482 ATGGATTTGAGGATAATAAACTTGTTCTACTGTACTGTGTGTTTCATGATTTCGAAGTTAGGAC

483 AAAATCAAACTTTGGGATCAGCGCCGCGTACTTGATATAAATTACATTATGTGAAATCTGTTGA

484 AAACGATTAATTGTATGGTCTTCTAAAGAAGGAAATGATATTTTATAGCCTCCCATCTGAATTG

485 GAAGGGCCAGTCAACGGAGGTTGCTTTCCATACCAAATTTATATTAATTGCAATTGTCAACTTC

486 TTAAATTGGACGTAATGAATATTACTTCCCCTACTAAAGGGGTGTTGATGGTAATCGCAACCCT

487 CGATGAATACGATTGCTCAAAGTGTCTATTGTCTTAGGCTGTTGAGCTCCTAAAAAAGAAAGGC

488 TGTCAATCGCATTCATTAGCAACGAAAATGATTCTAACTGGATACATAACCACACAGGACGAGA

489 AAGACCAACTATTTCTTCCTGCGAAAAGAATATTTAGAGGCTAATTTGATTACATTCTTCATTC

490 AAAGAGAAAACTGATTTCCATCAAAATTAAAAATTAACTGTCAGAACACTCAACGAATTGATAT

491 GTAATCGATGATACACATCGATGATAGTCTTCCCACATAGATAATTAATTCATGAGTGAGAGGG

492 CGTGAGTGAGGGGAAGGGAGGGGAGGAGAGGCGCGGTAAGTGCATAATCATTTCATCAGTCCTT

493 AATAAACATATAGTGGGTGGGAGGGGCCGGCCGATATATGTAATCTGGCTAATAACTTGATCTG

494 GAGGGGCGGTGGTGGGGGAGCAGGGGAGGGGAGCCATCGCGGGGCGAGGCCGGTGGAGGGGAGG

495 TCGGCACCCTGATTGGCCGAGAGCGGGGAGTGGGCGGCGGTGAGGGGGCGGGGCCTTGTCGGAC

496 ACGCCCACCGCCCCCTCCCCACCACCGCACAGCGCTCTCCCGACTTTGAAATCTTAGTTAGAAG

497 CTGTCAGCCGTTGACAGAAGCTCTCAATCGGATGTAGTGAGGCGAGGCCGGCCAACATGCCACC

498 CAAGCGCAAAACGCTTAACGCTGCGGCTGAGGCTAACGCTCATGCCGACGGACACGCCGACGGA

499 AACGCCGACGGACACGTGGCCAATACGGCCGCGTCCTCGAATAATGCGAGGTTCGCTGATCTCA

500 CTAACATCGATACTCCGGGTCTGGGACCCACAACTACGACCCTGCTCGTGGAACCAGCACGCTC

501 AAAGCGTCAACGAGTGTCCCGCGCATGCGACCAGTGCCGTGCAGCCCGAGAGAAATGCGACGGA

ATACAGCCTGCGTGTTTCCCGTGCGTTTCCCAGGGAAGGTCCTGCACTTATCAGGCTTCGCCGA

AAAAGAGGGGAGTTCAAACCGGTTATATTCGTACGCTGGAGCTCGCCCTCGCCTGGATGTTTGA

AAATGTCGCGCGTTCCGAAGATGCCTTGCATAACCTCCTCGTCCGTGACGCCGGACAAGGATCA

GCTCTGCTCGTTGGTAAAGATTCGCCGGCTGCCGAGCGACTCCATGCCCGTTGGGCTACTAGCC

GTGTCAATAAGAGCATTACCCGCCTCCTCCGTCAGTTGGAGCTCCCTCCTACCGCCACGGCTAC

GGCCTCGATAATGCCGCACGTGATGGAGCAGCCTCTCAGTACCAGCATTAACCCCGTCAACGAC

CGCTTCAACGGTATTCCCAACCCCACTCCGTATAACTCCGATGCAGCTCTCGATGCTATCACTC

AGACCAACGATTATGGAAGCGTAAATACACATGGTATCCTCTCTACTTACCCGCCACCGGCTAC

GCACCTTAATGAAGCTTCCGTCGCTCTCGCTCCCGGTGGCGCCCCCCCCCGACCGCCTCCTCCG

TATGTTGACAGCACGACCAATCACCCGCCGTACCACTCGAATCTGGTTCCAATGGCGAACTTTG

GTTACTCGACCGTTGATTACGATGCCATGGTTGACGATTTGGCTAGCATTGAATACACGGACGC

TGTGGATGTCGACCCACAGTTTATGACCAATCTGGGATTCGTTCCTGGATGTAACTTCTCCGAC

ATTAATACATACGAACAGTGATGACGTCTATCGATACCGTCGACTAAAGCCAAATAGAAAATTA

TTCAGTTCCTGGCTTAAGTTTTTAAAAGTGATATTATTTATTTGGTTGTAACCAACCAAAAGAA

TGTAAATAACTAATACATAATTATGTTAGTTTTAAGTTAGCAACAAATTGATTTTAGCTATATT

AGCTACTTGGTTAATAAATAGAATATATTTATTTAAAGATAATTGCGTTTTTATTGTCAGGGAG

TGAGTTTGCTTAAAAACTCGTTTAGATCCCGGTCACGTGTCACTGGGTCAGTGGGTAATCGCTT

ATCCTCGGATAAACAATTATCCTCACGGGTAATCGCTTATCCGCTCGGGTAATCGCTTATCCTC

GGGTAATCGCTTATCCTTGGGTAATCGCTTATCCTCGGATAAACAATTATCCTCACGGGTAATC

GCTTATCCGCTCGGGTAATCGCTTATCCTCGGGTAATCGCTTATCCTTGGGTAATCGCTTATCC

TCGGATAAACAATTATCCTCACGGGTAATCGCTTATCCGCTCGGGTAATCGCTTATCCTCGGGT

AATCGCTTATCCTTTCACGTTGGGACTCAGTGAGGAGGACCTGAATTCCTGCAGCCCGAGCGGA

GACTCTAGCGAGCGCCGGAGTATAAATAGAGGCGCTTCGTCTACGGAGCGACAATTCAATTCAA

ACAAGCAAAGTGAACACGTCGCTAAGCGAAAGCTAAGCAAATAAACAAGCGCAGCTGAACAAGC

TAAACAATCTGCAGTAAAGTGCAAGTTAAAGTGAATCAATTAAAAGTAACCAGCAACCAAGTAA

527 ATCAACTGCAACTACTGAAATCTGCCAAGAAGTAATTATTGAATACAAGAAGAGAACTCTGAAT

528 AGGGAATTGGGAATTCGTTAACAGATCGGGGGATCAATTCGTTAACATGGATAGCACCGAGGCA

529 GTGATCAAGGAGTTCATGCGGTTCAAGGTGCACATGGAGGGCTCCATGAACGGCCACGAGTTCG

530 AGATCGAGGGCGAGGGCGAGGGCCGCCCCTACGAGGGCACCCAGACCGCCAAGCTGAGGGTGAC

531 CAAGGGTGGCCCCCTGCCCTTCTCCTGGGACATCCTGTCCCCTCAGTTCATGTACGGCTCCAGG

532 GCCTTCACGAAGCACCCCGCCGACATCCCCGACTACTGGAAGCAGTCCTTCCCCGAGGGCTTCA

533 AGTGGGAGCGCGTGATGAACTTCGAGGACGGCGGCGCTGTGTCCGTGGCCCAGGACACCTCCCT

534 GGAGGACGGCACCCTGATCTACAAGGTGAAGCTCCGCGGCACCAACTTCCCTCCTGACGGCCCC

535 GTAATGCAGAAGAAGACAATGGGCTGGGAAGCATCCACCGAGCGGTTGTACCCCGAGGACGTCG

536 TGCTGAAGGGCGACATTAAGATGGCCCTGCGCCTGAAGGACGGCGGTCGCTACCTGGCGGACTT

537 CAAGACCACCTACAGGGCCAAGAAGCCCGTGCAGATGCCCGGCGCTTTCAACATCGACCGCAAG

538 TTGGACATCACATCCCACAACGAGGACTACACCGTGGTGGAACAGTACGAACGCTCCGTGGCCC

539 GCCACTCCACCGGCTAAAGCGGCCGCGACTCTAGATCATAATCAGCCATACCACATTTGTAGAG

540 GTTTTACTTGCTTTAAAAAACCTCCCACACCTCCCCCTGAACCTGAAACATAAAATGAATGCAA

541 TTGTTGTTGTTAACTTGTTTATTGCAGCTTATAATGGTTACAAATAAAGCAATAGCATCACAAA

542 TTTCACAAATAAAGCATTTTTTTCACTGCATTCTAGTTGTGGTTTGTCCAAACTCATCAATGTA

543 TCTTAAGGTTCTGTGAATTCAGATCTCCGGGGATCTAATTCAATTAGAGACTAATTCAATTAGA

544 GCTAATTCAATTAGGATTAATTCAATTAGAGACTAATTCAATTAGAGCTAATTCAATTAGGATT

545 AATTCAATTAGAGACTAATTCAATTAGAGCTAATTCAATTAGGATCCAAGCTTATCGATTTCGA

546 ACCCTCGACCGCCGGAGTATAAATAGAGGCGCTTCGTCTACGGAGCGACAATTCAATTCAAACA

547 AGCAAAGTGAACACGTCGCTAAGCGAAAGCTAAGCAAATAAACAAGCGCAGCTGAACAAGCTAA

548 ACAATCGAAGAATCAAAATGGTGAGCAAGGGCGAGGAGCTGTTCACCGGGGTGGTGCCCATCCT

549 GGTCGAGCTGGACGGCGACGTAAACGGCCACAAGTTCAGCGTGTCCGGCGAGGGCGAGGGCGAT

550 GCCACCTACGGCAAGCTGACCCTGAAGTTCATCTGCACCACCGGCAAGCTGCCCGTGCCCTGGC

551 CCACCCTCGTGACCACCCTGACCTACGGCGTGCAGTGCTTCAGCCGCTACCCCGACCACATGAA

GCAGCACGACTTCTTCAAGTCCGCCATGCCCGAAGGCTACGTCCAGGAGCGCACCATCTTCTTC

AAGGACGACGGCAACTACAAGACCCGCGCCGAGGTGAAGTTCGAGGGCGACACCCTGGTGAACC

GCATCGAGCTGAAGGGCATCGACTTCAAGGAGGACGGCAACATCCTGGGGCACAAGCTGGAGTA

CAACTACAACAGCCACAACGTCTATATCATGGCCGACAAGCAGAAGAACGGCATCAAGGTGAAC

TTCAAGATCCGCCACAACATCGAGGACGGCAGCGTGCAGCTCGCCGACCACTACCAGCAGAACA

CCCCCATCGGCGACGGCCCCGTGCTGCTGCCCGACAACCACTACCTGAGCACCCAGTCCGCCCT

GAGCAAAGACCCCAACGAGAAGCGCGATCACATGGTCCTGCTGGAGTTCGTGACCGCCGCCGGG

ATCACTCTCGGCATGGACGAGCTGTACAAGTAAAACTTGTTTATTGCAGCTTATAATGGTTACA

AATAAAGCAATAGCATCACAAATTTCACAAATAAAGCATTTTTTTCACTGCATTCTAGTTGTGG

TTTGTCCAAACTCATCAATGTATCTTGGTACCGGGCCCCCCCTCGAGGTCGACGGTATCGATAA

GCTTGATATCTATAACAAGAAAATATATATATAATAAGTTATCACGTAAGTAGAACATGAAATA

ACAATATAATTATCGTATGAGTTAAATCTTAAAAGTCACGTAAAAGATAATCATGCGTCATTTT

GACTCACGCGGTCGTTATAGTTCAAAATCAGTGACACTTACCGCATTGACAAGCACGCCTCACG

GGAGCTCCAAGCGGCGACTGAGATGTCCTAAATGCACAGCGACGGATTCGCGCTATTTAGAAAG

AGAGAGCAATATTTCAAGAATGCATGCGTCAATTTTACGCAGACTATCTTTCTAGGGTTAA

piggybac ITR: 238 bp(L), 305 bp(R)

Oncopeltus invected 2.4-kb upstream: 2435 bp

QF2: 1050 bp

hsp70 terminator: 257 bp

15xQUAS: 290 bp

Drosophila hsp70 promoter: 241 bp

mScarlet3: 672 bp

SV40 polyadenylation signal: 122 bp

Pax-6 homeodomain binding site: 11 bp x 9

Drosophila hsp70 promoter (minimal): 125 bp

EGFP: 717 bp

SV40 polyadenylation signal: 121 bp

Data S2. transposase protein sequence_261026

>0xNLS-hyPBase

MGSTMPRSPEFAATMGSSLDDEHILSALLQSDDELVGEDSDSEVSDHVSEDDVQSDTEE
AFIDEVHEVQPTSSGSEILDEQNVIEQPGSSLASNRILTLPQRTIRGKNKHCWSTSKPT
RRSRVSALNIVRSQRGPTRMCRNIYDPLLCFKLFFTDEIISEIVKWTNAEISLKRRESM
TSATFRDTNEDEIYAFFGILVMTAVRKDNHMSTDDLFDRSLSMVYVSVMSRDRFDFLIR
CLRMDDKSIRPTLRENDVFTPVRKIWDLFIHQCIQNYTPGAHLTIDEQLLGFRGRCPFR
VYIPNKPSKYGIKILMMCDSGTKYMINGMPYLGRGTQTNGVPLGEYYVKELSKPVHGSC
RNITCDNWFTSIPLAKNLLQEPYKLTIVGTVRSNKREIPEVLKNSRSRPVGTSMFCFDG
PLTLVSYKPKPAKMVYLLSSCDEDASINESTGKPQMVMYYNQTKGGVDTLDQMCSVMTC
SRKTNRWPMALLYGMINIACINSFIIYSHNVSSKGEKVQSRKKFMRNLYMGLTSSFMRK
RLEAPTLKRYLRDNISNILPKEVPGTSDDSTEEPVMKKRTYCTYCPSKIRRKASASCKK
CKKVICREHNIDMCQSCF

EPVMKKRTYCTYCPSKIRRKASASCKKCKKVI = predicted endogenous NLS

608 >1xNLS-hyPBase

609 MGSTMPKKKRKVPRSPEFAATMGSSLDDEHILSALLQSDDELVGEDSDSEVSDHVSEDD

610 VQSDTEEAFIDEVHEVQPTSSGSEILDEQNVIEQPGSSLASNRILTLPQRTIRGKNKHC

611 WSTSKPTRRSRVSALNIVRSQRGPTRMCRNIYDPLLCFKLFFTDEIISEIVKWTNAEIS

612 LKRRESMTSATFRDTNEDEIYAFFGILVMTAVRKDNHMSTDDLFDRSLSMVYVSVMSRD

613 RFDFLIRCLRMDDKSIRPTLRENDVFTPVRKIWDLFIHQCIQNYTPGAHLTIDEQLLGF

614 RGRCPFRVYIPNKPSKYGIKILMMCDSGTKYMINGMPYLGRGTQTNGVPLGEYYVKELS

615 KPVHGSCRNITCDNWFTSIPLAKNLLQEPYKLTIVGTVRSNKREIPEVLKNSRSRPVGT

616 SMFCFDGPLTLVSYKPKPAKMVYLLSSCDEDASINESTGKPQMVMYYNQTKGGVDTLDQ

617 MCSVMTCSRKTNRWPMALLYGMINIACINSFIIYSHNVSSKGEKVQSRKKFMRNLYMGL

618 TSSFMRKRLEAPTLKRYLRDNISNILPKEVPGTSDDSTEEPVMKKRTYCTYCPSKIRRK

619 ASASCKKCKKVICREHNIDMCQSCF

620

621 PKKKRKV = SV40 NLS

622 EPVMKKRTYCTYCPSKIRRKASASCKKCKKVI = predicted endogenous NLS

623

624

>3xNLS-hyPBase

MGSTMPKKKRKVPKKKRKVPKKKRKVPRSPEFAATMGSSLDDEHILSALLQSDDELVGE

DSDSEVSDHVSEDDVQSDTEEAFIDEVHEVQPTSSGSEILDEQNVIEQPGSSLASNRIL

TLPQRTIRGKNKHCWSTSKPTRRSRVSALNIVRSQRGPTRMCRNIYDPLLCFKLFFTDE

IISEIVKWTNAEISLKRRESMTSATFRDTNEDEIYAFFGILVMTAVRKDNHMSTDDLFD

RSLSMVYVSVMSRDRFDFLIRCLRMDDKSIRPTLRENDVFTPVRKIWDLFIHQCIQNYT

PGAHLTIDEQLLGFRGRCPFRVYIPNKPSKYGIKILMMCDSGTKYMINGMPYLGRGTQT

NGVPLGEYYVKELSKPVHGSCRNITCDNWFTSIPLAKNLLQEPYKLTIVGTVRSNKREI

PEVLKNSRSRPVGTSMFCFDGPLTLVSYKPKPAKMVYLLSSCDEDASINESTGKPQMVM

YYNQTKGGVDTLDQMCSVMTCSRKTNRWPMALLYGMINIACINSFIIYSHNVSSKGEKV

QSRKKFMRNLYMGLTSSFMRKRLEAPTLKRYLRDNISNILPKEVPGTSDDSTEEPVMKK

RTYCTYCPSKIRRKASASCKKCKKVICREHNIDMCQSCF

PKKKRKVPKKKRKVPKKKRKV = 3x SV40 NLS

EPVMKKRTYCTYCPSKIRRKASASCKKCKKVI = predicted endogenous NLS

643 >5xNLS-hyPBase

644 MGSTMPKKKRKVPKKKRKVPKKKRKVPKKKRKVPKKKRKVPRSPEFAATMGSSLDDEHI

645 LSALLQSDDELVGEDSDSEVSDHVSEDDVQSDTEEAFIDEVHEVQPTSSGSEILDEQNV

646 IEQPGSSLASNRILTLPQRTIRGKNKHCWSTSKPTRRSRVSALNIVRSQRGPTRMCRNI

647 YDPLLCFKLFFTDEIISEIVKWTNAEISLKRRESMTSATFRDTNEDEIYAFFGILVMTA

648 VRKDNHMSTDDLFDRSLSMVYVSVMSRDRFDFLIRCLRMDDKSIRPTLRENDVFTPVRK

649 IWDLFIHQCIQNYTPGAHLTIDEQLLGFRGRCPFRVYIPNKPSKYGIKILMMCDSGTKY

650 MINGMPYLGRGTQTNGVPLGEYYVKELSKPVHGSCRNITCDNWFTSIPLAKNLLQEPYK

651 LTIVGTVRSNKREIPEVLKNSRSRPVGTSMFCFDGPLTLVSYKPKPAKMVYLLSSCDED

652 ASINESTGKPQMVMYYNQTKGGVDTLDQMCSVMTCSRKTNRWPMALLYGMINIACINSF

653 IIYSHNVSSKGEKVQSRKKFMRNLYMGLTSSFMRKRLEAPTLKRYLRDNISNILPKEVP

654 GTSDDSTEEPVMKKRTYCTYCPSKIRRKASASCKKCKKVICREHNIDMCQSCF

655

656 PKKKRKVPKKKRKVPKKKRKVPKKKRKVPKKKRKV = 5x SV40 NLS

657 EPVMKKRTYCTYCPSKIRRKASASCKKCKKVI = predicted endogenous NLS

658

659

Supplementary Video Legends

Supplemental Video 1. Ventral view of a developing *O. fasciatus* embryo showing ubiquitous expression of H2B:mScarlet driven by the endogenous actin promoter identified herein. Over this 36 hour time course, katatrepsis (second inversion of the embryonic axes such that the head of the embryo moves from the posterior of the egg (right) to the anterior of the egg (left) (Panfilio, 2008)), and appendage elongation occur. The Green Fire Blue look up table implemented in Fiji (Schindelin et al., 2012) shows the highest intensity pixels in white, intermediate intensity pixels in green, and the lowest intensity pixels in black (see Figure 5D). Download Link

Supplemental Video 2. Dorsal view of a developing *O. fasciatus* embryo showing ubiquitous expression of H2B:mScarlet driven by the endogenous actin promoter identified herein. Over this 36 hour time course, the end of anatrepsis (first inversion of the embryonic anteroposterior axis such that the head of the embryo moves from the anterior of the egg (right) to the posterior of the egg (left)), and the whole of katatrepsis (second inversion of both anteroposterior and dorsoventral embryonic axes relative to those of the egg) occur (Panfilio, 2008). The Green Fire Blue look up table implemented in Fiji (Schindelin et al., 2012) shows the highest intensity pixels in white, intermediate intensity pixels in green, and the lowest intensity pixels in black (see Figure 5D). Download Link

Supplemental Video 3. Lateral view of a developing *O. fasciatus* embryo showing ubiquitous expression of H2B:mScarlet driven by the endogenous actin promoter identified herein. Over this 36 hour time course, the end of anatrepsis and the whole of

685 katatrepsis (Panfilio, 2008) occur as in Supplemental Video 3. From this lateral
686 viewpoint, emerging muscular contractions of the embryo are apparent beginning at
687 approximately 30 hours, the elongating appendages on the ventral side of the embryo
688 (bottom), and the dorsal movement (towards the top) of the lateral ectoderm that is
689 required for dorsal closure, are evident. The Green Fire Blue look up table implemented
690 in Fiji (Schindelin et al., 2012) shows the highest intensity pixels in white, intermediate
691 intensity pixels in green, and the lowest intensity pixels in black (see Figure 5D).
692 Download Link